Energy-based control design for mechanical systems

Muñoz Arias, Mauricio

Energy-based control design for mechanical systems

Applications of the port-Hamiltonian approach

Mauricio Muñoz Arias

university of groningen

The research described in this dissertation has been carried out at the Faculty of Mathematics and Natural Sciences, University of Groningen, The Netherlands, within the Engineering and Technology Institute Groningen (ENTEG).

The research reported in this dissertation is part of the research program of the Dutch Institute of Systems and Control (DISC). The author has successfully completed the educational program of DISC.

The research reported in this dissertation has been supported by the Costa Rica Institute of Technology.

Printed by Ipskamp Drukkers B.V.
Enschede, the Netherlands

ISBN (Book): 978-90-367-7797-1
ISBN (E-book): 978-90-367-7796-4

university of groningen

Energy-based control design for mechanical systems

Applications of the port-Hamiltonian approach

PhD thesis

to obtain the degree of PhD at the
University of Groningen
on the authority of the
Rector Magnificus Prof. E. Sterken
and in accordance with
the decision by the College of Deans.

This thesis will be defended in public on

Friday 24 April 2015 at 14:30 hours

by

Mauricio Muñoz Arias

born on 19 January 1981
in Heredia, Costa Rica.

Supervisor
Prof. dr. ir. J.M.A. Scherpen

Assessment committee
Prof. dr. A.J. van der Schaft
Prof. dr. B. Jayawardhana
Prof. dr. R. Babuska

To my mother:

Olga,

and my brothers and sisters:

Mariano, Ramiro,

Manfred, Andrea,

Isaac and Nicole.

Contents

Acknowledgments

First and foremost, I want to express my gratitude to my supervisor and promotor Jacquelien Scherpen, without whom this dissertation would not have happened. I deeply appreciate her advice, patience and guidance during my research. She always provided a friendly and inspirational research environment, her comments and remarks to improve the quality of my manuscripts are immeasurable.

I am grateful to my reading committee members, Arjan van der Schaft, Bayu Jayawardhana and Robert Babuska, who proofread the manuscript and suggested many improvements.

I would like to express my sincerest thanks to Daniel Dirksz, Alessandro Macchelli, and Mohamed El-Hawwary, who made very important collaborations on this manuscript. I appreciate our discussions full of constructive criticism based on your experiences and expertise.

Many thanks go to Jesús Barradas, Raymond Roepers, James Riehl and Héctor Garcia de Marina. I acknowledge here your willingness to help with the proofreading of this thesis.

A special debt is owed to the (former)collaborators of the DTPA Laboratory: Pim van den Dool, Herman Kruis, Sietse Achterop and Martin Stokroos. Their technical support was fundamental to demonstrating the a practical relevance of this work.

I want to thank Joël Mendels, Guus Nering Bögel, Martine Bos, Matthijs de Jong, Johan Siemonsma and Floorke Koops. The big impact of their hard work on the Philips Experimental Robot Arm during their Bachelor and Master projects is presented in every chapter of this thesis.

The design of the cover of this thesis dissertation would not be possible without the artistic skills of Emi Saliasi. I am heartily thankful to her.

My life in Groningen has been challenging, but also interesting and inspiring, thanks to my friends and colleagues. I have no words to express my gratitude to them all.

Finally, I wholeheartedly thank my family for their unconditional support during these years.

Mauricio Muñoz Arias,
Groningen, April 2015.

Chapter 1
Introduction

The focus of this thesis is on control of nonlinear mechanical systems, based on the port-Hamiltonian (PH) framework. Despite the fact that our control strategies are described for general mechanical systems, we focus our simulations and experimental results on a robotic manipulator in order to illustrate the applicability of the aforementioned control strategies. Firstly, we control position via feedback of the measurements provided by force sensors. Furthermore, we introduce results on force control and an impedance grasping strategy. This proposed control strategies are designed for systems that experience a non-contact to contact transition between an end-effector and an environment. Subsequently, a PH approach to vision control is introduced, which derives two control laws of practical interest that depend on the characteristics of the vision system. Lastly, a trajectory tracking control strategy for a robot manipulator is provided. Simulations and experimental results are shown in order to demonstrate the performance of the proposed controllers.

1.1 The energy-based setting

All physical systems are governed by definition by the laws of physics, out of which the *law of conservation of energy* states that energy is neither created nor destroyed, but just transformed, [50]. From this perspective, such systems act as energy transformation devices as discussed in detail in [44], where an intuitive and analytically powerful energy-based perspective is taken. This energy-based setting allows us to divide complex nonlinear systems into smaller subsystems, whose energies and energy interactions determine the overall system behavior.

An energy-based setting is the PH framework, which facilitates extension of systems and interconnections, in contrast to the classical Lagrangian approach [13, 55], where it is less straightforward. The Euler-Lagrange framework extensively documented in [40] is however comparable, but has a less clear physical structure and the interconnection is more involved.

In the sequel we give a brief introduction to the PH framework, together with its most relevant features and the control design methodology under this framework.

1.2 Port-Hamiltonian systems

The PH systems paradigm has succeeded in matching the "old" framework of port-based network modeling of multi-domain physical systems with the "new" framework of dynamical systems and control theory, [13]; "this paradigm provides the necessary tools for modeling, control and analysis via

1. the separation of the network interconnection structure of the system from the constitutive relations of its components;

2. the emphasis on power flow and the ensuing distinction between different kind of variables;

3. the analysis of the system through the properties of its interconnection structure and the component constitutive relations;

4. the achievement of control by interconnection, by means of stabilization by Casimir generation and energy shaping , energy routing control (transferring energy between components in the system), and port and impedance control.

Complex (nonlinear) systems from different fields can be modeled in the PH formalism, since it unifies the description of (nonlinear) physical systems from different domains" [13, 55]. Examples of such domains are mechanical, electrical, thermal, electromagnetic, and optical systems. Interconnection between two or more PH systems is realized via ports, and the resulting system is again PH. Since most of the PH systems are passive, the resulting system after the interconnection is also passive. This is a helpful property for control design, since passivity-based control for PH systems addresses complex problems in a more structured way. The PH system is based on a energy representation given by the Hamiltonian. The Hamiltonian function is suitable for stability analysis since it can be taken as candidate Lyapunov function. As presented by [13], the Hamiltonian approach has its roots in analytical mechanics and starts from the principle of least action, via the Euler-Lagrange equations and the Legendre transformation, towards the Hamiltonian equations of motion. The network approach proceeds from the electrical domain. Then, the PH framework systems combines the analysis of physical systems, and the network modeling of (complex) physical systems.

We base our work on the PH framework. We follow the control design methodologies of the PH framework since it allows a clearer interpretation of the proposed controllers.

1.3 Robotics in modern society

Even though both the PH framework and the results presented in this thesis are applicable to a more general class of mechanical systems, we focus our simulations and experimental results on a certain robotic manipulator in order to examine the performance of the proposed control strategies. In particular we make use of the Philips Experimental Robot Arm, [45].

Robotics are ubiquitous in our modern society, due to the ever rising production requirements of the industry, the ever increasing quality standards, and applications in other domains including *domotics*, and mobile robotics. Robots performing complex tasks amidst us have been a science fiction idea for years. However, science is rapidly bringing up this idea into reality. One example is the *Advanced Step In Innovative Motion* (ASIMO) shown in Figure 1.1, [47]. It is easy to associate this intelligent humanoid robot with the iconic science fiction author Isaac Asimov, who was the first to write about the *three laws of robotics*, see [2].

Figure 1.1: Multi-functional mobile assistant: ASIMO by Honda, [47].

In other fields in the modern society, robotics are influencing the incorporation of new health care methods, [39]. The robotic technology can improve existing medical procedures, and become less invasive. Furthermore, home automation, i.e., domotics, via service robots for the elderly and disabled are being studied and developed, [22].

In this thesis we investigate tasks performed by a robotic manipulator such as position control, force control, impedance grasping, vision control, and the trajectory tracking control problem, which are a step towards the practical applicability of the proposed control strategies. We elaborate on these contributions in the sequel.

1.4 Main contribution

This work extends the PH framework with new control strategies for nonlinear mechanical systems. We have the advantage of stability analysis since the Hamiltonian function can be taken as a Lyapunov function. Furthermore, the PH framework facilitates extensions of the system, and interconnections of multi-physical domains via its ports. Hence, we develop new strategies by strategically extending the dynamics of our mechanical systems. The new developments address the problems of position, force, impedance grasping, and trajectory tracking control, and we apply our new control strategies to a humanoid robot arm.

Skilled manipulation is required when a mechanical system, e.g. a robot, is in contact with the environment. In the robotics field, the number of possible tasks to perform is increased when the information about the dynamics of the contact with the environment is available. The interaction robot-environment is intentional in industrial applications such as grinding, polishing, cutting, excavating and non-industrial such as domotics and health care purposes [4, 21]. Implementation of all these tasks requires force feedback and force control. It becomes possible to feed back force of the manipulator links by installing force sensors. The force control in robot manipulators is thoroughly discussed in [4, 21, 38, 51, 53] in the Euler-Lagrange framework. Contrary to the EL strategies, it is the aim of this work to propose a dynamic extension for a class of mechanical system, and based on the PH formulation [13, 30] for force feedback and force control purposes. Furthermore, the problems of position control, and trajectory tracking control are addressed in this work. We design control methods based on force feedback, and an image-based vision strategy. Position control with force feedback is a strategy with more tunable properties in comparison with the classical results in the EL framework. Moreover, the PH framework allows us to include the nonlinear dynamics of a vision system in order to achieve position. PH systems include a large family of physical nonlinear systems, and since the PH framework is an efficient way to describe the environment, the physical systems, and the interactions between them, the dynamics of nonlinear controllers have a more suitable interpretation.

1.5 Outline of the thesis

The thesis is structured as follows. Chapter 2 provides the background for the main contributions presented in this thesis. We deal with the analysis of physical systems described in the PH framework, canonical transformations in order to obtain and stabilize an *error system*, and stability analysis in presence of disturbances in the input of system. Furthermore, modeling of the Philips Experimental Robot Arm is shown.

In Chapter 3, position control strategies via force feedback are presented for standard mechanical systems in the PH framework. The introduced control strategies require a set of coordinate transformations, since structure preservation of the PH system is not straightforward. With the coordinate transformations we can include force feedback in the input of the system. The PH formalism offers a modeling framework with a clear physical structure and other properties that can often be exploited for control design purposes, which is why we believe it is important to preserve the structure. The proposed control strategies offers an alternative solution to position control with more tuning freedom, and exploits knowledge of the system dynamics. Simulations results are provided in order to show the robustness of our control strategies.

The work of Chapter 4 is first devoted to a force control strategy of a class of standard mechanical systems in the PH framework. We provide a force control law that asymptotically stabilizes a mechanical system to a constant desired force. Experiments results are given to show the advantages of the force control strategy in presence of external forces. Furthermore, in Chapter 4 we introduce an impedance grasping strategy for mechanical systems in the PH framework. The presented control strategy requires a set of change of variables, since the impedance control in the PH framework with structure preservation is not straightforward. We then achieve impedance grasping control via a *virtual spring* with a variable rest-length. The force that is exerted by the virtual spring leads to a dissipation term in the impedance grasping controller, which is needed to obtain a smoother noncontact to contact transition. Simulations and experimental results are given in order to motivate our results.

The work of Chapter 5 is devoted to image-based visual servo control strategies for standard mechanical systems in the PH framework. We utilize a change of variables that transforms the PH system into one with constant mass-inertia matrix, and we use an interaction matrix that includes the depth information together with the image features variables of the image plane. We develop two control strategies. The first strategy utilizes a reduction principle to show closed-loop asymptotic stability. In the second strategy, the designed feedback renders a closed-loop system that is PH. The introduced approaches are applied to a three-link robot arm problem, and simulation results are provided.

Lastly, Chapter 6 introduces a trajectory tracking control strategy based on the main results of [17, 19]. We make use of a passivity-based control method, called stabilization via a canonical transformation. When a system cannot be stabilized by conventional state-feedback, the canonical transformations become of particular interest, because they are capable of dealing with a more general class of systems, e.g., time-varying systems. We finally provide simulations and experimental results to illustrate the stabilization of a link of the PERA to desired time-varying. trajectories.

1.6 List of publications

Journal papers

1. M. Munoz-Arias, J.M.A. Scherpen, and A. Macchelli, 2015, An impedance grasping strategy, *submitted*.

2. M. Munoz-Arias, M. El-Hawwary, and J.M.A. Scherpen, 2014, Imaged-based vision control strategies in the port-Hamiltonian framework, *submitted*.

3. M. Munoz-Arias, J.M.A. Scherpen, and D.A. Dirksz, 2013, Position control of a class of standard mechanical systems in the port-Hamiltonian framework, *submitted*.

Peer reviewed conference proceedings

1. M. Munoz-Arias, J.M.A. Scherpen, 2015, Trajectory tracking control of a robot manipulator, *submitted*.

2. M. Munoz-Arias, J.M.A. Scherpen, M. El-Hawwary, 2015, An image-based visual servo control strategy using the port-Hamiltonian approach, *submitted*.

3. M. Munoz-Arias, J.M.A. Scherpen, A. Macchelli, 2014, An impedance grasping strategy, in *Proceedings of the 53rd Annual Conference on Decision and Control (CDC2014)*, Los Angeles, CA, USA, pp. 1403-1408.

4. M. Munoz-Arias, J.M.A. Scherpen, and D.A. Dirksz, 2013, Position control of a class of standard mechanical systems in the port-Hamiltonian framework, in *Proceedings of the 52nd Annual Conference on Decision and Control (CDC2013)*, Florence, Italy, pp. 1622-1627.

5. M. Munoz-Arias, J.M.A. Scherpen, D.A. Dirksz, 2013, Force control of a class of standard mechanical system in the port-Hamiltonian framework, in *Proceedings of the 9th IFAC Symposium on Nonlinear Control Systems (NOLCOS2013)*, Toulouse, France, pp. 377-382.

6. M. Munoz-Arias, J.M.A. Scherpen, D.A. Dirksz, 2012, A class of standard mechanical system with force feedback in the port-Hamiltonian framework, in *Proceedings of the 4th IFAC Workshop on Lagrangian and Hamiltonian Methods for Nonlinear Control (LHMNLC2012)*, Bertinoro, Italy, pp. 90-95.

7. M. Munoz-Arias, J.M.A. Scherpen, D.A. Dirksz, 2012, Force feedback of a manipulator system in the port-Hamiltonian framework, in *Proceedings of the 20th Interna-*

tional Symposium on Mathematical Theory of Networks and Systems (MTNS2012), Melbourne, Australia.

Conferences with published abstracts

1. M. Munoz-Arias, J.M.A. Scherpen, A. Macchelli, 2014, An impedance grasping strategy, in *Proceedings of the 33rd Benelux Meeting on Systems and Control*, Heijden, The Netherlands, page 116.

2. M. Munoz-Arias, J.M.A. Scherpen, D.A. Dirksz, 2013, Force control of a class of standard mechanical systems in the port-Hamiltonian framework, in *Proceedings of the 32nd Benelux Meeting on Systems and Control*, Houffalize, Belgium, page 140.

3. M. Munoz-Arias, J.M.A. Scherpen, D.A. Dirksz, 2012, Force Feedback of a Manipulator System in the port-Hamiltonian Framework, in *Proceedings of the 31st Benelux Meeting on Systems and Control*, Heijden, The Netherlands, page 64.

4. M. Munoz-Arias, J.M.A. Scherpen, 2011, Euler-Lagrange modeling for a seven degrees of freedom manipulator, in *Proceedings of the 30st Benelux Meeting on Systems and Control*, Lommel, Belgium, page 190.

Abbreviations

In this thesis the abbreviation EL is used for Euler-Lagrange systems, PH for port-Hamiltonian, DOF for degrees of freedom, and PERA for Philips Experimental Robot Arm.

Chapter 2

Preliminaries

This chapter provides the background for the main contributions presented in this thesis. We deal here with the analysis of physical systems described in the PH framework, canonical transformations, and stability analysis in the presence of a disturbance, and a constant force in the input of system.

The chapter is organized as follows. In Section 2.1, we provide a general background in the PH framework [13]. In Section 2.2, we apply the results of [56] to equivalently describe the original PH system in a PH form which has a constant mass-inertia matrix in the Hamiltonian via a change of coordinates. This coordinate transformation simplifies the extension of the results in [31] to systems with a nonconstant mass-inertia matrix. A PH model of a robot manipulator of two-DOF is introduced in order to show a mass-inertia decomposition case. Furthermore, in Section 2.3 we briefly recall the Hamilton-Jacobi inequality related to $\mathscr{L}_2$ analysis. In Section 2.4, we recap the constructive procedure of [29] to modify the Hamiltonian function of a forced PH system in order to generate Lyapunov functions for nonzero equilibria, i.e. a system in the presence of nonzero constant external forces. Finally, concluding remarks are given in Section 2.5.

2.1 Port-Hamiltonian systems

We briefly recap the definition, properties and advantages of modeling and control with the PH formalism.

The PH framework is based on the description of systems in terms of energy variables, their interconnection structure, and power ports. PH systems include a large family of physical nonlinear systems. The transfer of energy between the physical system and the environment is given through energy elements, dissipation elements and power preserving ports [13, 30], based on the study of Dirac structures.

A class of PH system, introduced in [30], is described by

$$\Sigma = \begin{cases} \dot{x} = [J(x) - R(x)] \dfrac{\partial H(x)}{\partial x} + g(x) w \\ \\ y = g(x)^{\top} \dfrac{\partial H(x)}{\partial x} \end{cases} \tag{2.1}$$

with $x \in \mathbb{R}^{\mathscr{N}}$ the states of the system, the skew-symmetric interconnection matrix $J(x) \in \mathbb{R}^{\mathscr{N} \times \mathscr{N}}$, the positive-semidefinite damping matrix $R(x) \in \mathbb{R}^{\mathscr{N} \times \mathscr{N}}$, and the Hamiltonian $H(x) \in \mathbb{R}$. The matrix $g(x) \in \mathbb{R}^{\mathscr{N} \times \mathscr{M}}$ weights the action of the control inputs $w \in \mathbb{R}^{\mathscr{M}}$ on the system, and w, $y \in \mathbb{R}^{\mathscr{M}}$ with $\mathscr{M} \leqslant \mathscr{N}$, form a power port pair. We now restrict the description to a class of standard mechanical systems.

Consider a class of standard mechanical systems of n-DOF as in (2.1), e.g., an n-DOF rigid robot manipulator. Consider furthermore the addition of an external force vector. The resulting system is then given by

$$\begin{bmatrix} \dot{q} \\ \dot{p} \end{bmatrix} = \begin{bmatrix} 0_{n\times n} & I_{n\times n} \\ -I_{n\times n} & -D(q,p) \end{bmatrix} \begin{bmatrix} \dfrac{\partial H(q,p)}{\partial q} \\ \dfrac{\partial H(q,p)}{\partial p} \end{bmatrix} + \begin{bmatrix} 0_{n\times n} \\ G(q) \end{bmatrix} u + \begin{bmatrix} 0_{n\times n} \\ B(q) \end{bmatrix} f_e \tag{2.2}$$

$$y = G(q)^{\top} \frac{\partial H(q,p)}{\partial p} \tag{2.3}$$

with the vector of generalized configuration coordinates $q \in \mathbb{R}^n$, the vector of generalized momenta $p \in \mathbb{R}^n$, the identity matrix $I_{n\times n}$, the damping matrix $D(q,p) \in \mathbb{R}^{n\times n}$, $D(q,p) = D(q,p)^{\top} \geqslant 0$, $y \in \mathbb{R}^n$ the output vector, $u \in \mathbb{R}^n$ the input vector, $f_e \in \mathbb{R}^n$ the vector of external forces, $\mathscr{N} = 2n$, matrix $B(q) \in \mathbb{R}^{n\times n}$, and the input matrix $G(q) \in \mathbb{R}^{n\times n}$ everywhere invertible, i.e., the PH system is *fully actuated*. The Hamiltonian of the system is equal to the sum of kinetic and potential energy,

$$H(q,p) = \frac{1}{2} p^{\top} M^{-1}(q) p + V(q) \tag{2.4}$$

where $M(q) = M^{\top}(q) > 0$ is the $n \times n$ inertia (generalized mass) matrix and $V(q)$ is the potential energy.

We consider the PH system (2.2) as a class of standard mechanical systems with external forces.

Remark 2.1.1 The robot dynamics is given in joint space in (2.2), and here the *external forces* $f_e \in \mathbb{R}^n$ are introduced. Since f_e is a vector of external forces, $B(q) \in \mathbb{R}^{n\times n}$ is the transpose of the *geometric Jacobian* [53] that maps the forces in the *work space* to the

(generalized) forces in the *joint space*. In this paper the following holds,

$$f_e = \mathscr{J}(q)^\top F_e, \quad F_e \in \mathbb{R}^N, \tag{2.5}$$

and the geometric Jacobian is given by

$$\mathscr{J}(q) = \begin{bmatrix} \mathscr{J}_v(q) \\ \mathscr{J}_\omega(q) \end{bmatrix} \in \mathbb{R}^{6\times n} \tag{2.6}$$

where $\mathscr{J}_v(q) \in \mathbb{R}^{3\times n}$, and $\mathscr{J}_\omega(q) \in \mathbb{R}^{3\times n}$ are the linear, and angular geometric Jacobians, respectively, and $N = \{3,6\}$. If the Jacobian is full rank, we can always find $f_e \in \mathbb{R}^n$ that corresponds to F_e. Then, it is not a limitation to suppose $B(q) = I_n$. This separation between joint and work spaces is important here, because we control the robot by acting on the generalized coordinates q, i.e., in the joint space, but we grasp objects with the end-effector in the work space.

Example 2.1.2 Consider the system given by the two-DOF shoulder of the PERA, [45]. A picture of the PERA is shown in Figure 2.1. A *Denavit-Hartenberg* representation of the PERA, see [53], is given in Figure 2.2. The shoulder consists of a link actuated by two motors. The model of the shoulder consists of a mass m_s, a link length l_s, and a linear damping $d_s > 0$. The states of the system are $x = (q,p)^\top$, where $(q,p) \in \mathbb{R}^2$ are the generalized coordinates q_1, and q_2, and p_1, p_2 are the generalized momenta of the system. The system is described in the PH form by

$$\begin{bmatrix} \dot{q} \\ \dot{p} \end{bmatrix} = \begin{bmatrix} 0_{2\times2} & I_{2\times2} \\ -I_{2\times2} & D(q,p) \end{bmatrix} \begin{bmatrix} \dfrac{\partial V(q)}{\partial q} \\ M(q)^{-1} p \end{bmatrix} + \begin{bmatrix} 0 \\ G \end{bmatrix} u_s + \begin{bmatrix} 0 \\ B \end{bmatrix} f_e \tag{2.7}$$

$$y_s = G^\top M(q)^{-1} p \tag{2.8}$$

with an input matrix $G = I_{2\times2}$ (fully actuated), a vector of external forces $f_e \in \mathbb{R}^2$, an input-output port pair (u_s, y_s), Hamiltonian of the form

$$H(q,p) = \frac{1}{2} p^\top M(q)^{-1} p + V(q) \tag{2.9}$$

with $V(q)$ the potential energy, and a mass-inertia matrix $M(q) \in \mathbb{R}^{2\times2}$, s.t., $M(q) = diag(a,b)$ where

$$a = m_s l_s^2 \cos(q_2)^2 + \mathscr{I}_1 + \mathscr{I}_2 \tag{2.10}$$

$$b = m_s l_s^2 + \mathscr{I}_2 \tag{2.11}$$

and with $\mathscr{I}_1$, and $\mathscr{I}_2$ the inertias of the joints. Furthermore, the gravity vector is

$$\frac{\partial V(q)}{\partial q} = \begin{bmatrix} g m_s l_s \cos(q_2) \sin(q_1) \\ g m_s l_s \sin(q_2) \cos(q_1) \end{bmatrix} \tag{2.12}$$

with g the gravitational acceleration. The shoulder is experiencing Coulomb friction that we have determined, and also validated experimentally, [3, 26]. The dissipation matrix has the form

$$D(q,p) = D(\dot{q}) = diag(d_{s_1}(\dot{q}_1), d_{s_2}(\dot{q}_2)) \tag{2.13}$$

where $\dot{q} = M^{-1}(q)\, p$, and with

$$d_{s_i} = \left(F_{c_i} + (F_{s_i} - F_{c_i})\, e^{|\dot{q}_i| \dot{q}_{s_i}^{-1}}\right) \left(\alpha_{f_i} + \dot{q}_i^2\right)^{-0.5} + F_{v_i} \dot{q}_i \tag{2.14}$$

where F_{c_i}, F_{s_i}, and F_{v_i} are the are the Coulomb, static, and viscous friction coefficients, respectively, and the Coulomb friction force is approximated as in [20] with positive (small) constants α_i, $\dot{q}_{s_i}$ is the constant due to the Stribeck velocity [1], and $i = 1, 2$. □

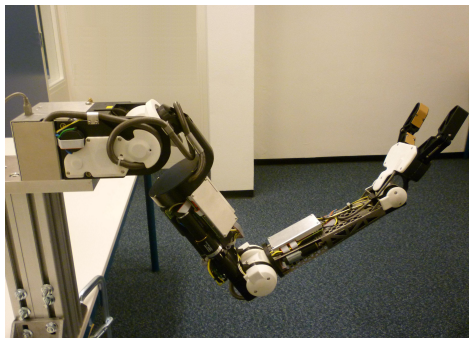

(a) PERA at the University of Groningen.

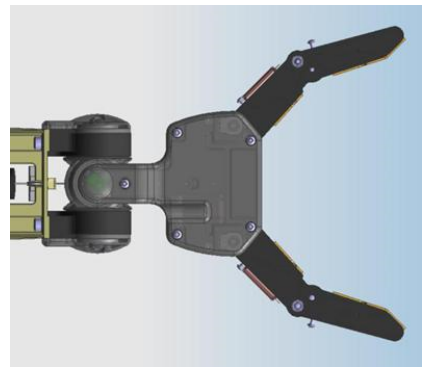

(b) Drawing of the gripper of the PERA.

Figure 2.1: Experimental setup

Example 2.1.3 Consider the one-DOF gripper (end-effector) of the PERA, [45]. A drawing of its gripper is shown in Figure 2.1b. The gripper consists of a shaft actuated by the motor of the gripper, which is attached to the fingers via cables. When the shaft moves counterclockwise; the gripper closes. When it moves clockwise; the gripper opens. The gripper is controlled via scripts developed in Matlab® with a sampling time of $10ms$.

The model of the gripper in the PH framework consists of a mass m_g, interconnected by a nonlinear spring, and a linear damping $d_g > 0$. The states of the system are $x = (q,p)^\top$, where q is the angular displacement between the two tips of the gripper, and p is the

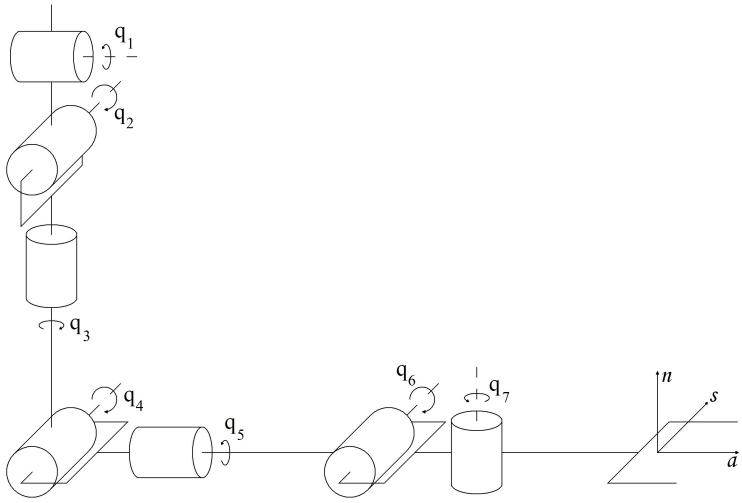

Figure 2.2: *Denavit-Hartenberg* representation of the PERA [26]

corresponding generalized momentum. The angular displacement of the two tips is directly proportional to the encoder of the motor. Coulomb friction forces and the gravitational forces can be neglected in the working space of the tips of the gripper.

The Hamiltonian of the system is given by

$$H(q,p) = \frac{1}{2} m_g^{-1} p^2 + V(q) \tag{2.15}$$

with a constant mass-inertia matrix, and where the potential energy $V(q)$ is given by a nonlinear spring, which stiffness coefficient $K_g(q)$ depends on the opening and closing of the gripper. We have obtained experimentally that

$$K_g(q) = \begin{cases} k_{g_1} & q - c_g \leqslant 0 \\ k_{g_2} & q - c_g > 0 \end{cases} \tag{2.16}$$

with a constant rest-length c_g, and positive spring constants k_{g_i}, and $i = 1,2$. We approximate this non-smooth stiffness constant of the nonlinear, such that

$$K_g(q) = \frac{1}{2}(k_{g_1} + k_{g_2}) + \frac{1}{2}(k_{g_1} - k_{g_2}) \frac{(q - c_g)}{\sqrt{a_f + (q - c_g)^2}} \tag{2.17}$$

Figure 2.3 illustrates the smooth transition of the gripper from opening to closing. From

(2.17), we have a potential energy function given by

$$\begin{aligned} V(q) = &\frac{1}{4}(k_{g_1}+k_{g_2})(q-c_g)^2 + \frac{a_f}{2}(k_{g_1}-k_{g_2})\ln\left(\sqrt{a_f}\right) \\ &+ \frac{1}{2}(k_{g_1}-k_{g_2})(q-c_g)\sqrt{a_f+(q-c_g)^2} \\ &- \frac{a_f}{2}(k_{g_1}-k_{g_2})\ln\left((q-c_g)+\sqrt{a_f+(q-c_g)^2}\right) \end{aligned} \tag{2.18}$$

with a positive (small) constant α_f. The system is described in the PH framework as

$$\begin{bmatrix} \dot{q} \\ \dot{p} \end{bmatrix} = \begin{bmatrix} 0 & 1 \\ -1 & -d_g \end{bmatrix} \begin{bmatrix} K_g(q)(q-c_g) \\ m_g^{-1}p \end{bmatrix} + \begin{bmatrix} 0 \\ G \end{bmatrix} u_g + \begin{bmatrix} 0 \\ B \end{bmatrix} f_e \tag{2.19}$$

$$y_g = G^\top m_g^{-1} p \tag{2.20}$$

with an input-output port pair $(u_g, y_g) \in \mathbb{R}^n$, and an external force vector $f_e \in \mathbb{R}^n$, with $n = 1$. □

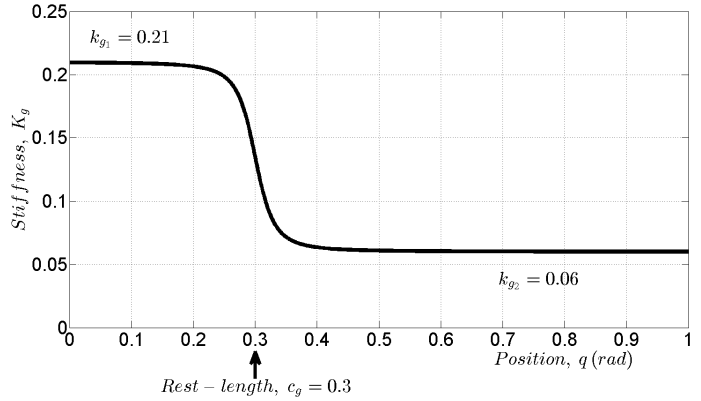

Figure 2.3: Smoothed stiffness of the one-DOF gripper of the PERA. Parameters $k_{g_1} = 0.21 Nm/rad$, $k_{g_2} = 0.06 Nm/rad$, and $c_g = 0.30 rad$ validated experimentally.

2.2 Canonical transformations of port-Hamiltonian systems

We recap here the results of [17, 19] in terms of generalized coordinate transformations for PH systems, and we apply the results of [56] to equivalently describe the original PH system in a PH form which has a constant mass-inertia matrix in the Hamiltonian.

A generalized canonical transformation of [19] is applied in (2.1) via a set of transformations

$$\bar{x} = \Phi(x) \tag{2.21}$$
$$\bar{H}(\bar{x}) = H(x) + U(x) \tag{2.22}$$
$$\bar{y} = y + \alpha(x) \tag{2.23}$$
$$\bar{u} = u + \beta(x) \tag{2.24}$$

that changes the coordinates x into $\bar{x}$, the Hamiltonian H into $\bar{H}$, the output y into $\bar{y}$, and the input u into $\bar{u}$. It is said to be a generalized canonical transformation for PH systems if it transforms a PH system (2.1) into another one.

The class of generalized canonical transformations are characterized by the following theorems.

Theorem 2.2.1 *[17] Consider the PH system* (2.1)*. For any smooth scalar function $U(x) \in \mathbb{R}$, and any smooth vector function $\beta(x) \in \mathbb{R}^{\mathscr{M}}$, there exists a pair of smooth functions $\Phi(x) \in \mathbb{R}^{\mathscr{N}}$ and $\alpha(x) \in \mathbb{R}^{\mathscr{M}}$ such that the set of equations* (2.21) *to* (2.24) *yields a generalized canonical transformation. The function $\Phi(x)$ yields a generalized canonical transformation with $U(x)$ and $\beta(x)$ if and only if the partial differential equation (PDE)*

$$\frac{\partial \Phi}{\partial(x,t)} \left(\begin{array}{c} (J-R)\dfrac{\partial U}{\partial x}^{\top} + (K-S)\dfrac{\partial (H+U)}{\partial x}^{\top} + g\beta \\ -1 \end{array} \right) = 0 \tag{2.25}$$

holds with a skew-symmetric matrix $K(x)$, and a symmetric matrix $S(x)$ satisfying $R(x) + S(x) \geqslant 0$. We have left out the arguments of $\Phi(x)$, $H(x)$, $J(x)$, $R(x)$, $S(x)$, $K(x)$, $U(x)$, $g(x)$, and $\beta(x)$, for notational simplicity. Furthermore, the change of output $\alpha(x)$, and the matrices $\bar{J}(\bar{x})$, $\bar{R}(\bar{x})$, and $\bar{g}(\bar{x})$, are given by

$$\alpha(x) = g(x)^{\top} \frac{\partial U(x)}{\partial x} \tag{2.26}$$
$$\bar{J}(\bar{x}) = \frac{\partial \Phi(x)}{\partial x} (J(x) + K(x)) \frac{\partial \Phi(x)}{\partial x}^{\top} \tag{2.27}$$
$$\bar{g}(\bar{x}) = \frac{\partial \Phi(x)}{\partial x} g(x) \tag{2.28}$$
$$\bar{R}(\bar{x}) = \frac{\partial \Phi}{\partial x} (R(x) + S(x)) \frac{\partial \Phi(x)}{\partial x}^{\top} \tag{2.29}$$

Theorem 2.2.2 *[17] Consider the PH system described by* (2.1) *and transform it by the generalized canonical transformation with $U(x)$ and $\beta(x)$ such that $H(x) + U(x) \geqslant 0$.*

Then the new input-output mapping $\bar{u} \to \bar{y}$ is passive with storage function $\bar{H}(\bar{x})$ if and only if

$$\frac{\partial (H+U)}{\partial (x)}^{\top} \begin{pmatrix} (J-R)\dfrac{\partial U}{\partial x}^{\top} - S\dfrac{\partial (H+U)}{\partial x}^{\top} + g\beta \\ -1 \end{pmatrix} \geqslant 0 \tag{2.30}$$

Suppose that (2.25) *holds, that $H(x)+U(x)$ is positive-definite and that the system is zero-state detectable. Then, the feedback $u = -\beta(x) - \mathscr{C}(x)(y+\alpha(x))$ with $\mathscr{C}(x) \geqslant \varepsilon I > 0$ renders the system asymptotically stable. Suppose moreover that $H+U$ is decrescent and that the transformed system is periodic. Then, the feedback renders the system uniformly asymptotically stable.*

Consider a class of standard mechanical systems (2.2) in the PH framework with a nonconstant mass-inertia matrix $M(q)$. The aim of this section is to transform the original system (2.2) into a PH formulation with a constant mass-inertia matrix via a generalized canonical transformation [19]. The proposed change of variables to deal with a nonconstant mass inertia matrix is first proposed in [56].

Consider the system (2.1) with nonconstant $M(q)$, and a coordinate transformation as

$$\bar{x} = \Phi(x) = \Phi(q,p) \triangleq \begin{pmatrix} \bar{q} \\ \bar{p} \end{pmatrix} = \begin{pmatrix} q - q_d \\ T(q)^{-1} p \end{pmatrix} = \begin{pmatrix} q - q_d \\ T(q)^{\top} \dot{q} \end{pmatrix} \tag{2.31}$$

with a constant desired position $q_d \in \mathbb{R}^n$, and where $T(q)$ is a lower triangular matrix such that

$$T(q) = T\left(\Phi^{-1}(q,p)\right) = \bar{T}(\bar{q}) \tag{2.32}$$

and

$$M(q) = T(q)\,T(q)^{\top} = \bar{T}(\bar{q})\,\bar{T}(\bar{q})^{\top} \tag{2.33}$$

Consider now the Hamiltonian $H(q,p)$ as in (2.4), and using (2.31), we realize $\bar{H}(\bar{x}) = H\left(\Phi^{-1}(\bar{x})\right)$ and $\bar{V}(\bar{q}) = V\left(\Phi^{-1}(\bar{q})\right)$ as

$$\bar{H}(\bar{x}) = \frac{1}{2}\bar{p}^{\top}\bar{p} + \bar{V}(\bar{q}) \tag{2.34}$$

The new form of the interconnection and damping matrices of the PH system are realized via the coordinate transformation (2.31), the mass-inertia matrix decomposition (2.33),

and the new Hamiltonian (2.34). The resulting [55] PH system is then given by

$$\begin{bmatrix} \dot{\bar{q}} \\ \dot{\bar{p}} \end{bmatrix} = \begin{bmatrix} 0_{n\times n} & \bar{T}(\bar{q})^{-\top} \\ -\bar{T}(\bar{q})^{-1} & \bar{J}_2(\bar{q},\bar{p}) - \bar{D}(\bar{q},\bar{p}) \end{bmatrix} \begin{bmatrix} \dfrac{\partial \bar{H}(\bar{q},\bar{p})}{\partial \bar{q}} \\ \dfrac{\partial \bar{H}(\bar{q},\bar{p})}{\partial \bar{p}} \end{bmatrix} + \begin{bmatrix} 0_{n\times n} \\ \bar{G}(\bar{q}) \end{bmatrix} v + \begin{bmatrix} 0_{n\times n} \\ \bar{B}(\bar{q}) \end{bmatrix} f_e \tag{2.35}$$

$$\bar{y} = \bar{G}(\bar{q})^{\top} \frac{\partial \bar{H}(\bar{q},\bar{p})}{\partial \bar{p}} \tag{2.36}$$

with a new input $v \in \mathbb{R}^n$, and where the skew-symmetric matrix $\bar{J}_2(\bar{q},\bar{p})$ takes the form

$$\bar{J}_2(\bar{q},\bar{p}) = \frac{\partial\left(\bar{T}(\bar{q})^{-1}\bar{p}\right)}{\partial \bar{q}} \bar{T}(\bar{q})^{-\top} - \bar{T}(\bar{q})^{-1} \frac{\partial\left(\bar{T}(\bar{q})^{-1}\bar{p}\right)}{\partial \bar{q}}^{\top} \tag{2.37}$$

with

$$(q,p) = \Phi^{-1}(\bar{q},\bar{p}) \tag{2.38}$$

together with the matrix $\bar{D}(\bar{q},\bar{p})$, and the input matrices $\bar{G}(\bar{q})$, and $\bar{B}(\bar{q})$, are described by

$$\bar{D}(\bar{q},\bar{p}) = \bar{T}(\bar{q})^{-1} D\left(\Phi^{-1}(\bar{q},\bar{p})\right) \bar{T}(\bar{q})^{-\top} \tag{2.39}$$

$$\bar{G}(\bar{q}) = \bar{T}(\bar{q})^{-1} G(\bar{q}) \tag{2.40}$$

$$\bar{B}(\bar{q}) = \bar{T}(\bar{q})^{-1} B(\bar{q}) \tag{2.41}$$

respectively. Via the transformation (2.31), we then obtain a class of mechanical systems with a constant (identity) mass inertia matrix in the Hamiltonian function as in (2.34), which equivalently describes the original system (2.2) with nonconstant mass-inertia matrix.

Example 2.2.3 Given a mass-inertia matrix $M(q) = diag(a,b)$ with a, and b as in (2.10) and (2.11), respectively, we compute a lower triangular matrix $T(q)$ as in (2.33), s.t.,

$$T(q) = \begin{bmatrix} \sqrt{a} & 0 \\ 0 & \sqrt{b} \end{bmatrix} \tag{2.42}$$

and based on $T(q)$, we can compute the matrices $\bar{J}_2(\bar{q},\bar{p})$, $\bar{D}(\bar{q},\bar{p})$, $\bar{G}(\bar{q})$, and $\bar{B}(\bar{q})$, as in (2.37), (2.39), (2.40), and (2.41), respectively. □

The coordinate transformation of this section is used in the rest of this thesis in order

to deal with non-constant mass-inertia matrices.

2.3 Hamilton-Jacobi inequality

In order to show the usefulness of some results on position control with force feedback presented later, we apply the Hamilton-Jacobi inequality useful for $\mathscr{L}_2$ gain analysis of nonlinear systems [55]. Towards this end we analyze the $\mathscr{L}_2$-gain of a closed-loop system w.r.t. an $\mathscr{L}_2$ disturbance δ.

Consider the time-invariant nonlinear system

$$\begin{aligned} \dot{\hat{x}} &= \mathscr{F}(\hat{x}) + \tilde{G}(\hat{x})\,\delta \\ \hat{y} &= h(\hat{x}) \end{aligned} \tag{2.43}$$

with states $\hat{x}$, input disturbance δ, output $\hat{y}$ and continuously differentiable vector functions $\mathscr{F}(\hat{x})$, $\tilde{G}(\hat{x})$ and $h(\hat{x})$. Let γ be a positive constant, then the $\mathscr{L}_2$-gain bound is found if for a γ there exists a continuously differentiable, positive semidefinite function $\mathscr{W}(\hat{x})$ that satisfies the Hamilton-Jacobi inequality (HJI)

$$\left(\frac{\partial \mathscr{W}(\hat{x})}{\partial \hat{x}}\right)^{\top} \mathscr{F}(\hat{x}) + \frac{1}{2}\frac{1}{\gamma^2}\left(\frac{\partial \mathscr{W}(\hat{x})}{\partial \hat{x}}\right)^{\top} \tilde{G}(\hat{x})\tilde{G}(\hat{x})^{\top}\frac{\partial \mathscr{W}(\hat{x})}{\partial \hat{x}} + \frac{1}{2}h(\hat{x})^{\top}h(\hat{x}) \leqslant 0 \tag{2.44}$$

for $\hat{x} \in \mathbb{R}^{\mathscr{N}}$. The system (2.43) is then finite-gain $\mathscr{L}_2$ stable and its gain is less than or equal to γ.

2.4 Stability analysis for constant external forces

Consider a class of PH system as described by (2.1). We now briefly recall the procedure of [29], i.e., we analyze the stability of the system (2.1) for a constant, and nonzero, input $w = \bar{u} \in \mathbb{R}^{\mathscr{M}}$, leading to a forced equilibrium $\check{x} \in \mathbb{R}^{\mathscr{N}}$. The forced equilibria $\check{x}$ are solutions of

$$[J(\check{x}) - R(\check{x})]\frac{\partial H}{\partial x}(\check{x}) + g(\check{x})\,\bar{u} = 0 \tag{2.45}$$

and if $[J(x) - R(x)]$ is invertible for every $x \in \mathbb{R}^{\mathscr{N}}$, the unique solution of (2.45) is $\dfrac{\partial H}{\partial x}(x) = \mathscr{K}(x)\,\bar{u}$ where

$$\mathscr{K}(x) = -[J(x) - R(x)]^{-1} g(x) \tag{2.46}$$

Based on (2.46), we define the matrices

$$J_s(x) \triangleq \mathscr{K}^\top(x) J(x) \mathscr{K}(x) \tag{2.47}$$

and

$$R_s(x) \triangleq \mathscr{K}^\top(x) R(x) \mathscr{K}(x) \tag{2.48}$$

which we use below to find the embedded Hamiltonian system. Clearly, $J_s(x)$ and $R_s(x)$ satisfy $J_s(x) = -J_s^\top(x)$, and $R_s(x) = R_s^\top(x) \geqslant 0$, respectively. Let us now consider the following PH system

$$\begin{bmatrix} \dot{x} \\ \dot{\zeta} \end{bmatrix} = [J_a(x) - R_a(x)] \begin{bmatrix} \dfrac{\partial H_a(x)}{\partial x} \\ \dfrac{\partial H_a(x)}{\partial \zeta} \end{bmatrix} \tag{2.49}$$

on the augmented state space $(x, \zeta) \in \mathbb{R}^{\mathscr{N}} \times \mathbb{R}^{\mathscr{M}}$, endowed with the structure matrices

$$J_a(x) = \begin{bmatrix} J(x) & J(x)\mathscr{K}(x) \\ -(J(x)\mathscr{K}(x))^\top & J_s(x) \end{bmatrix} \tag{2.50}$$

$$R_a(x) = \begin{bmatrix} R(x) & R(x)\mathscr{K}(x) \\ (R(x)\mathscr{K}(x))^\top & R_s(x) \end{bmatrix} \tag{2.51}$$

with $\mathscr{K}(x)$, $J_s(x)$, and $R_s(x)$ as in (2.46), (2.47), and (2.48), respectively, and with an augmented Hamiltonian

$$H_a(x, \zeta) \triangleq H(x) + H_s(\zeta), \quad H_s(\zeta) \triangleq -\bar{u}^\top \zeta \tag{2.52}$$

Theorem 2.4.1 *[29] Consider a class of PH system* (2.1) *with a constant input $w = \bar{u}$, and the matrix $[J(x) - R(x)]$ invertible for every $x \in \mathbb{R}^{\mathscr{N}}$. Define $\mathscr{K}(x)$ by* (2.46)*, and assume the functions $\mathscr{K}_{ij}$ to satisfy*

$$\frac{\partial \mathscr{K}_{ij}}{\partial x_k} = \frac{\partial \mathscr{K}_{kj}}{\partial x_i},\ i,k \in \bar{n} \triangleq \{1,\ldots,\mathscr{N}\},\ j \in \bar{m} \triangleq \{1,\ldots,\mathscr{M}\} \tag{2.53}$$

Also, assume that there exist locally smooth functions $\mathscr{C}_j : \mathbb{R}^{\mathscr{N}} \to \mathbb{R}$, called Casimirs [29], satisfying

$$\mathscr{K}_{ij}(x) = \frac{\partial \mathscr{C}_j}{\partial x_i}(x),\ j \in \bar{m},\ i \in \bar{n} \tag{2.54}$$

and $\zeta_j = \mathscr{C}_j(x) + c_j$, where $c_1,\ldots,c_{\mathscr{M}}$ depend on the initial conditions of $\zeta(t)$ in (2.49)*. Then the dynamics of* (2.1) *with input $u = \bar{u}$ is asymptotically stable at the equilibrium*

point $\check{x}$ fulfilling (2.45)*, and it can be alternatively represented by*

$$\dot{x} = [J(x) - R(x)] \frac{\partial H_r}{\partial x}(x) \tag{2.55}$$

where

$$H_r(x) \triangleq H(x) - \sum_{j=1}^{\mathscr{M}} \bar{u}_j \zeta_j \tag{2.56}$$

and H_r qualifies as a Lyapunov function for the forced dynamics (2.55)*.*

Remark 2.4.2 The $\mathscr{L}_2$-gain analysis of Section 2.3 gives a bound on the relation between an input δ and a output $\hat{y}$ as in (2.43) of a proposed closed-loop system for a $\mathscr{L}_2$-input disturbance δ. The $\mathscr{L}_2$-gain analysis differs from Theorem 2.4.1 in the sense that the $\mathscr{L}_2$-gain analysis is related to the output $\hat{y}$ while the analysis in this Section is for the case where the system is asymptotically stable, i.e., the system (2.35) has a new equilibrium point caused by a constant f_e.

2.5 Concluding remarks

Here we have recapitulated the important theorems, properties and examples for systems analysis used in this thesis. First, we provide a general background in the PH formalism, and we then equivalently describe the original PH system in a PH form, which has a constant mass-inertia matrix in the Hamiltonian. The transformation simplifies the control strategies developed in the following chapters. Furthermore, we present the Hamilton-Jacobi inequality as a tool to analyze a closed-loop system for disturbance attenuation properties. Finally, we provide the constructive procedure of [29] to modify the Hamiltonian function of a forced PH system in order to generate a Lyapunov function for nonzero equilibria.

Chapter 3
Position control via force feedback

The current technological advances continuously increase the demand for robots and intelligent systems that are fast, accurate and able to perform tasks under different circumstances. Sensing and using force measurements are examples of how reliability and performance of such robotic systems can be improved for almost all tasks in which a manipulator comes in contact with external objects [4, 21, 51]. Position control with force feedback for robotic systems has been thoroughly discussed in [4, 21, 38, 40, 53] and the references therein for the EL framework. In the EL framework, control design is based on selecting a suitable storage function that ensures position control. However, the desired storage function under the EL framework does not qualify as an energy function in any physical meaningful sense as stated in [4, 40].

In this chapter, we present position control strategies via force feedback for standard mechanical systems in the PH framework. The PH modeling framework of [30, 55] has received a considerable amount of interest in the last decade due to its insightful physical structure. Moreover, it is well known that a larger class of (nonlinear) physical systems can be described in the PH framework. The popularity of PH systems can be largely accredited to its application for analysis and control design of physical systems, as shown in [13, 17, 19, 42, 43, 55] and many others. Control laws in the PH framework are derived with a clear physical interpretation via direct shaping of the closed-loop energy, interconnection, and dissipation structure, see [13, 55]. In this chapter, we apply the PH modeling framework, since it allows extensions on the system coordinates, which facilitates the incorporation of force feedback in the input of the systems. Lastly, the presented control strategy preserves the PH structure, thus granting the aforementioned advantages to the closed-loop system.

The results presented in this chapter are based on [35], and extend the results presented in [31], [32] and [34]. In [31] a class of standard mechanical systems in the PH framework with force feedback and zero external forces has been introduced, for mechanical systems with a constant mass-inertia matrix. However, applying the results from [31] to systems with a nonconstant mass-inertia matrix is not trivial. In [34] preliminary results are presented for the more general class of mechanical systems with a nonconstant mass-inertia matrix. In this chapter, we combine these previous results into a PH framework for

position control with force feedback for standard mechanical systems.

The main contribution of this chapter is the introduction of an alternative position control strategy for mechanical systems that includes force feedback, in the PH framework. We present a control approach based on the *modeled* internal forces of a standard mechanical system; for this approach the system is extended with the internal forces into a PH system, which is then asymptotically stabilized. Furthermore, we analyze the disturbance attenuation properties to external forces, i.e., when the external forces are constant we show that the system has a constant steady-state error, and we apply an integral type control to compensate for position errors caused by these constant forces. We reformulate the stability analysis and analyze the robustness against external forces of the control strategy. The resulting controller has nicely tunable properties and interpretations, outperforming most of the existing force feedback control strategies. In addition, we develop a strategy assuming that we have force sensors that give measurements of the (real) total forces in the system, i.e., the internal plus external forces. Those measurements can be used to realize rejection of the external forces in the system.

The chapter is organized as follows. In Section 3.1, we realize a dynamic extension in order to include the modeled internal forces, while preserving the PH structure. In Section 3.2, we present the position control which uses feedback of the modeled forces. We also look at the disturbance attenuation properties when there are external forces, and we apply a type of integral control when the external forces are constant. For constant integral forces the system converges to a constant position different than the desired one, justifying the application of integral control. In Section 3.3, we assume that we have measurements of the total forces in the system, and use these measurements for control. Consequently, we show that we can realize rejection of the total forces in the system while preserving the PH structure. Finally, simulations are given in Section 3.4 to motivate our results for position control, and concluding remarks are provided in Section 3.5.

3.1 Force feedback via dynamic extension

In this Section, a force feedback strategy is introduced for a mechanical system in the PH framework. The force feedback is included to bring robustness and better tunable properties in the position control strategy. In comparison with force feedback in the EL framework [4, 51], the force feedback in the PH framework has nicely interpretable control strategies, as well as cleaner tuning opportunities that grant a better performance. The force feedback is achieved via a dynamic extension and a change of variables that introduces a new state for the PH system (2.35). The dynamics of the new state is realized such that it depends on the internal forces of the mechanical system. The internal forces are given by a set of kinetic, potential, and energy dissipating elements. The dynamic

extension is realized such that the extended system also has a PH structure. The present work is inspired by the results of [10, 12, 41].

Denote the internal forces on the system (2.2) by $f_{in}(q,p)$, i.e.,

$$f_{in}(q,p) = -\frac{\partial H(q,p)}{\partial q} - D(q,p)\frac{\partial H(q,p)}{\partial p} \tag{3.1}$$

with $H(q,p)$ as in (2.4). Define a new state $z \in \mathbb{R}^n$ with dynamics depending on the internal forces $f_{in}(q,p)$, such that,

$$\dot{z} = Y^\top T(q)^{-1} f_{in}(q,p) \tag{3.2}$$

with Y a constant matrix, to be defined later on. Consider now the coordinate transformation

$$\hat{p} = \bar{p} - Az \tag{3.3}$$

with $\bar{p}$ defined in (2.31), and with A a constant matrix that we use later to tune our controller. Furthermore, we can define for system (2.35) the control input

$$v = \bar{G}(\bar{q})^{-1} A\dot{z} + \bar{v} \tag{3.4}$$

where $\bar{v}$ is a new input, which realizes an extended PH system with states $\hat{p}$ and z, i.e.,

$$\begin{bmatrix} \dot{\bar{q}} \\ \dot{\hat{p}} \\ \dot{z} \end{bmatrix} = \underbrace{\begin{bmatrix} 0_{n\times n} & \bar{T}^{-\top} & \bar{T}^{-\top}Y \\ -\bar{T}^{-1} & \bar{J}_2 - \bar{D} & (\bar{J}_2 - \bar{D})Y \\ -Y^\top \bar{T}^{-1} & -Y^\top\left(\bar{J}_2^\top + \bar{D}\right) & -Y^\top\left(\bar{J}_2^\top + \bar{D}\right)Y \end{bmatrix}}_{\hat{J}(\bar{q},\hat{p},z) - \hat{R}(\bar{q},\hat{p},z)} \begin{bmatrix} \dfrac{\partial \hat{H}(\bar{q},\hat{p},z)}{\partial \bar{q}} \\ \dfrac{\partial \hat{H}(\bar{q},\hat{p},z)}{\partial \hat{p}} \\ \dfrac{\partial \hat{H}(\bar{q},\hat{p},z)}{\partial z} \end{bmatrix} + \begin{bmatrix} 0_{n\times n} \\ \bar{G}(\bar{q}) \\ 0_{n\times n} \end{bmatrix} \bar{v} + \begin{bmatrix} 0_{n\times n} \\ \bar{B}(\bar{q}) \\ 0_{n\times n} \end{bmatrix} f_e \tag{3.5}$$

$$\hat{y} = \bar{G}(\bar{q})^\top \frac{\partial \hat{H}(\bar{q},\hat{p},z)}{\partial \hat{p}} \tag{3.6}$$

with Hamiltonian

$$\hat{H}(\bar{q},\hat{p},z) = \frac{1}{2}\hat{p}^\top \hat{p} + \frac{1}{2} z^\top K_z^{-1} z + \bar{V}(\bar{q}) \tag{3.7}$$

where $K_z > 0$, and $Y = AK_z$. In (3.5) the arguments of $T(\bar{q})$, $\bar{J}_2(\bar{q},\hat{p})$, and $\bar{D}(\bar{q},\hat{p})$, are left out for notational simplicity.

Remark 3.1.1 Although in (3.5) the $\dot{z}$ dynamics are described in terms of $\bar{J}_2(\bar{q},\hat{p})$, $\bar{D}(\bar{q},\hat{p})$, and $\hat{H}(\bar{q},\hat{p},z)$, they are still the same as described by (3.2) with (3.1), in the new coordinates (2.31).

It can be verified that system (3.5) is PH, since

$$\hat{J}(\bar{q},\hat{p}) = \begin{bmatrix} 0_{n\times n} & \bar{T}(\bar{q})^{-\top} & \bar{T}(\bar{q})^{-\top}Y \\ -\bar{T}(\bar{q})^{-1} & \bar{J}_2(\bar{q},\hat{p}) & \bar{J}_2(\bar{q},\hat{p})Y \\ -Y^\top\bar{T}(\bar{q})^{-1} & -Y^\top\bar{J}_2(\bar{q},\hat{p})^\top & -Y^\top\bar{J}_2(\bar{q},\hat{p})^\top Y \end{bmatrix} \tag{3.8}$$

is skew-symmetric, while

$$\hat{R}(\bar{q},\hat{p}) = \begin{bmatrix} 0_{n\times n} & 0_{n\times n} & 0_{n\times n} \\ 0_{n\times n} & \bar{D}(\bar{q},\hat{p}) & \bar{D}(\bar{q},\hat{p})Y \\ 0_{n\times n} & Y^\top\bar{D}(\bar{q},\hat{p}) & Y^\top\bar{D}(\bar{q},\hat{p})Y \end{bmatrix} \tag{3.9}$$

can be shown to be positive-semidefinite via the Schur complement. Notice that by extending the dynamics of (2.35) with the internal forces $\dot{z}$ in the input (3.4), we include force-feedback and preserve the PH structure.

Remark 3.1.2 In [31] we present results for the case when the mass-inertia matrix is constant. The case for a constant M does not require the coordinate transformation (2.31), and system (3.5) is then described by $T = I$, $\bar{J}_2 = 0$, $\bar{D} = D$, $\bar{G} = G$, $\bar{B} = B$, $Y = M^{-1}AK_z$ and Hamiltonian

$$\hat{H}_c = \frac{1}{2}\hat{p}^\top M^{-1}\hat{p} + \frac{1}{2}z^\top K_z z + \bar{V}(\bar{q}) \tag{3.10}$$

instead of (3.7).

In this Section we have realized an extended mechanical system that includes force feedback and preserves the PH structure. In the next section we deal in more detail with position control and stability analysis.

3.2 Position control with modeled internal forces

In this Section, a position control strategy with force feedback is introduced. We feed back the modeled internal forces, and the resulting system preserves the PH structure. The control laws here presented are better tunable and more insightful solutions in comparison with the solutions given in the EL framework [4, 40].

3.2.1 Position control with zero external forces

In this Section, energy-shaping [25,40,55] and damping injection are combined with force feedback (of modeled forces) to realize position control.

Theorem 3.2.1 *Consider system* (3.5) *and assume* $f_e = 0$*. Then, the control input*

$$v = \bar{G}(\bar{q})^{-1}\left(\frac{\partial \bar{V}(\bar{q})}{\partial \bar{q}} - K_p(\bar{q} - q_d)\right) - C\hat{y} \tag{3.11}$$

with $K_p > 0$*,* $C > 0$*, and* q_d *being the desired constant position, asymptotically stabilizes the extended system* (3.5) *at* $(\bar{q}, \hat{p}, z) = (q_d, 0, 0)$*.*

Proof. This is a well known result, see [55], but we repeat the proof here for notational reasons and for ease of reading. The control input (3.11) applied to system (3.5) with $f_e = 0$ realizes the closed-loop system described by

$$\begin{bmatrix} \dot{\bar{q}} \\ \dot{\hat{p}} \\ \dot{z} \end{bmatrix} = \underbrace{\begin{bmatrix} 0_{n\times n} & \bar{T}^{-\top} & \bar{T}^{-\top}Y \\ -\bar{T}^{-1} & \bar{J}_2 - \bar{D} - \bar{G}C\bar{G}^\top & (\bar{J}_2 - \bar{D})Y \\ -Y^\top \bar{T}^{-1} & -Y^\top\left(\bar{J}_2^\top + \bar{D}\right) & -Y^\top\left(\bar{J}_2^\top + \bar{D}\right)Y \end{bmatrix} \begin{bmatrix} \frac{\partial \hat{H}_d}{\partial \bar{q}} \\ \frac{\partial \hat{H}_d}{\partial \hat{p}} \\ \frac{\partial \hat{H}_d}{\partial z} \end{bmatrix}}_{\mathscr{F}(\hat{x})} \tag{3.12}$$

$$\hat{y} = \bar{G}^\top \frac{\partial \hat{H}_d}{\partial \hat{p}} \tag{3.13}$$

with Hamiltonian

$$\hat{H}_d = \frac{1}{2}\hat{p}^\top \hat{p} + \frac{1}{2}(\bar{q} - q_d)^\top K_p(\bar{q} - q_d) + \frac{1}{2}z^\top K_z^{-1} z \tag{3.14}$$

where the arguments of $\hat{H}_d(\bar{q}, \hat{p}, z)$, $T(\bar{q})$, $\bar{J}_2(\bar{q}, \hat{p})$, $\bar{D}(\bar{q}, \hat{p})$, $\bar{G}(\bar{q})$, and $\bar{B}(\bar{q})$ are left out for simplicity. Take (3.14) as candidate Lyapunov function, which then gives

$$\dot{\hat{H}}_d = -\begin{bmatrix} \frac{\partial \hat{H}_d}{\partial \hat{p}} \\ \frac{\partial \hat{H}_d}{\partial z} \end{bmatrix}^\top \underbrace{\begin{bmatrix} \bar{D} + \bar{G}C\bar{G}^\top & -\bar{D}Y \\ -Y^\top \bar{D} & Y^\top \bar{D}Y \end{bmatrix}}_{K} \begin{bmatrix} \frac{\partial \hat{H}_d}{\partial \hat{p}} \\ \frac{\partial \hat{H}_d}{\partial z} \end{bmatrix} \tag{3.15}$$

Since $\bar{G}(\bar{q})$ is full rank and $C > 0$, via the Schur complement it can be shown that matrix K in (3.15) is positive definite. Subsequently, via LaSalle's invariance principle we can

prove that that the closed-loop system (3.12) is asymptotically stable in $\bar{q} = q_d$. ■

Substituting v in (3.4) by (3.11) then gives the total control input u for the original system (2.2), which in terms of the original coordinates (q, p) becomes

$$u = G(q)^{-1}T(q)\left(A\dot{z} + \frac{\partial V(q)}{\partial q} - K_p(q - q_d)\right) - CG(q)^{\top}\left(M(q)^{-1}p - T(q)^{-\top}Az\right) \tag{3.16}$$

with $\dot{z}$ as in (3.1). The above results correspond to the case when the external forces on the system are zero, i.e., $f_e = 0$. In the next subsection we look more in detail at the case when $f_e \neq 0$.

3.2.2 Disturbance attenuation properties

We now show the advantages of the proposed extended system with force feedback for disturbance attenuation to unknown external forces. The closed-loop PH system (3.12) with force feedback is asymptotically stable in the desired position q_d when it has zero forces exerted from the environment, i.e., $f_e = 0$. To look at the effect of f_e being different from zero, we analyze the $\mathscr{L}_2$-gain w.r.t. an $\mathscr{L}_2$ disturbance f_e, [55]. It follows that

Theorem 3.2.2 *Consider a closed-loop system* (3.12)*, an $\mathscr{L}_2$ disturbance f_e, and a constant matrix C with $\lambda_c \in \mathbb{R}^n$ being its set of eigenvalues. We then obtain a disturbance attenuation of f_e when the following conditions hold:*

$$\Gamma_1(q,p) = -D(q,p) + G(q)^{\top}\left(-C + \frac{1}{2}I_{n\times n}\right)G(q) + \frac{1}{2}\frac{1}{\gamma^2}B(q)B(q)^{\top}\frac{1}{2} \leqslant 0 \tag{3.17}$$

$$\begin{aligned}\Gamma_2(q) = {} & AT(q)^{-\top}G(q)^{\top}\left(-C + \frac{1}{2}I_{n\times n}\right)G(q)^{\top}T(q)^{-1}A \\ & + \frac{1}{2}\frac{1}{\gamma^2}AT(q)^{-1}B(q)B(q)^{\top}T(q)^{-\top}A \leqslant 0\end{aligned} \tag{3.18}$$

$$\Gamma_3(q) = \frac{1}{2}\frac{1}{\gamma^2}AT(q)^{-1}B(q)B(q)^{\top} \geqslant 0 \tag{3.19}$$

$$\lambda_c \geqslant \frac{1}{2} \tag{3.20}$$

with γ being a positive constant.

Proof. Consider the closed-loop system (3.12), but with $f_e \neq 0$, i.e,

$$\begin{bmatrix} \dot{\bar{q}} \\ \dot{\hat{p}} \\ \dot{z} \end{bmatrix} = \begin{bmatrix} 0_{n\times n} & \bar{T}^{-\top} & \bar{T}^{-\top}Y \\ -\bar{T}^{-1} & \bar{J}_2 - \bar{D} - \bar{G}C\bar{G}^\top & (\bar{J}_2 - \bar{D})Y \\ -Y^\top \bar{T}^{-1} & -Y^\top\left(\bar{J}_2^\top + \bar{D}\right) & -Y^\top\left(\bar{J}_2^\top + \bar{D}\right)Y \end{bmatrix} \begin{bmatrix} \frac{\partial \hat{H}_d}{\partial \bar{q}} \\ \frac{\partial \hat{H}_d}{\partial \hat{p}} \\ \frac{\partial \hat{H}_d}{\partial z} \end{bmatrix} + \begin{bmatrix} 0 \\ \bar{B} \\ 0 \end{bmatrix} f_e \tag{3.21}$$

$$\hat{y} = \bar{G}^\top \frac{\partial \hat{H}_d}{\partial \hat{p}} \tag{3.22}$$

where the arguments of $\hat{H}_d(\bar{q},\hat{p},z)$, $T(\bar{q})$, $\bar{J}_2(\bar{q},\hat{p})$, $\bar{D}(\bar{q},\hat{p})$, $\bar{G}(\bar{q})$, and $\bar{B}(\bar{q})$ are left out for notational simplicity. We analyze the HJI (2.44) first for system (3.21) with $\mathscr{W}(\hat{x}) = \hat{H}_d(\hat{x})$ to determine if this could be a solution. Given $\delta = f_e$ we obtain

$$-\left(\frac{\partial \hat{H}_d}{\partial \hat{x}}\right)^\top \tilde{R} \frac{\partial \hat{H}_d}{\partial \hat{x}} + \frac{1}{2}\frac{1}{\gamma^2}\left(\frac{\partial \hat{H}_d}{\partial \hat{p}}\right)^\top \bar{B}\bar{B}^\top \frac{\partial \hat{H}_d}{\partial \hat{p}} + \frac{1}{2}\hat{y}^\top \hat{y} \leqslant 0 \tag{3.23}$$

with $\hat{x} = (\bar{q},\hat{p},z)$, and

$$\tilde{R}(\hat{x}) = \begin{bmatrix} 0_{n\times n} & 0_{n\times n} & 0_{n\times n} \\ 0_{n\times n} & \bar{D}(\bar{q},\hat{p}) + \bar{G}(\bar{q})C\bar{G}(\bar{q})^\top & \bar{D}(\bar{q},\bar{p})Y \\ 0_{n\times n} & Y^\top \bar{D}(\bar{q},\hat{p}) & Y^\top \bar{D}(\bar{q},\hat{p})Y \end{bmatrix} \tag{3.24}$$

We compute the left hand-side term of the Hamilton-Jacobi inequality (2.44) based on the function $W(\hat{x}) = \hat{H}_d(\hat{x})$ with $\hat{H}_d(\hat{x})$ as in (3.14), and on the function $\mathscr{F}(\hat{x})$ of the closed-loop (3.12). Consequently, we obtain

$$\begin{aligned} \frac{\partial \mathscr{W}}{\partial \hat{x}}^\top \mathscr{F} &= \begin{bmatrix} \frac{\partial \hat{H}_d}{\partial \bar{q}} \\ \frac{\partial \hat{H}_d}{\partial \hat{p}} \\ \frac{\partial \hat{H}_d}{\partial z} \end{bmatrix}^\top \begin{bmatrix} 0 & \bar{T}^{-\top} & \bar{T}^{-\top}Y \\ -\bar{T}^{-1} & \bar{J}_2 - \bar{D} - \bar{G}C\bar{G}^\top & (\bar{J}_2 - \bar{D})Y \\ -Y^\top \bar{T}^{-1} & -Y^\top\left(\bar{J}_2^\top + \bar{D}\right) & -Y^\top\left(\bar{J}_2^\top + \bar{D}\right)Y \end{bmatrix} \begin{bmatrix} \frac{\partial \hat{H}_d}{\partial \bar{q}} \\ \frac{\partial \hat{H}_d}{\partial \hat{p}} \\ \frac{\partial \hat{H}_d}{\partial z} \end{bmatrix} \\ &= -\frac{\partial \hat{H}_d}{\partial \hat{p}}^\top \left(\bar{D} + \bar{G}C\bar{G}^\top\right)\frac{\partial \hat{H}_d}{\partial \hat{p}} - \frac{\partial \hat{H}_d}{\partial \hat{p}}^\top \bar{D}Y\frac{\partial \hat{H}_d}{\partial z} - \frac{\partial \hat{H}_d}{\partial z}^\top Y^\top \bar{D}\frac{\partial \hat{H}_d}{\partial \hat{p}} \\ &= -\left(\frac{\partial \hat{H}_d}{\partial \hat{p}} + Y\frac{\partial \hat{H}_d}{\partial z}\right)^\top \bar{D}\left(\frac{\partial \hat{H}_d}{\partial \hat{p}} + Y\frac{\partial \hat{H}_d}{\partial z}\right) - \frac{\partial \hat{H}_d}{\partial \hat{p}}^\top \bar{G}C\bar{G}^\top \frac{\partial \hat{H}_d}{\partial \hat{p}} \end{aligned} \tag{3.25}$$

where we have left out the arguments of $\mathscr{W}(\hat{x})$, $\mathscr{F}(\hat{x})$, $\bar{G}(\bar{q})$, $\bar{T}(\bar{q})$, $\hat{H}_d(\bar{q},\hat{p},z)$, and $\bar{D}(\bar{q},\hat{p})$, for notational simplicity. From $\hat{y}$ as in (3.13), $\hat{p}$ as in (3.3), $\bar{D}(\bar{q},\hat{p})$ as in (2.39), $\hat{x}=(\bar{q},\hat{p},z)$, and $Y=AK_z$, we rewrite (3.25) as

$$\begin{aligned}
\frac{\partial \mathscr{W}(\hat{x})}{\partial \hat{x}}^{\top} \mathscr{F}(\hat{x}) &= -\left(\hat{p}+YK_z^{-1}z\right)^{\top} \bar{D}(\bar{q},\hat{p})\left(\hat{p}+YK_z^{-1}z\right) - \hat{y}^{\top}C\hat{y} \\
&= -\left(\bar{p}-Az+AK_zK_z^{-1}z\right)^{\top} \bar{D}(\bar{q},\hat{p})\left(\bar{p}-Az+AK_zK_z^{-1}z\right) - \hat{y}^{\top}C\hat{y} \\
&= -\bar{p}^{\top}\bar{D}(\bar{q},\hat{p})\,\bar{p} - \hat{y}^{\top}C\hat{y} \\
&= -p^{\top}\bar{T}(\bar{q})^{-\top}\bar{T}(\bar{q})^{-1} D\left(\Phi^{-1}(\bar{q},\hat{p})\right)\bar{T}(\bar{q})^{-\top}\bar{T}(\bar{q})^{-1}p - \hat{y}^{\top}C\hat{y} \\
&= -p^{\top}M(q)^{-1}D(q,p)M(q)^{-1}p - \hat{y}^{\top}C\hat{y} \\
&= -\frac{\partial H(q,p)}{\partial p}^{\top} D(q,p)\frac{\partial H(q,p)}{\partial p} - \hat{y}^{\top}C\hat{y}
\end{aligned} \tag{3.26}$$

Based on a input matrix $\tilde{G}(\bar{q})$ defined as

$$\tilde{G}(\hat{x}) = \begin{bmatrix} 0_{n\times n} \\ \bar{B}(\bar{q}) \\ 0_{n\times n} \end{bmatrix} \tag{3.27}$$

with $\bar{B}(\bar{q})$ as in (2.41), we compute the second term of the left hand-side of the Hamilton-Jacobi inequality (2.44) as

$$\begin{aligned}
\tilde{Z}(\hat{x}) &= \frac{1}{2}\frac{1}{\gamma^2}\left(\frac{\partial \mathscr{W}(\hat{x})}{\partial \hat{x}}\right)^{\top} \tilde{G}(\hat{x})\tilde{G}^{\top}(\hat{x})\frac{\partial \mathscr{W}(\hat{x})}{\partial \hat{x}} \\
&= \frac{1}{2}\frac{1}{\gamma^2}\begin{bmatrix} \dfrac{\partial \hat{H}_d(\bar{q},\hat{p},z))}{\partial \bar{q}} \\ \dfrac{\partial \hat{H}_d(\bar{q},\hat{p},z))}{\partial \hat{p}} \\ \dfrac{\partial \hat{H}_d(\bar{q},\hat{p},z))}{\partial z} \end{bmatrix}^{\top} \begin{bmatrix} 0_{n\times n} \\ \bar{B}(\bar{q}) \\ 0_{n\times n} \end{bmatrix}\begin{bmatrix} 0_{n\times n} \\ \bar{B}(\bar{q}) \\ 0_{n\times n} \end{bmatrix}^{\top} \begin{bmatrix} \dfrac{\partial \hat{H}_d(\bar{q},\hat{p},z))}{\partial \bar{q}} \\ \dfrac{\partial \hat{H}_d(\bar{q},\hat{p},z))}{\partial \hat{p}} \\ \dfrac{\partial \hat{H}_d(\bar{q},\hat{p},z))}{\partial z} \end{bmatrix} \\
&= \frac{1}{2}\frac{1}{\gamma^2}\frac{\partial \hat{H}_d(\bar{q},\hat{p},z))}{\partial \hat{p}}^{\top} \bar{B}(\bar{q})\bar{B}(\bar{q})^{\top}\frac{\partial \hat{H}_d(\bar{q},\hat{p},z))}{\partial \hat{p}} \\
&= \frac{1}{2}\frac{1}{\gamma^2}\hat{p}^{\top}\bar{B}(\bar{q})\bar{B}(\bar{q})^{\top}\hat{p}
\end{aligned} \tag{3.28}$$

and we now substitute $\hat{p}$ as in (3.3) in (3.28). Hence, we obtain

$$\begin{aligned}\tilde{Z}(\hat{x}) &= \frac{1}{2}\frac{1}{\gamma^2}(\bar{p}-Az)^\top \bar{B}(\bar{q})\bar{B}(\bar{q})^\top(\bar{p}-Az) \\ &= \frac{1}{2}\frac{1}{\gamma^2}\left(\Upsilon(q,p)^\top\Upsilon(q,p)-\Upsilon(q,p)^\top Z - Z^\top\Upsilon(q,p)+Z^\top Z\right)\end{aligned} \tag{3.29}$$

where

$$Z(\hat{x}) = B(q)^\top T(q)^{-\top} Az \tag{3.30}$$

$$\Upsilon(q,p) = B(q)^\top \frac{\partial H(q,p)}{\partial p} \tag{3.31}$$

Finally, based on the output $\hat{y} = h(\hat{x})$, and the results (3.26), and (3.29), the Hamilton-Jacobi inequality (2.44) is rewritten as

$$-\frac{\partial H(q,p)}{\partial p}^\top D(q,p)\frac{\partial H(q,p)}{\partial p} - \hat{y}^\top C\hat{y} + \tilde{Z} + \frac{1}{2}\hat{y}^\top\hat{y} \leqslant 0 \tag{3.32}$$

with $\tilde{Z}(\hat{x})$ as in (3.29). We now rewrite $\hat{y}$ as

$$\hat{y} = \bar{G}(\bar{q})^\top \frac{\partial \hat{H}(\hat{x})}{\partial \hat{p}} = \bar{G}(\bar{q})^\top \hat{p} = G(q)^\top \frac{\partial H(q,p)}{\partial p} - G(q)^\top T(q)^{-1} A\hat{z} \tag{3.33}$$

and we replace (3.33) in (3.32). Lastly, we have that

$$\begin{bmatrix} \dfrac{\partial H(q,p)}{\partial p} \\ z \end{bmatrix}^\top \underbrace{\begin{bmatrix} \Gamma_1(q,p) & -\Gamma_3(q)^\top \\ -\Gamma_3(q) & \Gamma_2(q) \end{bmatrix}}_{P_{HJi}} \begin{bmatrix} \dfrac{\partial H(q,p)}{\partial p} \\ z \end{bmatrix} \leqslant 0 \tag{3.34}$$

The inequality (3.34) is satisfied when matrix $P_{HJi} \leqslant 0$, which is the case if matrix C of the control law (3.11) is designed such that the inequalities (3.17), (3.18), (3.19), and (3.20) hold, with $\lambda_c \in \mathbb{R}^n$ being the set of eigenvalues of C. ■

Remark 3.2.3 The Hamilton-Jacobi inequality (3.34) based on the closed-loop system (3.21) holds when the set of eigenvalues of the matrix C are chosen such that the conditions for $\Gamma_1(q,p)$, $\Gamma_2(q)$, $\Gamma_3(q)$, and λ_c are satisfied. It follows that increasing the eigenvalues of C allows for a smaller γ, and thus a smaller $\mathscr{L}_2$-gain bound. Increasing the eigenvalues of C corresponds to increasing the damping injection.

In the next subsection we look at the special case when f_e is unknown, but constant.

3.2.3 Stability analysis for constant external forces

Here, we propose an equivalent description of the system (3.12), with a different Hamiltonian function which can be used as a Lyapunov function for constant nonzero external forces, i.e., $f_e \in \mathbb{R}^n/\{0\}$. We embed the extended system into a larger PH system for which a series of Casimir functions are constructed. The analysis is based on the results of [29].

We proceed to apply the results in Section 2.4 to the closed-loop system (3.12) with constant nonzero external forces as input, i.e., $\bar{u} = f_e$. We compute matrix $\mathscr{K}(\hat{x})$ as in (2.46), and obtain

$$\mathscr{K}(\hat{x}) = -\begin{bmatrix} \bar{T}\left(-\bar{J}_2+\bar{D}\right)\bar{T}^\top & 0_{n\times n} & \bar{T}Y^{-\top} \\ 0_{n\times n} & \left(\bar{G}C\bar{G}^\top\right)^{-1} & -\left(\bar{G}C\bar{G}^\top\right)^{-1}Y^{-\top} \\ -Y^{-1}\bar{T}^\top & -Y^{-1}\left(\bar{G}C\bar{G}^\top\right)^{-1} & Y^{-1}\left(\bar{G}C\bar{G}^\top\right)^{-1}Y^{-\top} \end{bmatrix}\begin{bmatrix} 0_{n\times n} \\ \bar{B}(\bar{q}) \\ 0_{n\times n} \end{bmatrix} \tag{3.35}$$

Here, we left out the arguments of $\bar{T}(\bar{q})$, $\bar{G}(\bar{q})$, $\bar{J}_2(\bar{q},\hat{p})$, and $\bar{D}(\bar{q},\hat{p})$ for notational simplicity. If $\hat{G}(\bar{q}) = \left(\bar{G}(\bar{q})C\bar{G}(\bar{q})^\top\right)^{-1}$, then (3.35) leads to

$$\mathscr{K}(\hat{x}) = \begin{bmatrix} 0_{n\times n} \\ -\hat{G}(\bar{q})\bar{B}(\bar{q}) \\ Y^{-1}\hat{G}(\bar{q})\bar{B}(\bar{q}) \end{bmatrix} \tag{3.36}$$

Following the results of Theorem 2.4.1, we assume that the local smooth functions $\mathscr{C}_j(x)$, $j \in n$, satisfy the integrability condition (2.53). It follows that the dynamics of (3.21) can be alternatively represented by (2.55) where $H_r(\hat{x})$ is

$$\begin{aligned} H_r(\hat{x}) &= \hat{H}_d(\hat{x}) - \sum_{j=1}^{n} f_{e_j}\mathscr{C}_j(x) \\ &= \hat{H}_d(\hat{x}) + f_e^\top \hat{G}(\bar{q})\,\hat{p} - f_e^\top Y^{-1}\hat{G}(\bar{q})\,z + f_e^\top c \end{aligned} \tag{3.37}$$

where $\hat{x} = (\bar{q},\hat{p},z)$, and $\hat{H}_d(\hat{x})$ as in (3.14). If we choose the constant $c = -K_f f_e \in \mathbb{R}^n$, with $K_f > 0$. Then, we can rewrite (3.37) as

$$H_r(\hat{x}) = \frac{1}{2}\begin{bmatrix} \bar{q}-q_d \\ \hat{p} \\ z \\ f_e \end{bmatrix}^\top \underbrace{\begin{bmatrix} K_p & 0_{n\times n} & 0_{n\times n} & 0_{n\times n} \\ 0_{n\times n} & I_{n\times n} & 0_{n\times n} & \bar{B}^\top\hat{G}^\top \\ 0_{n\times n} & 0_{n\times n} & K_z^{-1} & -\bar{B}^\top\hat{G}^\top Y^{-\top} \\ 0_{n\times n} & \hat{G}\bar{B} & -Y^{-1}\hat{G}\bar{B} & K_f \end{bmatrix}}_{\hat{P}(\bar{q})}\begin{bmatrix} \bar{q}-q_d \\ \hat{p} \\ z \\ f_e \end{bmatrix} > 0 \tag{3.38}$$

where we have left out the arguments of $\bar{G}(\bar{q})$ and $\bar{B}(\bar{q})$ for notational simplicity. Since $\bar{G}(\bar{q})$ and $\bar{B}(\bar{q})$ are full rank, and $C > 0$, via the Schur complement it can be shown that matrix $\hat{P}(\bar{q})$ in (3.38) is positive definite, and then the inequality (3.38) holds. Furthermore, via Theorem 2.4.1, we have that

$$\dot{H}_r(\hat{x}) = -\frac{\partial H_r(\hat{x})}{\partial \hat{x}}^\top \tilde{R}(\hat{x}) \frac{\partial H_r(\hat{x})}{\partial \hat{x}} \leqslant 0 \tag{3.39}$$

and thus $H_r(\hat{x})$ qualifies as a Lyapunov function for the forced dynamics (2.55). Then, $\dot{H}_r(\hat{x}) \leqslant 0$, and given that $\frac{\partial \hat{H}_d(\hat{x})}{\partial \hat{p}} = \hat{p}$, and $\frac{\partial \hat{H}_d(\hat{x})}{\partial z} = K_z^{-1} z$, we know that $\hat{p}$, $z \to 0$ as $t \to \infty$. Given the dynamics of system (2.55), $\dot{\hat{p}} = \dot{z} = 0$, it can be verified that the largest invariant set for $\dot{H}_r(\hat{x}) = 0$ equals $\left(\bar{q} - q_d - K_p^{-1}\bar{B}(\bar{q}) f_e, \hat{p}, z\right) = (0,0,0)$. LaSalle's invariance then implies that the system is asymptotically stable in

$$\bar{q} = q_d + K_p^{-1}\bar{B}(\bar{q}) f_e \tag{3.40}$$

Remark 3.2.4 The $\mathscr{L}_2$-gain analysis of Section 3.2.2 gives a bound on the relation between input $\delta = f_e$ and the output $\hat{y}$ of the closed-loop system (3.21) for an $\mathscr{L}_2$-input disturbance δ. The $\mathscr{L}_2$-gain analysis differs from the results of Section 3.2.3 in the sense that the $\mathscr{L}_2$-gain analysis evaluates a bound on the output $\hat{y}$ in relation to the size of the input δ, while the analysis in Section 3.2.3 is for the case where the system is asymptotically stable, i.e. $\hat{y} \to 0$, with a new equilibrium point caused by a constant f_e. Notice that the $\mathscr{L}_2$-gain bound is related to the amount of damping injected, while the new equilibrium point (steady-state position) is related to the stiffness parameter K_p.

3.2.4 Integral position control

The analysis in the previous section shows that, under the assumption that f_e is constant, we can expect a constant steady-state error in the position of system (3.21). Furthermore, the analysis also justifies the application of integral control, since integral control compensates for constant steady-state errors. The main contribution of this section is to realize a type of integral position control for a class of standard mechanical systems with dissipation in the PH framework. For the extended system (3.5), with f_e constant, we propose a coordinate transformation to include the position error in the new output. By having the position error in the passive output, we can interconnect the closed-loop with an integrator in a passivity-preserving way, i.e., preserving the PH structure. The results of this section are inspired by the works of [10, 12, 41].

Theorem 3.2.5 *Consider system* (3.5) *and assume* $f_e \neq 0$ *and constant. Define the integrator state* ξ *with dynamics*

$$\dot{\xi} = -\bar{B}(\bar{q})^\top (\hat{p} + K_i(\bar{q} - q_d)) \tag{3.41}$$

q_d *the desired constant position and* K_i *a constant matrix. Then, the control input*

$$v = \bar{G}(\bar{q})^{-1} \left(\frac{\partial \bar{V}(\bar{q})}{\partial \bar{q}} - K_p(\bar{q} - q_d) - K_i \dot{\bar{q}} - \bar{B}(\bar{q})\xi \right) - C\bar{G}(\bar{q})^\top (\hat{p} + K_i(\bar{q} - q_d)) \tag{3.42}$$

with $K_p > 0$*, and* $C > 0$*, asymptotically stabilizes the extended system* (3.5) *at* $(\bar{q}, \hat{p}, z) = (q_d, 0, 0)$*, i.e., zero steady-state error.*

Proof. We use the results of [12]. Consider first the coordinate transformation

$$\tilde{p} = \hat{p} + K_i(\bar{q} - q_d) \tag{3.43}$$

with a constant matrix K_i, which then implies that

$$\dot{\tilde{p}} = \dot{\hat{p}} + K_i \dot{\bar{q}} \tag{3.44}$$

since q_d is constant. The control input (3.42) with integrator dynamics (3.41) then realizes the closed-loop system

$$\begin{bmatrix} \dot{\bar{q}} \\ \dot{\tilde{p}} \\ \dot{z} \\ \dot{\xi} \end{bmatrix} = \begin{bmatrix} -K_i K_p^{-1} & \bar{T}^{-\top} & \bar{T}^{-\top} Y & 0 \\ -\bar{T}^{-1} & \bar{J}_2 - \bar{D} - \bar{G}C\bar{G}^\top & (\bar{J}_2 - \bar{D})Y & \bar{B} \\ -Y^\top \bar{T}^{-1} & -Y^\top \left(\bar{J}_2^\top + \bar{D}\right) & -Y^\top \left(\bar{J}_2^\top + \bar{D}\right) Y & 0 \\ 0 & -\bar{B}^\top & 0 & 0 \end{bmatrix} \begin{bmatrix} \frac{\partial \hat{H}_i}{\partial \bar{q}} \\ \frac{\partial \hat{H}_i}{\partial \tilde{p}} \\ \frac{\partial \hat{H}_i}{\partial z} \\ \frac{\partial \hat{H}_i}{\partial \xi} \end{bmatrix} \tag{3.45}$$

$$\tilde{y} = \bar{G}^\top \frac{\partial \hat{H}_i}{\partial \tilde{p}} \tag{3.46}$$

with Hamiltonian

$$\hat{H}_i = \frac{1}{2}\tilde{p}^\top \tilde{p} + \frac{1}{2}(\bar{q} - q_d)^\top K_p (\bar{q} - q_d) + \frac{1}{2} z^\top K_z^{-1} z + \frac{1}{2}(f_e - \xi)^\top (f_e - \xi) \tag{3.47}$$

where the arguments of $\hat{H}_i(\bar{q},\tilde{p},z,\xi)$, $T(\bar{q})$, $\bar{J}_2(\bar{q},\tilde{p})$, $\bar{D}(\bar{q},\tilde{p})$, $\bar{G}(\bar{q})$, and $\bar{B}(\bar{q})$ are left out for notational simplicity. Furthermore, notice that

$$\tilde{y} = \bar{G}(\bar{q})^\top \tilde{p} = \bar{G}(\bar{q})^\top (\hat{p} + K_i(\bar{q} - q_d)) \tag{3.48}$$

Take (3.47) as candidate Lyapunov function, which then gives

$$\dot{\hat{H}}_i = -\begin{bmatrix} \frac{\partial \hat{H}_i}{\partial \bar{q}} \\ \frac{\partial \hat{H}_i}{\partial \tilde{p}} \\ \frac{\partial \hat{H}_i}{\partial z} \end{bmatrix}^\top \underbrace{\begin{bmatrix} K_i K_p^{-1} & 0 & 0 \\ 0 & \bar{D}(\bar{q},\tilde{p}) + \bar{G}(\bar{q}) C \bar{G}(\bar{q})^\top & -\bar{D}(\bar{q},\tilde{p}) Y \\ 0 & -Y^\top \bar{D}(\bar{q},\tilde{p})^\top & Y^\top \bar{D}(\bar{q},\tilde{p})^\top Y \end{bmatrix}}_{U(\bar{q},\tilde{p})} \begin{bmatrix} \frac{\partial \hat{H}_i}{\partial \bar{q}} \\ \frac{\partial \hat{H}_i}{\partial \tilde{p}} \\ \frac{\partial \hat{H}_i}{\partial z} \end{bmatrix} \tag{3.49}$$

Since $\bar{G}(\bar{q})$ is full rank, $\bar{D}(\bar{q},\tilde{p}) \geqslant 0$, $K_i > 0$, $K_p > 0$, $C > 0$, $K_z > 0$, $Y = AK_z$ and A being a constant matrix, via the Schur complement it can be shown that matrix $U(\bar{q},\tilde{p}) \geqslant 0$, and thus $\dot{\hat{H}}_i \leqslant 0$ holds. Define the set $\mathbb{O} = \left\{ (\bar{q},\tilde{p},z,\xi) \mid \dot{\hat{H}}_i(\bar{q},\tilde{p},z,\xi) = 0 \right\}$. Given that $\dot{\hat{H}}_i(q_d,0,0,\xi) = 0$, $\forall \xi$, hence ξ is free. Assume $\xi - f_e = c_1 \neq 0$ constant with $c_1 \in \mathbb{R}^n$, thus $\dot{\xi} = 0$. Then, the dynamics $\dot{\tilde{p}}$ is

$$\dot{\tilde{p}} = \bar{B}(q_d)(c_1 + f_e) \neq 0 \tag{3.50}$$

Since (3.50) is constant, then $\tilde{p}$ will change over time, and hence a contradiction. Thus the largest invariant set in $\mathbb{O}$ is $\mathbb{M} = \{q_d, 0, 0, f_e\}$. Via LaSalle's invariance principle we conclude that the system (3.45) is asymptotically stable at $(\bar{q},\tilde{p},z,\xi) = (q_d,0,0,f_e)$, which means that the constant disturbance is compensated by ξ, i.e., $\xi \to f_e$. ■

Substituting v in (3.4) by (3.42) then gives the total control input u for the original system (2.2), which in terms of the original coordinates q, p becomes

$$\begin{aligned} u =& G(q)^{-1} T(q) \left(A\dot{z} + \frac{\partial V(q)}{\partial q} - K_p(q - q_d) - K_i \dot{q} \right) - G(q)^{-1} B(q) \xi \\ & - C G(q)^\top \left(M(q)^{-1} p - T(q)^{-\top} A z - T(q)^{-\top} K_i (q - q_d) \right) \end{aligned} \tag{3.51}$$

with $\dot{z}$ as in (3.2).

3.3 Position control with measured forces

In the previous section we have presented a position control strategy that exploits feedback of the modeled internal forces. In other words, the forces used for feedback are based on

the dynamical model and the measured positions and velocities. In this Section we assume we have force sensors, which provide the (real) total forces working on the system. Then, we feed back the readings of the force sensors in the input of the system (2.35). Notice that the measured total forces f in the system can be described by

$$f(q,p) = f_{in}(q,p) + B(q) f_e \tag{3.52}$$

with $f_{in}(q,p)$ as in (3.1). In the previous section we used (3.1) to model and compute the internal forces for feedback control. We can still use (3.1) to describe the internal forces, while adding the external forces to model the total forces in the system. Let $\bar{f}(\bar{q},\bar{p})$ be the total forces multiplied by the matrix $T(q)$ in (2.31), i.e.,

$$\bar{f}\left(\Phi^{-1}(\bar{q},\bar{p})\right) = \bar{f}(q,p) = T(q)^{-1} f(q,p) \tag{3.53}$$

Consider now system (2.35). Notice that in terms of the coordinates $\bar{q},\bar{p}$ that $\bar{f}(\bar{q},\bar{p})$ is then described by

$$\bar{f}(\bar{q},\bar{p}) = -\bar{T}(\bar{q})^{-1} \frac{\partial \bar{H}(\bar{q},\bar{p})}{\partial \bar{q}} + \left(\bar{J}_2(\bar{q},\bar{p}) - \bar{D}(\bar{q},\bar{p})\right) \frac{\partial \bar{H}(\bar{q},\bar{p})}{\partial \bar{p}} + \bar{B}(\bar{q}) f_e \tag{3.54}$$

Define for system (2.35) the input

$$v = -\bar{G}(\bar{q})^{-1} \bar{f}(\bar{q},\bar{p}) + \bar{v} \tag{3.55}$$

with $\bar{v}$ being a new input vector, which then changes (2.35) into the PH system

$$\begin{bmatrix} \dot{\bar{q}} \\ \dot{\bar{p}} \end{bmatrix} = \begin{bmatrix} 0 & \bar{T}(\bar{q})^{-\top} \\ -\bar{T}(\bar{q})^{-1} & 0 \end{bmatrix} \begin{bmatrix} \dfrac{\partial \bar{H}_\tau(\bar{q},\bar{p})}{\partial \bar{q}} \\ \dfrac{\partial \bar{H}_\tau(\bar{q},\bar{p})}{\partial \bar{p}} \end{bmatrix} + \begin{bmatrix} 0 \\ \bar{G}(\bar{q}) \end{bmatrix} \bar{v} \tag{3.56}$$

$$\bar{y} = \bar{G}(\bar{q})^{\top} \frac{\partial \bar{H}_\tau(\bar{q},\bar{p})}{\partial \bar{p}} \tag{3.57}$$

with Hamiltonian

$$\bar{H}_\tau(\bar{q},\bar{p}) = \frac{1}{2} \bar{p}^{\top} \bar{p} \tag{3.58}$$

We then obtain (2.35), with all forces canceled. We can thus control the system without the problems described in Section 3.2.2. Notice that we need to describe (2.2) in the equivalent form (2.35) in order to realize force rejection and preserve the PH structure. In the original coordinates (q,p) the control input (3.55) is given by

$$u = -G(q)^{-1} f(q,p) + \bar{v} \tag{3.59}$$

with $f(q,p)$ as in (3.52). Notice that the advantage here is that we can apply control methods without having to worry about the external forces (disturbances) and internal forces (potential forces and friction). However, equation (3.59) implies that there is no tuning possible in the application of force feedback. In Section 3.2.2 the disturbances are not rejected, however, we have the possibility to tune the force feedback with the matrix A.

In the next section we illustrate, via simulation of the system (2.7), the results of Sections 3.2, and 3.3 for obtaining asymptotic stability in a desired position.

3.4 Simulation results: Two-DOF shoulder system

We have determined the parameters of the two-DOF shoulder system of Figure 2.1a as $\mathscr{I}_i = \{0.013, 1.692\}$, $F_{c_i} = \{0.005, 0.025\}$, $F_{s_i} = \{1.905, 2.257\}$, $F_{v_i} = \{4.119, 4.973\}$, and $\dot{q}_{s_i} = \{0.167, 0.170\}$. We have a link length of $l_c = 0.249m$, $m = 3.9kg$; matrices $A = diag\,(0.5, 0.7)$, $K_z = diag\,(2,2)$, $K_p = diag\,(15,15)$, and $C = diag\,(10,10)$; an initial position $q(0) = (0,0)$, and desired position $q_d = (1, 0.5)\,rad$. We obtain the desired position $q_d = (1,0.5)^\top$ from an initial position $q\,(0) = (0,0)^\top$ at $t = t_1 \geqslant 3s$ with the control law (3.11). Then, we apply a constant nonzero force, i.e., $f_e = (3,-3)^\top$, at $t_2 =\geqslant 5s$, to the closed-loop system (3.12). Results are shown in Figure 3.1. The new position is $q = K_p^{-1} f_e + q_d = (1.2, 0.3)^\top$ (blue line) which corresponds to a different equilibrium point as in (3.40). The results presented here validate the fact that the PH system (3.12) remains stable with a constant nonzero input $\bar{u} = f_e$. Furthermore, we want to recover the desired position by applying the integral control law (3.51) to the PH system (3.12) at $t_3 \geqslant 10s$, with a matrix $K_i = diag\,(1, 0.5)$. We observe how the system is stabilized again at the desired position q_d at $t \geqslant 11s$ without a steady state error.

Finally, we apply a constant nonzero force, i.e., $f_e = (3,-3)^\top$, to the two-DOF inputs of the to the system (2.7), and apply (3.59) at $t = t_2 \geqslant 5s$, which includes the measured forces of the sensors. Then, the equilibrium is achieved immediately, independent of f_e as seen in Figure 3.1.

3.5 Concluding remarks

This chapter is devoted to the development of strategies for position control via force feedback for mechanical systems in the PH framework. Our main driver is to propose an alternative solution to the classical methods for position control problem via force feedback in the EL formalism, since PH modeling and control strategies provide better tuning. We have shown that via coordinate transformations force feedback can be realized while preserving the PH structure. In the first part of the chapter we have presented a control

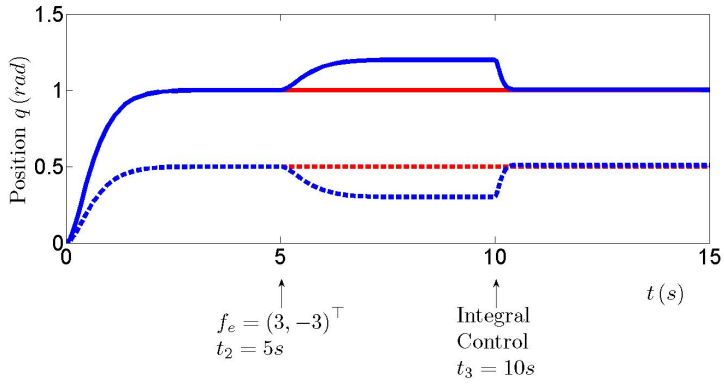

Figure 3.1: Position control via force feedback (blue line) with $f_e = col\,(0,0)^\top$ at $t \leqslant 5s$. Integral control (blue line) with $f_e = col\,(3,-3)^\top$ at $t \geqslant 10s$. Total force rejection (red line) at $t \geqslant 0$. Initial conditions $(q\,(0)\,,p\,(0))^\top = (0,0,0,0)^\top$. Solid line q_1. Dashed line q_2.

strategy based on modeled internal forces of a mechanical system with a nonconstant mass-inertia matrix. When the external forces acting on the aforementioned system are constant nonzero, we have shown via Theorem 3.2.5 that a type of integral control compensates for position errors. The integral control design strategy follows naturally from the PH structure, which gives us a clear physical interpretation. In the second part, we assume that force sensors are present to give measurements of the (real) total forces in the system, i.e., the internal and external forces. Lastly, we show that we can use the force measurements to realize rejection of the total forces in the system.

Chapter 4

Force control and an impedance grasping strategy

In order to perform complex robotic tasks involving the interaction of an end-effector and an external environment, strategies with dexterous manipulation are required. This chapter addresses two such control strategies, i.e., force and impedance grasping, for mechanical systems. These strategies involve a noncontact to contact transition. Force control is suitable when a task requires extensive contact with the environment such as griding, deburring, and polishing [21, 53]. Impedance grasping control is necessary for constraining objects with an end-effector (gripper) [23, 51, 53].

We assume here that total measurements of the internal and external forces acting on the system are available; we will use those measurements to design controllers for the system (2.2). The presented control strategies asymptotically stabilize a mechanical system to a desired constant force. We obtain a desired constant force by introducing a set of change of variables in the dynamics of the PH system in (2.2). Preserving the PH structure while implementing force control and impedance grasping is not straightforward task. Accordingly, we follow a control design strategy inspired by the position control via force feedback of our previous chapter. In Section 3.3 we have assumed a system with force sensors that provide the (real) total forces working on the system. Exploiting the fact that many new systems are equipped with such force sensors, we then consider our force control strategy as a continuation of the PH system with total force rejection in (3.56). The force control strategy requires the desired force to be directly fed back in the input of the system in (2.2). We then asymptotically stabilize the extended PH system with a type of integral action over the constant desired force. Impedance grasping control strategy is achieved via a *virtual spring* with a variable *rest-length*. The grasping force that is exerted by the virtual spring leads to a (co)dissipation term in the impedance grasping controller, which is needed to obtain a smoother noncontact to contact transition. We finally asymptotically stabilize the PH system to a desired grasping force under a zero-state detectability assumption. Both strategies show a zero steady-state error.

This chapter is organized as follows. In Section 4.1 we obtain an asymptotically stable desired contact force via the proposed force control strategy. Experimental results based on our force control strategy are given in Section 4.1.2. Furthermore, in Section 4.2 we introduce an impedance grasping strategy based on passivity-based control, and on a type

of modified integral control action in order to avoid steady-state errors. This integral control depends on a variable rest-length of the virtual spring interpretation. In Section 4.2 we show how a change of variables yields a PH framework without losing its structure in order to realize the modified integral control. We then obtain an asymptotically stable desired grasping force. Simulations and experimental results are given in Section 4.2.2 and 4.2.3, respectively, to motivate our results for impedance grasping control. Lastly, Section 4.3 provides concluding remarks.

4.1 Force control

The present section introduces an extension of the PH system in (2.2) to obtain force control instead of position control in presence of external forces in the input of the system. The preliminary results of Section 3.1 are based on an extension on the system coordinates in order to include a type of integral action over the force sensor measurements. Furthermore, in Section 3.3, the total forces of system (2.2) are modeled as in (3.52). The control input (3.55) realizes a system in (3.56) with all forces canceled.

The main result of this section relies on a new strategy for force control for a class of standard mechanical systems in the PH framework. The force control in robot manipulators is thoroughly discussed in [4,21,38,51,53] in the EL framework. Contrary to EL strategies, the aim of this Section to propose a dynamic extension for a class of mechanical system based on the PH formulation [13,30] for force control purposes. The main strategy adopted here is to realize a force control law in the equivalent PH system (2.35) via a change of variables. We provide the Lyapunov candidate function of a closed-loop system in order to prove asymptotic stability to the desired constant force. The main advantage of the PH formulation with force feedback modeling is that we obtain a robust force control strategy with a clear physical interpretation.

4.1.1 Control law

In this section, a dynamic extension and a change of variables are introduced for the PH system (2.35) as it was done in Sections 3.1 and 3.3. The dynamics of the new state depend on the sum of the internal and external forces acting on the mechanical system. We assume here, as in Section 3.3, that we have force sensors working on the system, which feed back readings to the input of the system (2.35). The internal forces are given by a set of kinetic, potential, and energy dissipation elements. The external forces are exerted from the environment and are modeled as generalized force vectors, which are preliminarily presented in the PH framework (2.2). Particularly, the dynamic extension is included via a change of variables in order to preserve the structure of the transformed PH

system.

As previously stated, assume that the system (2.2) has force sensors that measure the internal and external forces given by $f(q,p)$ as in (3.52). We propose a state $\hat{z}$ as the dynamic extension of the PH system. The extension is realized in order to include the internal and the external forces while preserving the PH structure. We define then the dynamics of the new state as a function of the forces, i.e.,

$$\dot{\hat{z}} = -Y^{\top} T(q)^{-1} f(q,p) = -Y^{\top} \bar{f}(\bar{q},\bar{p}) \tag{4.1}$$

with a constant gain matrix Y over the internal and external forces, where the symmetric part of Y is positive definite, i.e., $Y + Y^{\top} > 0$, $Y \in \mathbb{R}^{n\times n}$, and $T(q)$ is the matrix decomposition as in (2.33), and $\bar{f}(\bar{q},\bar{p})$ in (3.54) being the internal and external forces of (2.2). The Y-matrix is defined later on.

Given now the sensor readings and the dynamic extension $\hat{z}$ as in (4.1), we have constant desired forces

$$f_d = Y^{\top} T(q_z)\, \dot{z}_d \tag{4.2}$$

where $f_d \in \mathbb{R}^n$, with $\dot{z}_d \in \mathbb{R}^n$ a constant that depends on the desired forces (4.2), and the position vector $q_z \in \mathbb{R}^n$ given by the solution of the equation

$$-Y^{\top} T(q_z)^{-1} \left(\frac{\partial \bar{H}(q_z)}{\partial q_z} + \bar{B}(q_z) f_e \right) - \dot{z}_d = 0 \tag{4.3}$$

and with a new state $\hat{z}$ as in (4.1), and a function of a type of integral action over the desired forces, i.e., z_d being two times differentiable, we define a new adapted momenta as

$$\hat{p} = \bar{p} - A(\hat{z} - z_d) \tag{4.4}$$

with a constant diagonal matrix $A > 0$, $A \in \mathbb{R}^{n\times n}$. We then feed back the force by application of the input

$$v = \bar{G}(\bar{q})^{-1} A \left(\dot{\hat{z}} - \dot{\hat{z}}_d \right) + \omega_z \tag{4.5}$$

into the system (2.35), and a new input ω_z, which then realizes a new PH system under the condition that $\bar{G}(\bar{q})$, as in (2.40), is invertible.

Based on the forced mechanical systems in the PH framework (2.35), we now want to attain asymptotic stability over a type of integral action considering the desired force vector f_d as in (4.2). We assume that there are lower and upper bounds such that the

matrices $\bar{T}(\bar{q})$, $\tilde{D}(\bar{q},\hat{p})$, and $\bar{G}(\bar{q})$ satisfy,

$$\rho_1 I_{n\times n} \leqslant \quad \bar{T}(\bar{q}) \quad \leqslant \rho_2 I_{n\times n} \tag{4.6}$$

$$d_1 I_{n\times n} \leqslant \quad \tilde{D}(\bar{q},\hat{p}) \quad \leqslant d_2 I_{n\times n} \tag{4.7}$$

$$g_1 I_{n\times n} \leqslant \quad \bar{G}(\bar{q}) \quad \leqslant g_2 I_{n\times n} \tag{4.8}$$

with ρ_1, ρ_2, d_1, d_2, g_1, and g_2 being positive constants. Based on the conditions (4.6), (4.7), and (4.8), we define a force control law for the system (2.35), i.e.,

Theorem 4.1.1 *Consider the PH system* (2.35)*, and the assumptions* (4.6)*,* (4.7)*, and* (4.8)*. Let $\hat{z}$ be the dynamics of the new state as in* (4.1) *with nonzero external forces f_e, and an adapted momenta $\hat{p}$ as in* (4.4)*. Then, the control input*

$$v = \bar{G}(\bar{q})^{-1}\left(\bar{T}(\bar{q})^{-1}\frac{\partial \bar{H}(\bar{q},\bar{p})}{\partial \bar{q}} + A\left(\dot{\hat{z}} - \dot{z}_d\right)\right) - C\hat{p} \tag{4.9}$$

with $C > 0$, $Y = AK_z$, s.t.,

$$c_1 I_{n\times n} \leqslant \quad C \quad \leqslant c_2 I_{n\times n} \tag{4.10}$$

$$\kappa_1 I_{n\times n} \leqslant \quad K_z \quad \leqslant \kappa_2 I_{n\times n} \tag{4.11}$$

$$\gamma_1 I_{n\times n} \leqslant \quad Y \quad \leqslant \gamma_2 I_{n\times n} \tag{4.12}$$

with c_1, c_2, κ_1, κ_2, γ_1, and γ_2 being positive constants, and

$$\sqrt{\frac{1}{\kappa_1}} > \varepsilon \tag{4.13}$$

$$\frac{\gamma_2 d_2 \kappa_1}{\gamma_1 d_1 \sqrt{\kappa_2}} > \varepsilon \tag{4.14}$$

$$\frac{\gamma_1}{\gamma_2}\sqrt{\frac{\left(d_1 + c_1 g_1^2\right) d_1 \kappa_2}{\left(d_2 + c_2 g_2^2\right) d_2 \kappa_1}} > \varepsilon \tag{4.15}$$

for a sufficiently small ε, asymptotically stabilizes the system (2.35) *with zero steady-state error at $\bar{x} = \bar{x}^* = (q_z, 0)$. Hence $\dot{\hat{z}} = \dot{z}_d$ and, based on* (4.2)*, $f(q,p) = f_d$.*

Proof. Consider first the the change of variables (4.4) with a constant matrix A, which implies

$$\dot{\hat{p}} = \dot{\bar{p}} - A\left(\dot{\hat{z}} - \dot{z}_d\right) \tag{4.16}$$

with z_d being two times differentiable. The control input (4.9) then realizes the closed-loop

$$\begin{bmatrix} \dot{\bar{q}} \\ \dot{\hat{p}} \\ \dot{\hat{z}} \end{bmatrix} = \begin{bmatrix} 0_{n\times n} & \bar{T}^{-\top} & \bar{T}^{-\top}Y \\ -\bar{T}^{-1} & \bar{J}_2 - \bar{D} - \bar{G}C\bar{G}^{\top} & (\bar{J}_2 - \bar{D})Y \\ -Y^{\top}\bar{T}^{-1} & -Y^{\top}\left(\bar{J}_2^{\top} + \bar{D}\right) & -Y^{\top}\left(\bar{J}_2^{\top} + \bar{D}\right)Y \end{bmatrix} \begin{bmatrix} \dfrac{\partial H_z(\bar{q},\hat{p},\hat{z})}{\partial \bar{q}} \\ \dfrac{\partial H_z(\bar{q},\hat{p},\hat{z})}{\partial \hat{p}} \\ \dfrac{\partial H_z(\bar{q},\hat{p},\hat{z})}{\partial \hat{z}} \end{bmatrix} \tag{4.17}$$

$$\hat{y} = \bar{G}^{\top}\frac{\partial H_z(\bar{q},\hat{p},\hat{z})}{\partial \hat{p}} \tag{4.18}$$

with Hamiltonian

$$H_z(\bar{q},\hat{p},\hat{z}) = \frac{1}{2}\hat{p}^{\top}\hat{p} + \frac{1}{2}(\hat{z}-z_d)^{\top}K_z^{-1}(\hat{z}-z_d) \tag{4.19}$$

where the arguments of $T(\bar{q})$, $\bar{J}_2(\bar{q},\hat{p})$, $\bar{D}(\bar{q},\hat{p})$, and $\bar{G}(\bar{q})$ are left out for simplicity. Denote now by $\underline{\lambda}(\mathscr{S}) = s_1$, and $\overline{\lambda}(\mathscr{S}) = s_2$, the upper, and lower bounds of the norm of a positive semidefinite matrix $\mathscr{S}$, i.e.,

$$s_1 I_{n\times n} \leqslant \mathscr{S} \leqslant s_2 I_{n\times n} \tag{4.20}$$

Consider then a candidate Lyapunov function

$$\mathscr{H}(\bar{q},\hat{p},\hat{z}) = H_z(\bar{q},\hat{p},\hat{z}) + \varepsilon\hat{p}^{\top}(\hat{z}-z_d) \tag{4.21}$$

with a constant $\varepsilon > 0$. Notice that the function (4.21) can be written in a matrix form as

$$\mathscr{H}(\bar{q},\hat{p},\hat{z}) = \frac{1}{2}\begin{bmatrix} \hat{z}-z_d \\ \hat{p} \end{bmatrix}^{\top}\begin{bmatrix} K_z^{-1} & \varepsilon \\ \varepsilon & I \end{bmatrix}\begin{bmatrix} \hat{z}-z_d \\ \hat{p} \end{bmatrix} \tag{4.22}$$

Then, the function (4.22) satisfies

$$\mathscr{H}(\bar{q},\hat{p},\hat{z}) \geqslant \frac{1}{2}\begin{bmatrix} \|\hat{z}-z_d\| \\ \|\hat{p}\| \end{bmatrix}^{\top}\underbrace{\begin{bmatrix} \underline{\lambda}\left(K_z^{-1}\right) & \varepsilon \\ \varepsilon & I \end{bmatrix}}_{P_1}\begin{bmatrix} \|\hat{z}-z_d\| \\ \|\hat{p}\| \end{bmatrix} \tag{4.23}$$

and from the definition of K_z, the matrix P_1 is positive definite if $\underline{\lambda}\left(K_z^{-1}\right) - \varepsilon^2 > 0$, i.e.,

$$\sqrt{\frac{1}{\kappa_1}} > \varepsilon \tag{4.24}$$

We now want to prove that $\dot{\mathscr{H}}(\bar{q},\hat{p},\hat{z}) \leqslant 0$, along the trajectories of (2.35). First, we write $\dot{\mathscr{H}}(\bar{q},\hat{p},\hat{z})$ as

$$\dot{\mathscr{H}}(\bar{q},\hat{p},\hat{z}) = \frac{\partial \mathscr{H}(\bar{q},\hat{p},\hat{z})}{\partial \bar{q}}^{\top} \dot{\bar{q}} + \frac{\partial \mathscr{H}(\bar{q},\hat{p},\hat{z})}{\partial \hat{p}}^{\top} \dot{\hat{p}} + \frac{\partial \mathscr{H}(\bar{q},\hat{p},\hat{z})}{\partial \hat{z}}^{\top} \dot{\hat{z}} \tag{4.25}$$

Since $\dfrac{\partial H_z(\bar{q},\hat{p},\hat{z})}{\partial \bar{q}} = 0$, $\dfrac{\partial H_z(\bar{q},\hat{p},\hat{z})}{\partial \hat{p}} = \hat{p}$, and $K_z \dfrac{\partial H_z(\bar{q},\hat{p},\hat{z})}{\partial \hat{z}} = (\hat{z} - z_d)$, and based on the closed-loop dynamics (4.17), we replace $\dot{\bar{q}}$, $\dot{\hat{p}}$, and $\dot{\hat{z}}$, in (4.25), i.e.,

$$\begin{aligned}
\dot{\mathscr{H}} = &- \left(\frac{\partial H_z(\bar{q},\hat{p},\hat{z})}{\partial \hat{p}} + Y \frac{\partial H_z(\bar{q},\hat{p},\hat{z})}{\partial \hat{z}} \right)^{\top} \bar{D}(\bar{q},\hat{p}) \left(\frac{\partial H_z(\bar{q},\hat{p},\hat{z})}{\partial \hat{p}} + Y \frac{\partial H_z(\bar{q},\hat{p},\hat{z})}{\partial \hat{z}} \right) \\
&- \varepsilon \left(Y \frac{\partial H_z(\bar{q},\hat{p},\hat{z})}{\partial \hat{p}} + K_z \frac{\partial H_z(\bar{q},\hat{p},\hat{z})}{\partial \hat{z}} \right)^{\top} \bar{D}(\bar{q},\hat{p}) \left(\frac{\partial H_z(\bar{q},\hat{p},\hat{z})}{\partial \hat{p}} + Y \frac{\partial H_z(\bar{q},\hat{p},\hat{z})}{\partial \hat{z}} \right) \\
&- \left(\frac{\partial H_z(\bar{q},\hat{p},\hat{z})}{\partial \hat{p}} + \varepsilon K_z \frac{\partial H_z(\bar{q},\hat{p},\hat{z})}{\partial \hat{z}} \right)^{\top} \bar{G}(\bar{q}) C \bar{G}(\bar{q})^{\top} \frac{\partial H_z(\bar{q},\hat{p},\hat{z})}{\partial \hat{p}}
\end{aligned} \tag{4.26}$$

We have left out the arguments of $\dot{\mathscr{H}}(\bar{q},\hat{p},\hat{z})$ for notational simplicity. From (4.26), we obtain

$$\begin{aligned}
\dot{\mathscr{H}}(\bar{q},\hat{p},\hat{z}) = &- \varepsilon \begin{bmatrix} \dfrac{\partial H_z(\bar{q},\hat{p},\hat{z})}{\partial \hat{p}} \\ \dfrac{\partial H_z(\bar{q},\hat{p},\hat{z})}{\partial \hat{z}} \end{bmatrix}^{\top} \begin{bmatrix} \tilde{S}(\bar{q},\hat{p}) & \dfrac{1}{\varepsilon}\tilde{S}(\bar{q},\hat{p})^{\top} \\ \dfrac{1}{\varepsilon}\tilde{S}(\bar{q},\hat{p}) & K_z \tilde{S}(\bar{q},\hat{p})^{\top} \end{bmatrix} \begin{bmatrix} \dfrac{\partial H_z(\bar{q},\hat{p},\hat{z})}{\partial \hat{p}} \\ \dfrac{\partial H_z(\bar{q},\hat{p},\hat{z})}{\partial \hat{z}} \end{bmatrix} \\
&- \varepsilon \begin{bmatrix} \dfrac{\partial H_z(\bar{q},\hat{p},\hat{z})}{\partial \hat{p}} \\ \dfrac{\partial H_z(\bar{q},\hat{p},\hat{z})}{\partial \hat{z}} \end{bmatrix}^{\top} \begin{bmatrix} \dfrac{1}{\varepsilon}\tilde{G}(\bar{q},\hat{p}) & \tilde{S}(\bar{q},\hat{p}) Y \\ K_z \tilde{G}(\bar{q},\hat{p}) & \dfrac{1}{\varepsilon}\tilde{S}(\bar{q},\hat{p}) Y \end{bmatrix} \begin{bmatrix} \dfrac{\partial H_z(\bar{q},\hat{p},\hat{z})}{\partial \hat{p}} \\ \dfrac{\partial H_z(\bar{q},\hat{p},\hat{z})}{\partial \hat{z}} \end{bmatrix}
\end{aligned} \tag{4.27}$$

where $\tilde{S}(\bar{q},\hat{p})$, and $\tilde{G}(\bar{q},\hat{p})$ are

$$\tilde{S}(\bar{q},\hat{p}) = Y^{\top} \bar{D}(\bar{q},\hat{p}) \tag{4.28}$$

$$\tilde{G}(\bar{q},\hat{p}) = \bar{D}(\bar{q},\hat{p}) + \bar{G}(\bar{q}) C \bar{G}(\bar{q})^{\top} \tag{4.29}$$

respectively. We now write (4.27) in terms of the vectors $\hat{p}$, and $\hat{z}-z_d$, as

$$\begin{aligned}\dot{\mathscr{H}}(\bar{q},\hat{p},\hat{z}) = &-\varepsilon \begin{bmatrix} \hat{p} \\ \hat{z}-z_d \end{bmatrix}^\top \begin{bmatrix} \tilde{S} & \frac{1}{\varepsilon}\tilde{S}^\top K_z^{-1} \\ \frac{1}{\varepsilon}K_z^{-1}\tilde{S} & \tilde{S}^\top K_z^{-1} \end{bmatrix} \begin{bmatrix} \hat{p} \\ \hat{z}-z_d \end{bmatrix} \\ &-\varepsilon \begin{bmatrix} \hat{p} \\ \hat{z}-z_d \end{bmatrix}^\top \begin{bmatrix} \frac{1}{\varepsilon}\tilde{G}(\bar{q},\hat{p}) & \tilde{S}YK_z^{-1} \\ \tilde{G}(\bar{q},\hat{p}) & \frac{1}{\varepsilon}K_z^{-1}\tilde{S}YK_z^{-1} \end{bmatrix} \begin{bmatrix} \hat{p} \\ \hat{z}-z_d \end{bmatrix}\end{aligned} \tag{4.30}$$

and furthermore the dynamics of $\dot{\mathscr{H}}(\bar{q},\hat{p},\hat{z})$ as in (4.27) satisfy

$$\begin{aligned}\dot{\mathscr{H}}(\bar{q},\hat{p},\hat{z}) \leqslant &-\varepsilon \begin{bmatrix} \|\hat{p}\| \\ \|\hat{z}-z_d\| \end{bmatrix}^\top \underbrace{\begin{bmatrix} \underline{\lambda}\left(\tilde{S}\right) & \frac{1}{\varepsilon}\overline{\lambda}\left(\tilde{S}^\top K_z^{-1}\right) \\ \frac{1}{\varepsilon}\overline{\lambda}\left(K_z^{-1}\tilde{S}\right) & \underline{\lambda}\left(\tilde{S}^\top K_z^{-1}\right) \end{bmatrix}}_{Q_1(\bar{q},\hat{p})} \begin{bmatrix} \|\hat{p}\| \\ \|\hat{z}-z_d\| \end{bmatrix} \\ &-\varepsilon \begin{bmatrix} \|\hat{p}\| \\ \|\hat{z}-z_d\| \end{bmatrix}^\top \underbrace{\begin{bmatrix} \frac{1}{\varepsilon}\underline{\lambda}\left(\tilde{G}(\bar{q},\hat{p})\right) & \overline{\lambda}\left(\tilde{S}YK_z^{-1}\right) \\ \overline{\lambda}\left(\tilde{G}(\bar{q},\hat{p})\right) & \frac{1}{\varepsilon}\underline{\lambda}\left(K_z^{-1}\tilde{S}YK_z^{-1}\right) \end{bmatrix}}_{Q_2(\bar{q},\hat{p})} \begin{bmatrix} \|\hat{p}\| \\ \|\hat{z}-z_d\| \end{bmatrix}\end{aligned} \tag{4.31}$$

where we left out the arguments of $\tilde{S}(\bar{q},\hat{p})$ for notational simplicity, and with $Q_1(\bar{q},\hat{p})$, and $Q_2(\bar{q},\hat{p})$ matrices with the diagonal elements depending on the lower bounds and the off-diagonal elements depending on the upper bounds, which give conditions for ε such that (4.31) is negative definite. The previous results in

$$\frac{\overline{\lambda}\left(\tilde{S}(\bar{q},\hat{p})\right)\overline{\lambda}\left(\tilde{S}(\bar{q},\hat{p})^\top K_z^{-1}\right)}{\underline{\lambda}\left(K_z^{-1}\tilde{S}(\bar{q},\hat{p})\right)\underline{\lambda}\left(\tilde{S}(\bar{q},\hat{p})^\top K_z^{-1}\right)} > \varepsilon^2 \tag{4.32}$$

$$\frac{\underline{\lambda}\left(\tilde{G}(\bar{q},\hat{p})\right)\underline{\lambda}\left(\tilde{S}(\bar{q},\hat{p})YK_z^{-1}\right)}{\overline{\lambda}\left(\tilde{G}(\bar{q},\hat{p})\right)\overline{\lambda}\left(K_z^{-1}\tilde{S}(\bar{q},\hat{p})YK_z^{-1}\right)} > \varepsilon^2 \tag{4.33}$$

and replacing $\tilde{S}(\bar{q},\hat{p})$ as in (4.28), and $\tilde{G}(\bar{q},\hat{p})$ as in (4.29), in (4.32), and (4.33), we

obtain

$$\frac{\overline{\lambda}\left(Y^{\top}\bar{D}\left(\bar{q},\hat{p}\right)\right)\overline{\lambda}\left(\bar{D}\left(\bar{q},\hat{p}\right)YK_z^{-1}\right)}{\underline{\lambda}\left(K_z^{-1}Y^{\top}\bar{D}\left(\bar{q},\hat{p}\right)\right)\underline{\lambda}\left(\bar{D}\left(\bar{q},\hat{p}\right)YK_z^{-1}\right)} > \varepsilon^2 \tag{4.34}$$

$$\frac{\underline{\lambda}\left(\bar{D}\left(\bar{q},\hat{p}\right)+\bar{G}\left(\bar{q}\right)C\bar{G}\left(\bar{q}\right)^{\top}\right)\underline{\lambda}\left(Y^{\top}\bar{D}\left(\bar{q},\hat{p}\right)YK_z^{-1}\right)}{\overline{\lambda}\left(\bar{D}\left(\bar{q},\hat{p}\right)+\bar{G}\left(\bar{q}\right)C\bar{G}\left(\bar{q}\right)^{\top}\right)\overline{\lambda}\left(Y^{\top}\bar{D}\left(\bar{q},\hat{p}\right)YK_z^{-1}\right)} > \varepsilon^2 \tag{4.35}$$

respectively. The evaluation of the inequalities (4.34), and (4.35) based on the assumptions (4.6), (4.7), (4.8), (4.10), (4.11), and (4.12) results in the conditions

$$\frac{\gamma_2 d_2 \kappa_1}{\gamma_1 d_1 \sqrt{\kappa_2}} > \varepsilon \tag{4.36}$$

$$\frac{\gamma_1}{\gamma_2}\sqrt{\frac{\left(d_1+c_1 g_1^2\right)d_1\kappa_2}{\left(d_2+c_2 g_2^2\right)d_2\kappa_1}} > \varepsilon \tag{4.37}$$

respectively. Furthermore, for a sufficiently small ε, the inequalities (4.24), (4.36), and (4.37), hold. Then, (4.21) is positive semidefinite and its time derivative along the trajectories of (4.17) is negative semidefinite, i.e., $\mathscr{H}\left(\bar{q},\hat{p},\hat{z}\right) \geqslant 0$ and $\mathscr{H}\left(\bar{q},\hat{p},\hat{z}\right) \leqslant 0$ both hold. Lyapunov stability theory along with LaSalle's Invariance Principle, implies asymptotic stability of system (4.17) in (2.35) in $(\bar{q},\hat{p},\hat{z}) = (q_z,0,z_d)$, which means that the system (2.35) is asymptotically stable in $(\bar{q},\bar{p}) = (q_z,0)$, and hence a type of integral control over the desired force vector f_d as in (4.2) is finally realized. ■

We have realized a force control law for the PH system in (2.35). We know that from the proposed integrator dynamics (4.1), we obtain structure preservation in the closed-loop system (4.17), which is useful for force control. Furthermore, we have realized an asymptotically stable closed-loop system in (4.17) via the control law (4.9). In Section 4.1.2, we motivate the present PH approach with an example of a class of standard mechanical systems with a constant mass-inertia matrix.

4.1.2 Experimental results

For experimental purposes, we have grasped a *squash ball*, which represents a nonzero external force vector with the gripper of the PERA (Figure 2.1b). The model representation is given by the Example 2.1.3 in the PH framework.

We have a mass $m_g = 0.5kg$, a rest-length $c_g = 0.30rad$ (gripper open) with stiffness coefficients being $k_{g_i} = \{0.21, 0.06\} Nm/rad$, a damping coefficient $d_g = 0.10$ with $\alpha_f = 0.001$; constants $A = 1$, $K_p = 1$, and $C = 5$; an initial position $q(0) = 0.30rad$, and a desired force of $f_d = 3.50N$. Based on these parameters, we can see how the conditions

(4.13), (4.14), and (4.15) are given for a small ε. We apply the control law (4.9) to the PH system (2.35). Figure 4.1 shows the experimental results. The noncontact to contact transition occurs at $t_1 \geqslant 0.50s$. We obtain the desired force f_d at $t \geqslant 1.50s$ with a zero steady-state error.

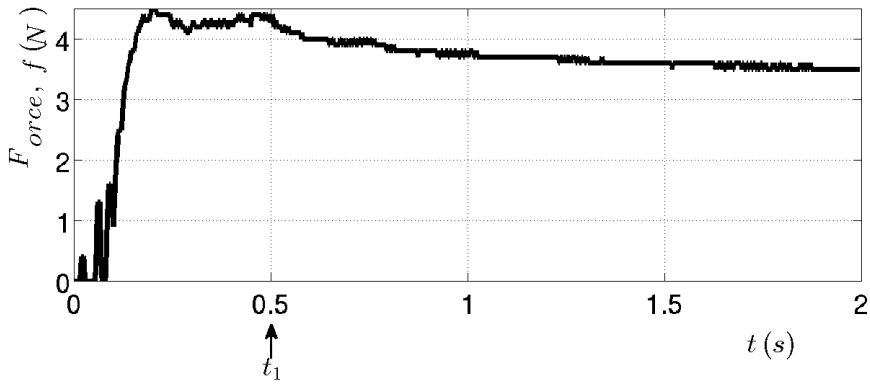

Figure 4.1: Force control of the tips of the gripper of the PERA via the control law (4.9). Initial conditions $(q(0), p(0))^\top = (3,0)^\top$.

4.2 An impedance grasping strategy

A conventional impedance control strategy in the EL framework is a feedback transformation such that the closed-loop system is equivalent to a mechanical system with the desired behavior, [4, 23, 53]. More recently in the EL framework, the concept of contact estimation in order to improve the classical results of impedance control is introduced in [5], and kinematic redundancy for safe interaction of the robot system with the environment is given by [46]. Passivity-based control in the EL framework is based on selecting a storage energy function which ensures the desired behavior between the environment and the mechanical system. However, the desired storage function does not qualify as an energy function in any meaningful physical sense as stated in [4, 40]. In contrast to the EL framework, the PH framework has cleaner tuning opportunities, resulting in a better performance [13, 19, 55]. An impedance grasping control approach in the PH framework is given by [54]. This approach introduces the concept of *virtual object*, and its interconnection with the end-effector and the environment via *configuration springs*. The grasping of the real object (environment) is obtained via an indirect control of the position of the virtual object. In [54] actual contact points and measuring of contact forces are not

considered for embedding in an impedance control strategy. In addition, an impedance control design methodology in the PH framework with Casimir functions is proposed by [48] where the input of the mechanical system is different from the standard case, i.e., it is not a torque but a fluid flow.

The main contribution of this Section is to present an alternative impedance grasping control strategy for mechanical systems. We realize a passivity-based control strategy, and a type of modified integral control action. The control is achieved by shaping a *virtual potential energy* function represented by a virtual spring-stored energy, whose rest-length can be modified. This means that we can shape the minimum potential energy relative to a grasping force. Furthermore, a coordinate transformation is presented to include a *virtual position* error in the passive output of the transformed PH system . The present work is inspired by the results of [10, 54], and presented in [36, 37].

This chapter presents a grasping strategy that combines impedance control and force control. Basically, impedance control is employed to manage the *transient behaviour* of the grasping, namely the way in which the system interacts with the object, e.g., by improving the response of the system during noncontact to contact transitions. On the other hand, force control is employed to deal with the steady-state response of the system, i.e., we specify how strong (or weak) is the grasp.

We design the rest-length dynamics of the virtual spring in such a way that it depends on the output of the system, i.e., the velocity. When the end-effector is getting close to the object to be grasped, it experiences a decreasing speed due to the damping injection interpretation via the rest-length. Our impedance control strategy behaves as the classical impedance control proposed by [23], by controlling a virtual desired position during contact. This strategy becomes of greater relevance for nonrigid environments due to its non destructive behavior.

The grasping force depends on the object (environment) dynamics and position. We compensate here for nonlinear dynamics of the nonrigid body by the feed back of the measurements of the force sensors [33]. In principle, estimation techniques via position-based visual servo control or image-based visual servo control, as in [24], leads to a priori knowledge of the position of the object. Thus, we are able to successfully implement the proposed impedance grasping strategy. Vision control in the PH setting is the scope of the following chapter [9, 11, 27], which is promising to connect to our setting in future research.

4.2.1 Control law

In this Section, a control law strategy is introduced in order to achieve an impedance grasping interaction between a mechanical system and its environment, in a noncontact

to contact transition. Here, we combine two strategies, i.e., impedance control and force control. First, impedance control is used to manage transient behavior of the grasping, i.e., the interaction between an end-effector and the environment (object). We improve the response of the system during noncontact to contact transitions in comparison to former impedance control methods such as [23, 46, 48]. Secondly, force control is employed to deal with the steady-state response of the system. The problem of stabilization is to find a control law, which brings the grasping force to a desired force f_d. In order to avoid steady-state errors, we include dynamics in such a way that the PH structure is preserved. Then, via a change of variables for the canonical momenta of system (2.35), we realize a passive output in the transformed system that includes the grasping error. The key idea implemented here lies in the virtual potential energy shaping. The virtual potential energy is represented as virtual spring-stored energy, whose rest-length can be varied. This means that we can shape the minimum potential energy relative to a grasping force. Then, when the system experiences the noncontact to contact transition, we obtain asymptotic stability to a desired force which is related to a virtual desired position q_f. The results presented here are inspired by [10, 54].

We define a *virtual spring* with a variable rest-length q_{rl}. The force that is exerted by the virtual spring leads to a dissipation term in the impedance grasping controller, which is needed to obtain a smoother noncontact to contact transition. Of importance here is to make the dynamics of the rest-length dependent on the port output of the system. Then, the incorporation of a virtual spring force with a variable rest-length fundamentally improves mechanical impedance between the mechanical system and the environment. In order to implement the virtual spring force we define a *virtual potential energy* $H_c(\bar{q}, q_{rl})$ as

$$H_c(\bar{q}, q_{rl}) = \frac{1}{2}(\bar{q} - q_{rl})^\top K_p(\bar{q} - q_{rl}) + \frac{1}{2} q_{rl}^\top K_{rl} q_{rl} \tag{4.38}$$

with a constant matrix $K_p > 0$. A desired grasping force f_d is related to a virtual desired position q_f, a virtual potential energy $H_c(\bar{q}, q_{rl})$ as in (4.38), a rest-length q_{rl}, and a generalized coordinate q. Based now on the classical concept of impedance control introduced by [23], f_d or q_f is given when (q, q_{rl}) are asymptotically stabilized to zero, i.e.,

$$\begin{aligned} f_d &= -\left.\frac{\partial H_c(\bar{q}, q_{rl})}{\partial \bar{q}}\right|_{q_{rl}\to 0,\, q\to 0} \\ &= -K_p(\bar{q} - q_{rl})|_{q_{rl}\to 0,\, q\to 0} \\ &= -K_p(q - q_f - q_{rl})\big|_{q_{rl}\to 0,\, q\to 0} \\ &= K_p q_f \end{aligned} \tag{4.39}$$

Remark 4.2.1 The virtual potential energy (4.38) is defined in the joint space, but the idea is to apply a desired vector force $F_d \in \mathbb{R}^n$ in the work space in steady state. Then, the meaning of (4.39) is that it is necessary to find $f_d \in \mathbb{R}^n$, $K_d \in \mathbb{R}^{n\times n}$, and $q_f \in \mathbb{R}^{n\times n}$ such that

$$f_d = \mathscr{J}^\top(q_f) F_d = K_p q_f. \tag{4.40}$$

$K_p > 0$ is interpreted as a desired elastic behavior in the joint space, and q_f is the reference position in steady state. When the dynamics of q_{rl} is given, we basically have a desired impedance, i.e., we specify the way in which robot and object interact. Hence, the desired impedance is defined in joint space.

In order to incorporate the variable rest-length in the port output of the system, we realize a coordinate transformation

$$\hat{p} = \bar{p} + \bar{T}(\bar{q})^\top K_p(\bar{q} - q_{rl}) \tag{4.41}$$

which then implies

$$\dot{\hat{p}} = \dot{\bar{p}} + \bar{T}(\bar{q})^\top K_p(\dot{\bar{q}} - \dot{q}_{rl}) + \dot{\bar{T}}(\bar{q})^\top K_p(\bar{q} - q_{rl}) \tag{4.42}$$

The new output becomes

$$\hat{y} = \bar{G}(\bar{q})^\top \hat{p} = \bar{G}(\bar{q})^\top \left(\bar{p} + \bar{T}(\bar{q})^\top K_p(\bar{q} - q_{rl})\right) \tag{4.43}$$

and finally the dynamics of the rest-length is chosen as a modified integrator, i.e.,

$$\dot{q}_{rl} = -\hat{y} - K_p(\bar{q} - q_{rl}) - K_{rl} q_{rl} \tag{4.44}$$

with a constant matrix $K_{rl} > 0$.

Remark 4.2.2 It can be seen that a new port-pair (u_{rl}, y_{rl}) is now given by the following dynamics

$$u_{rl} = \dot{q}_{rl} \tag{4.45}$$

$$y_{rl} = \bar{G}(\bar{q})^\top \frac{\partial\left(\bar{H}(\bar{q},\bar{p}) + H_c(\bar{q}, q_{rl})\right)}{\partial q_{rl}} = \bar{G}(\bar{q})^\top \left(K_p(\bar{q} - q_{rl}) + K_{rl} q_{rl}\right) \tag{4.46}$$

with $\bar{H}(\bar{q},\bar{p})$ as in (2.34), $H_c(\bar{q}, q_{rl})$ as in (4.38), and the dynamics of q_{rl} as in (4.44).

We now define an impedance grasping control law of the PH system (2.35) with measurable external forces, i.e.,

Theorem 4.2.3 *Consider the PH system* (2.35) *with* $\bar{D}(\bar{q},\bar{p})$*, constant matrices* $K_p > 0$ *and* $K_{rl} > 0$*, invertible matrices* $\bar{G}(\bar{q})$ *and* $\bar{B}(\bar{q})$*, and that we have information of the vector of external forces* f_e *via force sensors. Furthermore, consider a passive output* $\hat{y}$ *as in* (4.43)*, and assume that the system is zero-state detectable with respect to* $\bar{x}$*. Then, the control input*

$$\begin{aligned} v =& \bar{G}(\bar{q})^{-1}\left[\bar{T}(\bar{q})^{-1}\frac{\partial \bar{H}(\bar{q},\bar{p})}{\partial \bar{q}} + \bar{G}(\bar{q})K_{rl}q_{rl} - \bar{B}(\bar{q})f_e \right. \\ &+ \left(\bar{G}(\bar{q})\bar{T}(\bar{q})^{-\top} - \bar{T}(\bar{q})^{-\top} + \bar{J}_2(\bar{q},\hat{p}) - \bar{D}(\bar{q},\hat{p})\right)\bar{T}(\bar{q})^{\top}K_p(\bar{q}-q_{rl}) \\ &\left. -\bar{T}(\bar{q})^{\top}K_p(\dot{\bar{q}}-\dot{q}_{rl}) - \dot{\bar{T}}(\bar{q})^{\top}K_p(\bar{q}-q_{rl})\right] - C\hat{y} \end{aligned} \tag{4.47}$$

with $C > 0$*, asymptotically stabilizes the system* (2.35) *with zero steady-state error at* $\bar{q}^* = 0$*.*

Proof. The coordinate transformation $\bar{x}$ as in (2.31) results in $\dot{\bar{q}}$ as

$$\dot{\bar{q}} = \dot{q} = M(q)^{-1}p = \bar{T}(\bar{q})^{-\top}\bar{p} \tag{4.48}$$

Based on the adapted momenta $\hat{p}$ as in (4.41), we rewrite the dynamics $\dot{\bar{q}}$ as in (4.48) in terms of $(\bar{q},\hat{p},q_{rl})$, i.e.,

$$\dot{\bar{q}} = -K_p(\bar{q}-q_{rl}) + \bar{T}(\bar{q})^{-\top}\hat{p} \tag{4.49}$$

We differentiate both sides of the change of variables (4.41) as

$$\dot{\hat{p}} = \dot{\bar{p}} + \bar{T}(\bar{q})^{\top}K_p(\dot{\bar{q}}-\dot{q}_{rl}) + \dot{\bar{T}}(\bar{q})^{\top}K_p(\bar{q}-q_{rl}) \tag{4.50}$$

and with the dynamics of $\dot{\bar{p}}$ as in (2.35) as

$$\begin{aligned} \dot{\bar{p}} &= -\bar{T}(\bar{q})^{-1}\frac{\partial \bar{H}(\bar{q},\bar{p})}{\partial \bar{q}} + (\bar{J}_2(\bar{q},\bar{p}) - \bar{D}(\bar{q},\bar{p}))\frac{\partial \bar{H}(\bar{q},\bar{p})}{\partial \bar{p}} + \bar{G}(\bar{q})v + \bar{B}(\bar{q})f_e \\ &= -\bar{T}(\bar{q})^{-1}\frac{\partial \bar{H}(\bar{q},\bar{p})}{\partial \bar{q}} + (\bar{J}_2(\bar{q},\bar{p}) - \bar{D}(\bar{q},\bar{p}))\bar{p} + \bar{G}(\bar{q})v + \bar{B}(\bar{q})f_e \end{aligned} \tag{4.51}$$

we substitute the dynamics of $\dot{\bar{p}}$ as in (4.51), and the control law v as in (4.47) in (4.50). It leads to the dynamics $\dot{\hat{p}}$ in terms of $(\bar{q},\hat{p},q_{rl})$, i.e.,

$$\dot{\hat{p}} = \left(\bar{J}_2(\bar{q},\bar{p}) - \bar{D}(\bar{q},\bar{p}) - \bar{G}(\bar{q})C\bar{G}(\bar{q})^{\top}\right)\hat{p} - K_p(\bar{q}-q_{rl}) + \bar{G}(\bar{q})\left(K_p(\bar{q}-q_{rl}) + K_{rl}q_{rl}\right) \tag{4.52}$$

with $\hat{p}$ as in (4.41), and $\hat{y}$ as in (4.43). Furthermore, the dynamics of the variable rest-length

$\dot{q}_{rl}$ as in (4.44) can be rewritten as

$$\dot{q}_{rl} = -\bar{G}(\bar{q})^{\top}\hat{p} - K_p(\bar{q} - q_{rl}) - K_{rl}q_{rl} \tag{4.53}$$

Finally, we choose a smooth function $\bar{U}(\bar{q},\bar{p},q_{rl})$ such as

$$\begin{aligned}\bar{U}(\bar{q},\bar{p},q_{rl}) =& \bar{p}^{\top}\bar{T}(\bar{q})^{\top}K_p(\bar{q}-q_{rl}) - \bar{V}(\bar{q}) \\ &+ \frac{1}{2}(\bar{q}-q_{rl})^{\top}K_p\bar{T}(\bar{q})\bar{T}(\bar{q})^{\top}K_p(\bar{q}-q_{rl}) \\ &+ \frac{1}{2}(\bar{q}-q_{rl})^{\top}K_p(\bar{q}-q_{rl}) + \frac{1}{2}q_{rl}^{\top}K_{rl}q_{rl}\end{aligned} \tag{4.54}$$

with matrices $K_p > 0$, $K_{rl} > 0$, and where $\bar{V}(\bar{q})$ is the potential energy function of (2.35). We then realize a candidate Lyapunov function $\hat{H}(\bar{q},\hat{p},q_{rl}) = \bar{H}(\bar{q},\bar{p}) + \bar{U}(\bar{q},\bar{p},q_{rl})$, with $\hat{H}(\bar{q},\hat{p},q_{rl}) > 0$, and $\bar{H}(\bar{q},\bar{p})$ as in (2.34), $\bar{U}(\bar{q},\bar{p},q_{rl})$ as in (4.54), and the change of variables $\bar{p}$ as in (4.41), i.e.,

$$\hat{H}(\bar{q},\hat{p},q_{rl}) = \frac{1}{2}\hat{p}^{\top}\hat{p} + \frac{1}{2}(\bar{q}-q_{rl})^{\top}K_p(\bar{q}-q_{rl}) + \frac{1}{2}q_{rl}^{\top}K_{rl}q_{rl} \tag{4.55}$$

Based now on the dynamics $\dot{\bar{q}}$ as in (4.49), $\dot{\hat{p}}$ as in (4.52), and $\dot{q}_{rl}$ as in (4.53), we obtain the closed-loop

$$\begin{bmatrix} \dot{\bar{q}} \\ \dot{\hat{p}} \\ \dot{q}_{rl} \end{bmatrix} = \begin{bmatrix} -I_{n\times n} & \bar{T}(\bar{q})^{-\top} & 0_{n\times n} \\ -\bar{T}(\bar{q})^{-1} & \bar{J}_2(\bar{q},\hat{p}) - \bar{D}(\bar{q},\hat{p}) - \bar{G}(\bar{q})C\bar{G}(\bar{q})^{\top} & \bar{G}(\bar{q}) \\ 0_{n\times n} & -\bar{G}(\bar{q})^{\top} & -I_{n\times n} \end{bmatrix} \begin{bmatrix} \dfrac{\partial\hat{H}}{\partial\bar{q}} \\ \dfrac{\partial\hat{H}}{\partial\hat{p}} \\ \dfrac{\partial\hat{H}}{\partial q_{rl}} \end{bmatrix} \tag{4.56}$$

with Hamiltonian (4.55), and where we have left out the arguments of $\hat{H}(\bar{q},\hat{p},q_{rl})$ for notational simplicity.

Take now (4.55) as a candidate Lyapunov function, $\hat{H}(\bar{q},\hat{p},q_{rl}) > 0$. It can be verified via the dynamics of $\bar{q}$, $\hat{p}$ and q_{rl}, as in (4.49), (4.52), and (4.53), respectively, that $(\bar{q},\hat{p},q_{rl}) = (0,0,0)$ is an equilibrium point of (4.56). We now compute the power balance $\dot{\hat{H}}(\bar{q},\hat{p},q_{rl})$ as

$$\dot{\hat{H}}(\bar{q},\hat{p},q_{rl}) = -\begin{bmatrix} \bar{q}^{\top} & \hat{p}^{\top} & \hat{q}_{rl}^{\top} \end{bmatrix}^{\top} U(\bar{q},\hat{p}) \begin{bmatrix} \hat{q} \\ \hat{p} \\ \hat{q}_{rl} \end{bmatrix} \tag{4.57}$$

with $\hat{q} = \bar{q} - q_{rl}$, $\hat{q}_{rl} = K_p(\bar{q} - q_{rl}) + K_{rl}q_{rl}$, and a matrix $U(\bar{q}, \hat{p})$, such that,

$$U = \begin{bmatrix} K_p K_p & 0_{n\times n} & 0_{n\times n} \\ 0_{n\times n} & \bar{D}(\bar{q},\hat{p}) + \bar{G}(\bar{q})C\bar{G}(\bar{q})^\top & 0_{n\times n} \\ 0_{n\times n} & 0_{n\times n} & I_{n\times n} \end{bmatrix} \tag{4.58}$$

Since $\bar{G}(\bar{q})$ is full rank, $\bar{D}(\bar{q},\hat{p}) \geqslant 0$, and C, K_p and K_{rl} are positive definite, then $U(\bar{q},\hat{p}) > 0$, and thus $\dot{\hat{H}}(\bar{q},\hat{p},q_{rl}) < 0$. Hence, since the system is zero-state detectable (see [19]), then the closed-loop system (4.56) is asymptotically stable in $(\bar{q},\hat{p},q_{rl}) = (0,0,0)$, and hence $\bar{q}^* = 0$. ■

Remark 4.2.4 Since the new output $\hat{y}$ as in (4.43) includes a position error $\bar{q}$ and a variable rest-length q_{rl}, we have realized here an additional (co)dissipation term $K_p K_p > 0$ in our power balance $\dot{\hat{H}}(\bar{q},\hat{p},q_{rl})$ as in (4.57). This additional dissipation term realized by our impedance strategy (4.47) leads to a smoother noncontact to contact transition during the grasping.

We have realized an impedance grasping control law via passivity-based control, and damping injection. Via the control law (4.47) we are able to stabilize the system (2.35) to a virtual desired position q_f which means a realization of a grasping force f_d as in (4.39) in a noncontact to contact transition. We assume here that the end-effector is within a grasping distance with respect to the environment [38]. We now motivate the present PH approach for impedance grasping control with an example of an end-effector system.

4.2.2 Simulation results

In this Section we illustrate, via a simulation of the system (2.19), in order to obtain a desired force via the impedance grasping strategy of Theorem 4.2.3.

By experimental means, we have determined the parameters of the gripper. We want to grasp a *rigid body*, and a *compliant body*, that are located at a grasping distance, e.g., $q_f = 0.20rad$. We then apply the grasping impedance control law (4.47) to the PH system (2.19), i.e.,

$$v = \frac{\partial V(q)}{\partial q} - d_g K_p(\bar{q} - q_{rl}) - K_p(\dot{q} - \dot{q}_{rl}) + K_{rl}q_{rl} - C(m_g\dot{q} + K_p(\bar{q} - q_{rl})) - f_e \tag{4.59}$$

where $\bar{q} = q - q_f$, $\dot{\bar{q}} = \dot{q}$, $k_{g_i} = \{0.21, 0.06\}$, $d_g = 0.1$, $m_g = 0.5kg$, $\alpha_f = 0.001$, and $c_g = 0.30rad$. We have constants $K_p = 1$, $K_{rl} = 0.5$ and $C = 3$; an initial position $q(0) = 0.30rad$, input matrices $G = 1$ (fully actuated), $B(q) = 1$, a desired force $f_d = 0.20N$,

and based on (4.39), a virtual position of $q_f = K_p^{-1} f_d = 0.20 rad$. We have compared our strategy with the classical impedance control law ([23], Part II, equation (15), page 10) for this gripper given by

$$\bar{u} = \frac{\partial D(q,\dot{q})}{\partial \dot{q}} + \frac{\partial V(q)}{\partial q} - K_{Hp}(q - q_f) - K_{Hd}(\dot{q} - \dot{q}_f) \tag{4.60}$$

where $q_f, \dot{q}_f \in \mathbb{R}^n$ are the desired virtual position and desired velocity vectors, respectively, $K_{Hp} > 0$ and $K_{Hd} > 0$ are the $n \times n$ constant matrices of the proportional and differential terms, respectively, $\frac{\partial V(q)}{\partial q} \in \mathbb{R}^n$ is the potential energy vector, and $\frac{\partial D(q,\dot{q})}{\partial \dot{q}} \in \mathbb{R}^n$ is the vector of dissipation forces. In addition, we include the vector of external forces $f_e \in \mathbb{R}^n$ in (4.60) since this matches a fair comparison. Hence, the classical impedance control law plus external force feedback is given by the equation

$$u = \bar{u} - f_e \tag{4.61}$$

Then, by adding an external force rejection strategy in the classical impedance control law, we are able to compare our results with the variable rest-length strategy. Given the dynamics of the gripper (2.19) with Hamiltonian (2.15), we implement here the control law (4.60) with $\frac{\partial D(q,\dot{q})}{\partial \dot{q}} = d_g \dot{q} = 0.1\dot{q}$, $K_g(q)(q - c_g)$ with $K_g(q)$ as in (2.17), and the parameters $K_{Hp} = 1$, $K_{Hd} = 3$, $k_{g_i} = \{0.21, 0.06\} Nm/rad$, $\alpha_f = 0.001$, $c_g = 0.30 rad$, $q_f = 0.20 rad$, and $\dot{q}_f = 0$ (note that we choose $K_{Hp} = K_p$, and $K_{Hd} = C$).

The compliant body is modeled by linear mass-spring-damper system in a PH framework. The system has a generalized coordinate $q \in \mathbb{R}$, generalized momentum $p \in \mathbb{R}$; mass m_c, with dissipation d_c, a potential energy function $V_c(q) = \frac{1}{2} K_c (q - q_c)^2$ with a constant rest-length q_c, and Hamiltonian

$$H_c(q,p) = \frac{1}{2} m_c^{-1} p^2 + V_c(q) = \frac{1}{2} m_c^{-1} p^2 + \frac{1}{2} K_c (q - q_c)^2 \tag{4.62}$$

The PH model is

$$\begin{bmatrix} \dot{q} \\ \dot{p} \end{bmatrix} = \begin{bmatrix} 0 & 1 \\ -1 & -d_c \end{bmatrix} \begin{bmatrix} K_c(q - q_c) \\ m_c^{-1} p \end{bmatrix} + \begin{bmatrix} 0_{n \times n} \\ 1 \end{bmatrix} u_c \tag{4.63}$$

$$y_c = m_c^{-1} p \tag{4.64}$$

with an input-output port pair $(u_c, y_c) \in \mathbb{R}$. The noncontact to contact transition between the gripper system (2.19), and the compliant body (4.63) is modeled as an interconnection

of two PH systems, i.e.,

$$f_e = -y_c \tag{4.65}$$

$$u_c = y_g \tag{4.66}$$

with f_e being an external force applied to the gripper system (2.19), y_g as in (2.20), and the output input-output port pair (u_c, y_c) of the compliant body as in (4.63), and (4.64), respectively. We furthermore apply the grasping impedance control law (4.59) to the PH system (2.19), with an initial position of $q(0) = 0.30rad$, input matrices $G = 1$ (fully actuated), $B(q) = 1$; constants $K_p = 1$, $K_{rl} = 0.25$ and $C = 1.5$; compliant body parameters $K_c = 0.1$, $d_c = 0.1$, and a rest-length $q_c = 0.30rad$; a desired force $f_d = 0.20N$, and based on (4.39), a virtual position of $q_f = K_p^{-1} f_d = 0.20rad$. We compare our strategy with the classical impedance control law [23] for this gripper given by (4.60). Subsequently, we include the vector of external forces $f_e \in \mathbb{R}^n$ in (4.60). Hence, the classical impedance control law with external forces compensation is given by (4.61), with the parameters $K_{Hp} = 1$, $K_{Hd} = 3$, $k_{g_i} = \{0.21, 0.06\} Nm/rad$, $\alpha_f = 0.001$, $c_g = 0.30rad$, $q_f = 0.20rad$ and $\dot{q}_f = 0$ (note that we choose $K_{Hp} = K_p$, and $K_{Hd} = C$).

The simulation results of the impedance grasping strategies are shown in Figures 4.2, 4.3, 4.4, and 4.5, of the grasping position and force of a rigid and a compliant bodies. When grasping a rigid body, we observe in Figure 4.2 that a noncontact to contact transition occurs at $t_1 = 0.60s$ with our control law (4.59) (solid-blue), and at $t_2 = 0.80s$ with the classical control law with and without external forces compensation, i.e., (4.60) (dotted-black), and (4.61) (dashed-red) on top. When grasping the compliant body, (4.63), a noncontact to contact transition results at $t_1 = 0.80s$ and $t_2 = 1.30s$, as shown in Figures 4.4, and 4.5. We observe that the noncontact to contact transition is faster with our strategy (solid-blue) due to the damping injection of the variable rest-length dynamics. In Figures 4.3 and 4.5, we show that our controller (solid-blue) is faster in convergence in terms of the forces of the system. When grasping a rigid body, as shown in Figure 4.3, we obtain lower impact forces (solid-blue, $f = 0.10N$) than the impact force obtained with the classical controller with and without an external force rejection strategy (dashed-red, $f = 0.40N$, and dotted-black, $f = 0.60N$). Similarly, when we grasp a compliant body, as shown in Figure 4.5, we obtain the impact forces $f = 0.00N$ (solid-blue), $f = 0.20N$ (dashed-red), and $f = 0.30N$ (dotted-black). Furthermore, the grasping force of $f_d = 0.20N$ is obtained at $t > 0.90s$ with a zero steady-state error via the rest-length strategy of (4.59) when grasping a rigid and a compliant body, while the classical strategies of (4.60) and (4.61) take $t > 2s$, and $t > 2.5s$. An asymptotically stable desired grasping force is then obtained together with a nondestructive behavior. The noncontact to contact transition using a compliant body is smoother than with a rigid body. This is due to its linear mass-spring-

damping effect modeled as in (4.63), and the interconnection of two PH systems given by (4.65) and (4.66).

4.2.3 Experimental results

The experimental set-up is shown in Figure 4.6. An alloy and a foam are localized within a grasping distance, $q_f = 0.20rad$. The alloy is modeled as a rigid body, and the foam is modeled as a linear mass-spring-damper system as in (4.63) with output (4.64). We grasp the alloy and the foam with a desired force $f_d = 0.20N$. For a fair comparison with the simulation results, we implement the grasping control laws (4.59), (4.60), and (4.61) with the parameters of Section 4.2.2. Results are shown in Figures 4.7 and 4.8 for the alloy, and 4.9 and 4.10 for the foam. We observe in Figures 4.7 and 4.9 how the noncontact to contact transition occurs at $t \geqslant 0.55s$ and $t \geqslant 0.78s$, respectively, with the control law (4.59) (solid-blue). Our rest-length strategy has a faster convergence due to the (co)dissipation effect of the variable rest-length of our virtual nonlinear spring in comparison with the classical control laws (4.60) (dashed-red), and (4.61) (dotted-black). Moreover, we observe in Figures 4.8 and 4.10 how the rest-length control strategy (4.59) (solid-blue) achieves the desired force at $t \geqslant 0.70s$, and $t \geqslant 1.20s$ with zero steady-state error. Additionally, the classical impedance control law with and without external forces compensation, i.e., (4.61) (dashed-red) and (4.60) (dotted-black), have impact forces of $f = 0.25N$ (dashed-red), and $f = 0.40N$ (dotted-black), when grasping the alloy (Figure 4.8). When the gripper grasps the foam, the impact forces are $f = 0.05N$ (dashed-red), and $f = 0.15N$ (dotted-black) (Figure 4.10). We furthermore observe that these impact forces are reduced to $f = 0.05N$ when grasping the alloy, and $f = 0.00N$ when grasping the foam via our impedance grasping strategy. The performance of the controllers on the gripper system validate our simulation results of Section 4.2.2.

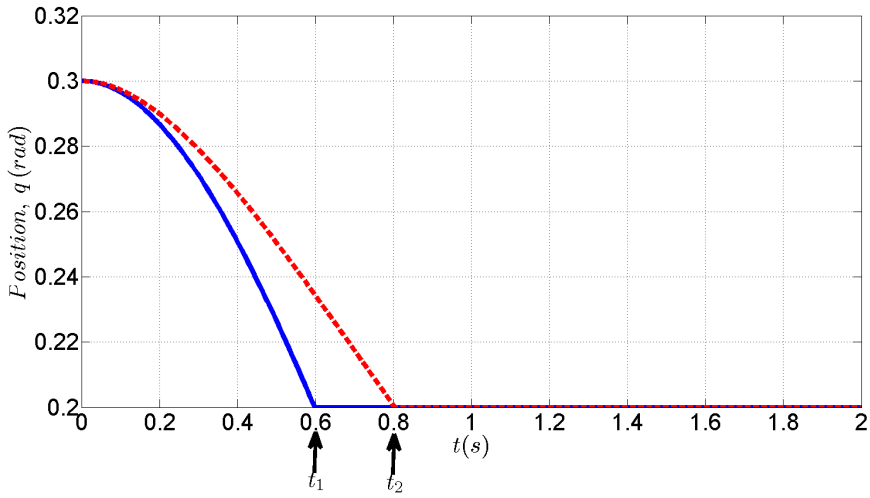

Figure 4.2: Grasping position of a rigid body located at $q_f = 0.20rad$. Initial conditions $(q, p) = (0.3rad, 0)$. Simulation results obtained via the rest-length strategy (4.59) (solid-blue), and the classical impedance strategy (4.61) (dashed-red) with external force compensation, which is on top of the classical impedance control without external force compensation given by (4.60) (dotted-black).

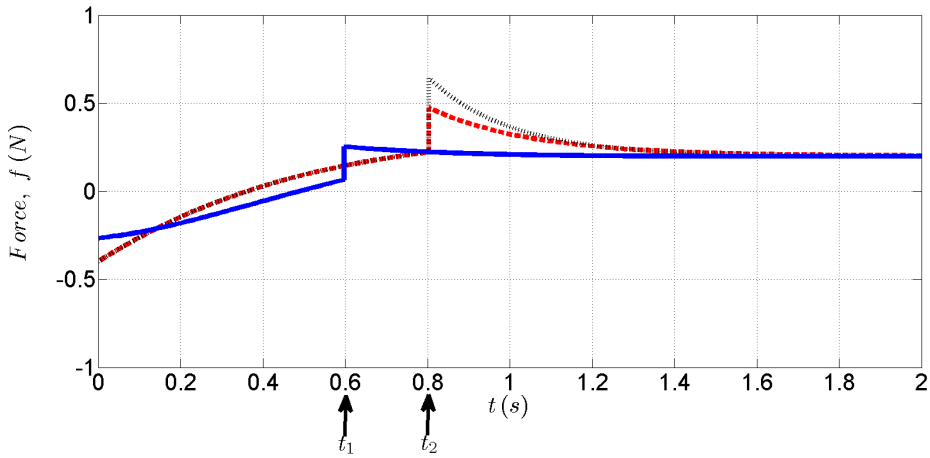

Figure 4.3: Grasping force of a rigid body at $f_d = 0.20N$. Simulation results obtained via the rest-length strategy (4.59) (solid-blue), and the classical impedance strategy (4.61) (dashed-red), both with external forces compensation. The classical impedance control without external force compensation is given by (4.60) (dotted-black).

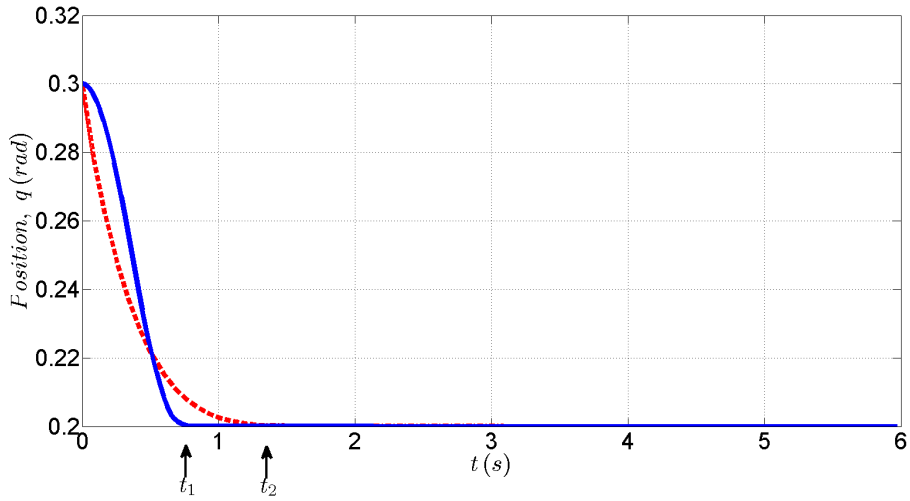

Figure 4.4: Grasping position of a compliant body located at $q_f = 0.20rad$. Initial conditions $(q, p) = (0.3rad, 0)$. Simulation results obtained via the rest-length strategy (4.59) (solid-blue), and the classical impedance strategy (4.61) (dashed-red) with external force compensation, which is on top of the classical impedance control without external force compensation given by (4.60) (dotted-black).

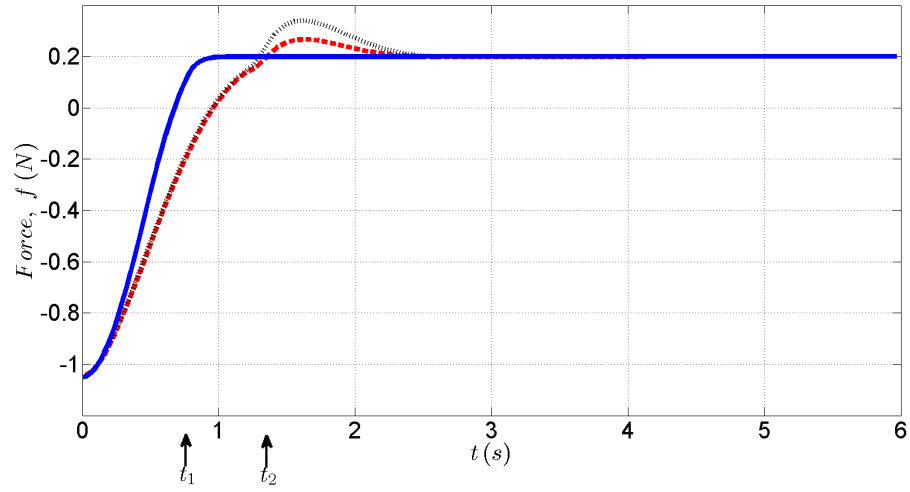

Figure 4.5: Grasping force of a compliant body at $f_d = 0.20N$. Simulation results obtained via the rest-length strategy (4.59) (solid-blue), and the classical impedance strategy (4.61) (dashed-red), both with external forces compensation. The classical impedance control without external force compensation is given by (4.60) (dotted-black).

(a) Rigid body at a grasping distance.

(b) Gripper grasping a rigid body.

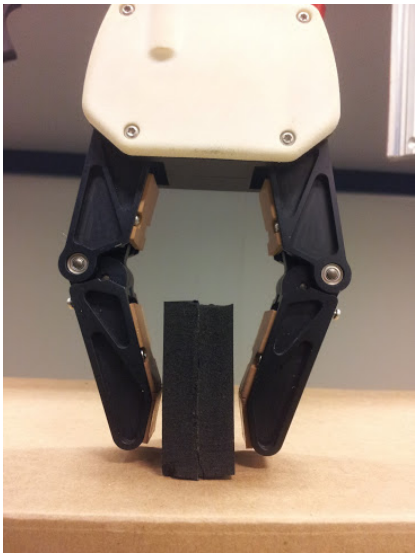

(c) Compliant body in (4.63) at a grasping distance.

(d) Gripper grasping a compliant body as in (4.63).

Figure 4.6: Experimental setup

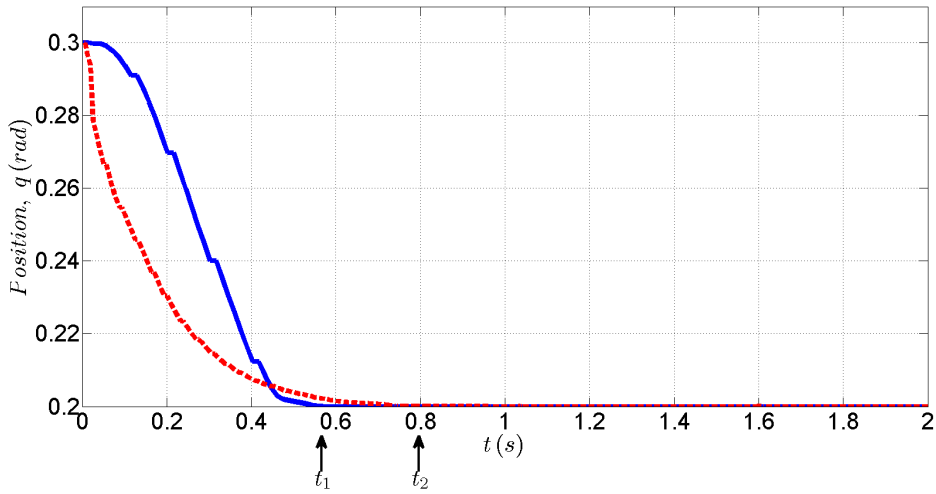

Figure 4.7: Grasping position of a rigid body located at $q_f = 0.20rad$. Initial conditions $(q, p) = (0.3rad, 0)$. Experimental results obtained via the rest-length strategy (4.59) (solid-blue), and the classical impedance strategy (4.61) (dashed-red) with external force compensation, which is on top of the classical impedance control without external force compensation given by (4.60) (dotted-black).

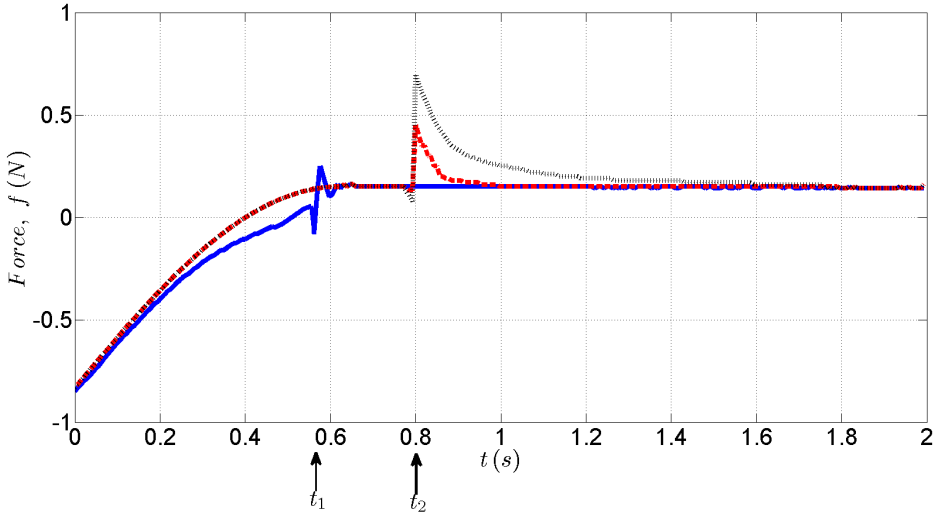

Figure 4.8: Grasping force of a rigid body at $f_d = 0.20N$. Experimental results obtained via the rest-length strategy (4.59) (solid-blue), and the classical impedance strategy (4.61) (dashed-red), both with external forces compensation. The classical impedance control without external force compensation is given by (4.60) (dotted-black).

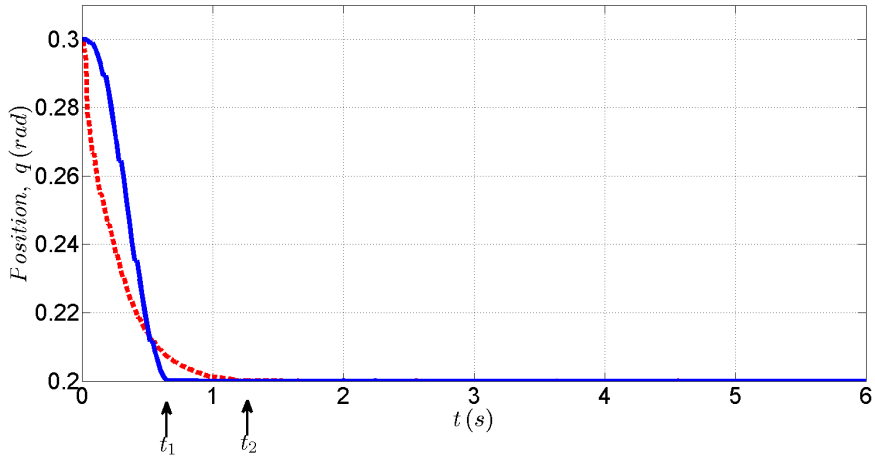

Figure 4.9: Grasping position of a compliant body located at $q_f = 0.20rad$. Initial conditions $(q, p) = (0.3rad, 0)$. Experimental results obtained via the rest-length strategy (4.59) (solid-blue), and the classical impedance strategy (4.61) (dashed-red) with external force compensation, which is on top of the classical impedance control without external force compensation given by (4.60) (dotted-black).

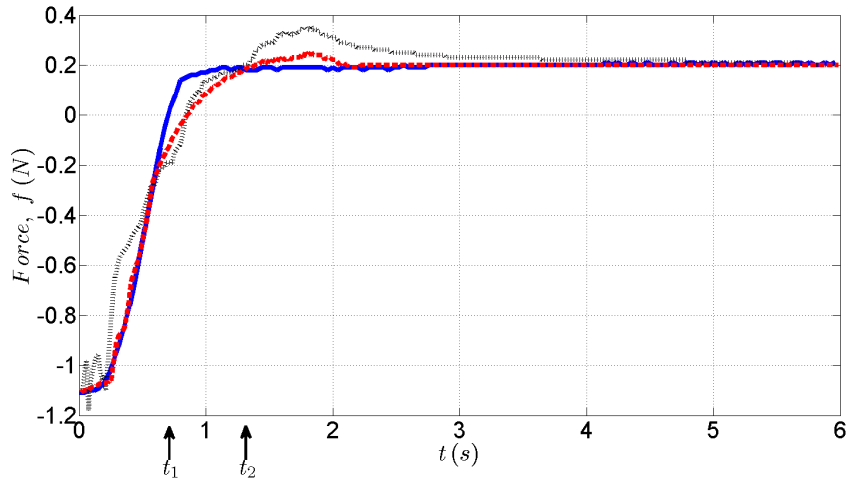

Figure 4.10: Grasping force of a compliant body at $f_d = 0.20N$. Experimental results obtained via the rest-length strategy (4.59) (solid-blue), and the classical impedance strategy (4.61) (dashed-red), both with external forces compensation. The classical impedance control without external force compensation is given by (4.60) (dotted-black).

4.3 Concluding remarks

This chapter is devoted to the development new strategies of force control and impedance grasping control in the PH framework, and in a noncontact to contact transition. Our main motivation is given by the proposition of an alternative to the classical impedance control and force control methods in the EL framework. A type of integral action over the force sensor output, and a change of variable, are the main strategies to realize a force control in presence of external forces. Force control is then realizable when we have (total) measurements of the internal and external forces of our system. Furthermore, we have given an impedance control law complemented with a virtual spring force. The incorporation of a virtual spring force with a variable rest-length that can be varied fundamentally improves the mechanical impedance between the system and the environment. Better convergence and lower impact forces are obtained with our impedance grasping strategy in comparison with the classical one from [23]. This behavior is due to the additional (co)dissipation term in the power balance of the system. Both strategies achieve asymptotic stability in the closed-loop system with a zero steady-state error, and both have been validated through simulation and experimental results.

Chapter 5

A port-Hamiltonian approach to visual servo control

The current emerging technologies have given rise to an ever increasing demand of robots and systems with skilled manipulation, which are able to perform under unknown environments. However, the environment is normally contrived to suit the robot characteristics. An alternative for increasing the dexterity of robots and mechanical systems is the integration of visual information, as a reactive measure instead of constraining the environment. The inclusion of vision in contemporary robotic systems results in enhanced sensory capabilities, since it resembles the human sense of vision, and allows for noncontact measurement of the environment as extensively documented in [24]. Control applications are suitable, due to the modern computing power capabilities of visual systems commercially available. The results of this research, when combined with previous results on mechanical impedance grasping control as in [35, 37], should enable the reader to implement a complete experimental setup where a robot manipulator is capable of converging to a grasping configuration via vision sensors, and performing a smooth noncontact to contact transition with the environment (object) via force sensors.

Via the geometric information of the imaging process, we are able to control the robot to a determined target. Generally, vision systems provide projections to an *image plane* where the visual sensor is located [24, 51]. The vision literature compiles two projection models: perspective projection and scaled orthographic projection. The orthographic projection models are valid for scenes where the relative depth of the points is small compared with the distance from the camera to the scene, which is not the case here. With perspective projection we make use of a well-known model that includes *image features variables* in the image plane. Based on this projection, we find the most popular classifications of visual servo control in the vision literature: position-based visual servo (PBVS) control and image-based visual servo (IBVS) control. In PBVS control, visual servoing features are extracted from the image, and used to estimate the pose of the target with respect to the camera. The feedback control is computed via the error of the estimated pose. In IBVS control, the control feedback is directly computed from the image parameters. Both classifications have received considerable attention and it is out of the scope of this chapter to summarize all of them. For more details we refer to the interested reader to [24].

In this chapter a standard mechanical system with an eye-in-hand configuration is considered. Similar to many works on robot vision control, we apply perspective projection to model the camera dynamics. The main contribution of this chapter is to control a mechanical system (robot manipulator) to a desired position based on the image features of the object to be grasped. First, we derive an extended *interaction matrix* that includes a *depth*-type dynamics. The depth variable is the length as seen by the camera, and it complements the image features variables of the image plane found in the classical IBVS control strategies. We then realize an extended system in order to include the nonlinear dynamics of the camera, and the image features variables together with the depth-type variable. The resulting extended system has no structure preservation. Subsequently, we implement change of variables, i.e., *adapted momenta*, that include the dynamics of the vision system. We propose then two control strategies that asymptotically stabilizes the system in desired image features. The first makes use of a reduction-based design, and is independent of the invertibility properties of the interaction matrix with no preservation of a PH structure. The second strategy realizes a PH system with structure preservation. However, it depends on the geometric properties of the interaction matrix.

The PH modeling framework of [30,55] has received a considerable amount of interest in the last decade because of its insightful physical structure. It is well known that a large class of (nonlinear) physical systems can be described in the PH framework. The popularity of PH systems can be largely accredited to its application for analysis and control design of physical systems, as shown in [13, 19, 30, 55], and many others. Control laws in the PH framework are derived with a clear physical interpretation via direct shaping of the closed-loop energy, interconnection, and dissipation structure, see [13,55]. We apply the PH modeling framework since it allows extensions of the system coordinates which facilitates the incorporation of the nonlinear dynamics of the camera. However, IBVS control in the PH framework is not straightforward when we desire structure preservation. We then implement a set of change of variables to deal with this problem.

To the best of our knowledge, [28] is the first PH approach to visual servo control. Contrary to this chapter, in [28] they deal with an aerial robot and apply a spherical image representation, while we apply perspective projection as in [9, 11]. In [27] they deal with a general class of lossless standard mechanical systems, and they introduce an extension that compensates for unknown depth dependence of the interaction matrix by a kind of depth observer. In this chapter, we deal with a standard class of mechanical systems with a nonconstant mass-inertia matrix and with nonlinear friction. Contrary to [27], we use the length of the object in the image plane together with a perspective projection relation as in [24] to determine the depth.

This work is based on the results of [9, 11] where the problem of image-based visual servo control of a pick and place system is addressed in a PH framework. The results

of [9] are given for a constant mass-inertia matrix with linear damping. Full knowledge of the mass-inertia and damping matrices is required for the control strategy in [9], while a later work presented in [11] realizes a different controller, which only requires partial knowledge of the system parameters. Here we extend this work to deal with nonconstant mass-inertia matrices, and to deal with nonlinear damping, which is a more realistic situation. Furthermore, opposite to [9, 11], our interaction matrix is handling rotational systems as well.

The remainder of this chapter is organized as follows. In Section 5.1, the equivalent PH system with the constant mass-inertia matrix of Section 2.2 is extended by including the nonlinear dynamics of the vision system. Subsequently, we realize an interaction matrix that includes the depth-type of information together with the image features of the image plane. We then introduce in Section 5.2 IBVS control strategies based on the geometric information of the vision system, e.g., the interaction matrix. Specifically, we present two control strategies with and without dependency on the constrains given by the nonlinear vision system. Via the control strategies, we attain asymptotic stability in the desired image features. In Section 5.3, we compare the advantages and disadvantages of both control laws. Finally, simulations are given in Section 5.4 to motivate our results for IBVS control, and Section 5.5 provides concluding remarks.

5.1 Extended system-camera dynamics

This paper studies a system consisting of an n-dof robot manipulator with an eye-in-hand camera configuration, i.e., the camera is attached to the wrist of the manipulator. The robot manipulator has model (2.2) with Hamiltonian (2.4). Here we develop an extended model of the robot manipulator with camera dynamics.

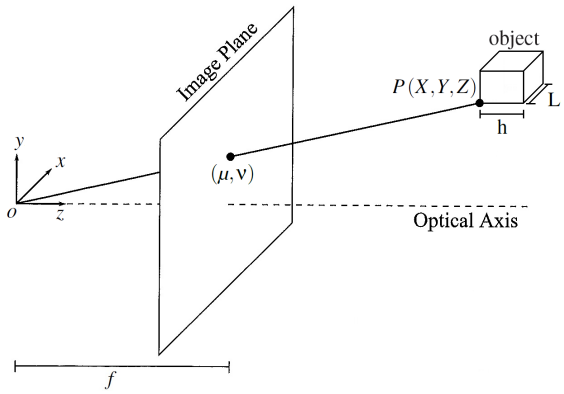

Figure 5.1: Camera Pinhole model as in [53].

First, we consider a *pinhole* image model [53] as depicted in Figure 5.1. The image plane is the plane that contains the sensing array. Behind the image plane, at a distance f (focal length), is located the origin $o(x,y,z)$ of a camera coordinate frame. We consider the lens as an ideal pinhole, described by (μ,ν) in Figure 5.1, at the focal center of the lens where μ, ν are used to parametrize the image plane, and referred to as *image plane coordinates*. For any point $P(X,Y,Z)$ in an inertial frame, let its projection on the image plane be (μ,ν). Then, under the pinhole assumption, the points P, (μ,ν), and o are collinear.

The measurement of one point of the object only gives an (X,Y) position information, i.e., the horizontal position of the object with respect to the camera frame. Then, using the fact that the object has a constant length L, that length as seen by the camera, and denoted here l, can be used as the third state of the camera mode. The length l increases when the camera approaches the object, and decreases when the camera moves away by the factor f/Z. It is desired to bring the gripper with the camera to a position such that the object is seen in a desired form in the image plane (usually the center of the image plane), refer to Figure 5.2. When this is achieved the gripper is ready to grasp the object.

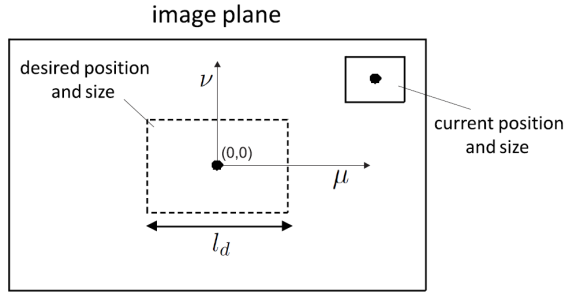

Figure 5.2: Image plane as in [11].

The three image coordinates are therefore given by

$$\begin{bmatrix} \mu \\ \nu \\ l \end{bmatrix} = \frac{f}{Z} \begin{bmatrix} X \\ Y \\ L \end{bmatrix} \tag{5.1}$$

with dynamics

$$\begin{bmatrix} \dot{\mu} \\ \dot{\nu} \\ \dot{l} \end{bmatrix} = \begin{bmatrix} \frac{f}{Z} & 0 & -\frac{\mu}{Z} \\ 0 & \frac{f}{Z} & -\frac{\nu}{Z} \\ 0 & 0 & \frac{l}{Z} \end{bmatrix} \begin{bmatrix} \dot{X} \\ \dot{Y} \\ \dot{Z} \end{bmatrix} \tag{5.2}$$

The desired values for μ, ν, and l are given by the constants μ_d, ν_d, and l_d, respectively.

Now, let $\xi = col\,(v,\omega)$, with $v,\omega \in \mathbb{R}^3$, be the camera velocity vector in inertial frame where $v = col\,(v_X, v_Y, v_Z)$, and $\omega = col\,(\omega_X, \omega_Y, \omega_Z)$, are the linear and angular velocity, respectively. Using these variables, the relationship between the position of the gripper with a camera in inertial frame, and the position of the object in camera frame can be given by

$$\begin{bmatrix} \dot{\mu} \\ \dot{\nu} \\ \dot{l} \end{bmatrix} = \underbrace{\begin{bmatrix} -\frac{l}{L} & 0 & \frac{l\mu}{fL} & \frac{\mu\nu}{f} & -f-\frac{\mu^2}{f} & \nu \\ 0 & -\frac{l}{L} & \frac{l\nu}{fL} & f+\frac{\nu^2}{f} & -\frac{\nu\mu}{f} & -\mu \\ 0 & 0 & -\frac{l^2}{fL} & \frac{l\nu}{f} & -\frac{l\mu}{f} & 0 \end{bmatrix}}_{\Delta(\mu,\nu,l)} \begin{bmatrix} v_X \\ v_Y \\ v_Z \\ \omega_X \\ \omega_Y \\ \omega_Z \end{bmatrix} \tag{5.3}$$

where $\Delta(\mu,\nu,l) \in \mathbb{R}^{3\times 6}$ denotes the *interaction matrix* (image Jacobian) [9, 11, 24]. The steps to construct the interaction matrix are based on the Section 12.3.2 of [53]. The interaction matrix relates the camera velocity to image features velocity and it is a function of the image coordinates [15, 53].

Let $\tau = col\,(\mu,\nu,l)$, $\tau \in \mathbb{R}^3$, denote the vector of feature values that can be measured in an image. Its derivative $\dot{\tau} \in \mathbb{R}^3$ is referred to as an *image features velocity*. We now turn attention back to system (2.2). Using the kinematic equation

$$\xi = \begin{bmatrix} v \\ \omega \end{bmatrix} = \begin{bmatrix} \mathscr{J}_v(q)\,\dot{q} \\ \mathscr{J}_\omega(q)\,\dot{q} \end{bmatrix} = \mathscr{J}(q)\,\dot{q} \tag{5.4}$$

where $\mathscr{J}_v(q) \in \mathbb{R}^{3\times n}$, and $\mathscr{J}_\omega(q) \in \mathbb{R}^{3\times n}$ are the linear, and angular geometric Jacobians, respectively, and

$$\mathscr{J}(q) = \begin{bmatrix} \mathscr{J}_v(q) \\ \mathscr{J}_\omega(q) \end{bmatrix} \in \mathbb{R}^{6\times n} \tag{5.5}$$

is the geometric Jacobian of a robot manipulator [53]. The dynamics of the visual servo takes the form

$$\dot{\tau} = \Delta(\tau)\,\xi = \underbrace{\Delta(\tau)\,\mathscr{J}(q)}_{\Delta_\tau(q,\tau)}\dot{q} = \Delta_\tau(q,\tau)\,M(q)^{-1}\,p = \Delta_\tau(q,\tau)\,T(q)^{-\top}\,T(q)^{-1}\,p \tag{5.6}$$

where $\Delta_\tau(q,\tau) \in \mathbb{R}^{3\times n}$. Using the coordinate transformation (2.31), (2.32), $\bar{H}(\bar{q},\bar{p})$ as in (2.34), and

$$\bar{\Delta}(\bar{q},\bar{\tau}) = \Delta_\tau\left(\Phi^{-1}(\bar{q}),\bar{\tau}\right) \tag{5.7}$$

we then rewrite (5.6) as

$$\dot{\tau} = \bar{\Delta}(\bar{q},\bar{\tau})\,\bar{T}(\bar{q})^{-\top}\,\bar{p} = \bar{\Delta}(\bar{q},\bar{\tau})\,\bar{T}(\bar{q})^{-\top}\,\frac{\partial \bar{H}(\bar{q},\bar{p},\tau)}{\partial \bar{p}} \tag{5.8}$$

Using this and (2.35), the extended system-camera dynamics is written as

$$\begin{bmatrix} \dot{\bar{q}} \\ \dot{\bar{p}} \\ \dot{\tau} \end{bmatrix} = \begin{bmatrix} 0_{n\times n} & \bar{T}(\bar{q})^{-\top} & 0_{n\times n} \\ -\bar{T}(\bar{q})^{-1} & \bar{J}_2(\bar{q},\bar{p}) - \bar{D}(\bar{q},\bar{p}) & 0_{n\times n} \\ 0_{n\times n} & \bar{\Delta}(\bar{q},\bar{\tau})\,\bar{T}(\bar{q})^{-\top} & 0_{n\times n} \end{bmatrix} \begin{bmatrix} \dfrac{\partial \bar{H}(\bar{q},\bar{p},\tau)}{\partial \bar{q}} \\ \dfrac{\partial \bar{H}(\bar{q},\bar{p},\tau)}{\partial \bar{p}} \\ \dfrac{\partial \bar{H}(\bar{q},\bar{p},\tau)}{\partial \tau} \end{bmatrix} + \begin{bmatrix} 0_{n\times n} \\ \bar{G}(\bar{q}) \\ 0_{n\times n} \end{bmatrix} v \tag{5.9}$$

with $\bar{H}(\bar{q},\bar{p},\tau)$ as in (2.34). Note that the matrix

$$\tilde{J}(\bar{q},\bar{p},\tau) = \begin{bmatrix} 0_{n\times n} & \bar{T}(\bar{q})^{-\top} & 0_{n\times n} \\ -\bar{T}(\bar{q})^{-1} & \bar{J}_2(\bar{q},\bar{p}) & 0_{n\times n} \\ 0_{n\times n} & \bar{\Delta}(\bar{q},\bar{\tau})\,\bar{T}(\bar{q})^{-\top} & 0_{n\times n} \end{bmatrix} \tag{5.10}$$

is not skew-symmetric, and so (5.9) is not a port-Hamiltonian system representation.

5.2 Image-based visual servo control

Consider the system in (5.9) modeling the n-dof robot manipulator with eye-in-hand camera, discussed in the previous section. The objective of this section is to design a feedback $v(\bar{q},\bar{p},\tau)$ to stabilize (5.9) to a desired position of a fixed object to be grasped. This can be stated as the objective to design $v(\bar{q},\bar{p},\tau)$ to asymptotically stabilize the set $\{(\bar{q},\bar{p},\tau) : \bar{p} = 0, \tau = \tau_d\}$ for (5.9), where $\tau_d = col\,(\mu_d, \nu_d, l_d) \in \mathbb{R}^3$, denotes the desired value of the image features variables τ (refer to the image plane in Figure 5.2). Note that in order for this objective to be feasible, τ_d has to correspond to point(s) that lie within the reach space of the manipulator.

Remark 5.2.1 The final position of the end-effector (gripper) in terms of the generalized coordinates, $q = q_d \in \mathbb{R}^n$, is given by substituting τ_d in (5.1) in order to obtain the coordinates (X,Y,Z) (see Figure 5.2), with L, and f being known constants, and then by solving the inverse kinematic problem [53], i.e., $\bar{\tau} = \phi_{\bar{q}}(\bar{q})$ with $\phi_{\bar{q}}$ nonsingular.

Two control design strategies are presented in this Section. One utilizes reduction-based design, while the other relies on realizing a closed-loop port-Hamiltonian system. A key tool in both approaches is the design of new momentum functions, i.e., $\hat{p}$, and

$\tilde{p}$, that incorporate the generalized momentum of the system, $\bar{p}$, and the image features error, $\bar{\tau} = \tau - \tau_d$. This idea is inspired by previous results regarding force, position, and mechanical impedance control of [33, 34, 36], respectively. The work here is also inspired by an IBVS control strategy in the PH framework for a simpler pick and place system in [9, 11], and the change of variables in [10].

5.2.1 Reduction-based approach

Let

$$\bar{\tau} = \tau - \tau_d \tag{5.11}$$

denote the error in the image features variables, and consider the following new momentum variables

$$\hat{p} = \bar{p} + \bar{T}(\bar{q})^{\top} K_{\tau} \bar{\tau} \tag{5.12}$$

where $K_{\tau} \in \mathbb{R}^{n \times 3}$ is a constant matrix, and $\bar{T}(\bar{q})$ is as in (2.33). The time derivative of $\hat{p}$ along the dynamics (5.9) takes the form

$$\begin{aligned} \dot{\hat{p}} &= \dot{\bar{p}} + \bar{T}(\bar{q})^{\top} K_{\tau} \dot{\bar{\tau}} + \dot{\bar{T}}(\bar{q})^{\top} K_{\tau} \bar{\tau} \\ &= \left(\bar{J}_2(\bar{q}, \bar{p}) - \bar{D}(\bar{q}, \bar{p})\right) \frac{\partial \bar{H}(\bar{q}, \bar{p})}{\partial \bar{p}} + \bar{G}(\bar{q}) v + \bar{T}(\bar{q})^{\top} K_{\tau} \dot{\bar{\tau}} + \dot{\bar{T}}(\bar{q})^{\top} K_{\tau} \bar{\tau} \end{aligned} \tag{5.13}$$

where $\bar{H}(\bar{q}, \bar{p})$ is given in (2.34), $\dot{\bar{T}}(\bar{q})$ is the time derivative of $\bar{T}(\bar{q})$ along (5.9), and

$$\dot{\bar{\tau}} = \bar{\Delta}(\bar{q}, \bar{\tau}) \bar{T}(\bar{q})^{-\top} \frac{\partial \bar{H}(\bar{q}, \bar{p})}{\partial \bar{p}} \tag{5.14}$$

Using (2.34) and (5.12), this can be rewritten as

$$\dot{\bar{\tau}} = \bar{\Delta}(\bar{q}, \bar{\tau}) \bar{T}(\bar{q})^{-\top} \hat{p} - \bar{\Delta}(\bar{q}, \bar{\tau}) K_{\tau} \bar{\tau} \tag{5.15}$$

Consider the following feedback

$$\begin{aligned} v = &\bar{G}(\bar{q})^{-1} \Big(-K_p \hat{p} + \left(\bar{J}_2(\bar{q}, \bar{p}) - \bar{D}(\bar{q}, \bar{p})\right) \bar{T}(\bar{q})^{\top} K_{\tau} \bar{\tau} - \dot{\bar{T}}(\bar{q})^{\top} K_{\tau} \bar{\tau} \\ &- \bar{T}(\bar{q})^{\top} K_{\tau} \left(\bar{\Delta}(\bar{q}, \bar{\tau}) \bar{T}(\bar{q})^{-\top} \hat{p} - \bar{\Delta}(\bar{q}, \bar{\tau}) K_{\tau} \bar{\tau} \right) \Big) \end{aligned} \tag{5.16}$$

where $K_p \in \mathbb{R}^{n \times n}$ is a constant positive definite matrix. We assume here that $\bar{G}(\bar{q})^{-1}$ is well defined for all $\bar{q}$ in the reach space of the manipulator. Substituting this feedback into (5.13) gives

$$\dot{\hat{p}} = \left(\bar{J}_2(\bar{q}, \bar{p}) - \bar{D}(\bar{q}, \bar{p})\right) \hat{p} - K_p \hat{p} \tag{5.17}$$

Now, consider the candidate Lyapunov function

$$\tilde{V} = \frac{1}{2}\hat{p}^\top \hat{p} \tag{5.18}$$

Using (5.17), the time derivative of $\tilde{V}$ along the closed-loop system (5.9)-(5.16) takes the form

$$\dot{\tilde{V}} = -\hat{p}^\top \left(D\left(\bar{q},\bar{p}\right) + K_p\right)\hat{p} \tag{5.19}$$

This implies that the set $\{(\bar{q},\bar{p},\tau) : \hat{p} = 0\}$ (the zero level set of $\tilde{V}$, $\tilde{V}^{-1}(0)$) is asymptotically (in fact exponentially) stable for the closed-loop system, and globally so if all closed-loop solution are well defined.

Note that the previous feedback renders $\tilde{V}^{-1}(0)$ positively invariant. The restriction of the dynamics (5.15) to this set takes the form

$$\dot{\bar{\tau}} = -\bar{\Delta}\left(\bar{q},\bar{\tau}\right) K_\tau \bar{\tau} \tag{5.20}$$

From this it follows that a necessary condition for the set $\{(\bar{q},\bar{p},\tau) : \bar{p} = 0, \tau = \tau_d\}$ to be asymptotically stable for the closed-loop system (5.9)-(5.16) is that the origin of the dynamics (5.20) is asymptotically stable. The question then becomes whether this condition is also necessary. This question lies in what is called the *reduction problem*. This problem was first addressed for the stability of compact sets in [49].

The following result follows from the previous developments.

Theorem 5.2.2 *Consider system* (5.9)*. The feedback*

$$\begin{aligned} v = &\bar{G}\left(\bar{q}\right)^{-1}\Big(-K_p\hat{p} + \left(\bar{J}_2\left(\bar{q},\bar{p}\right) - \bar{D}\left(\bar{q},\bar{p}\right)\right)\bar{T}\left(\bar{q}\right)^\top K_\tau \bar{\tau} - \dot{\bar{T}}\left(\bar{q}\right)^\top K_\tau \bar{\tau} \\ &-\bar{T}\left(\bar{q}\right)^\top K_\tau \Big(\bar{\Delta}\left(\bar{q},\bar{\tau}\right)\bar{T}\left(\bar{q}\right)^{-\top}\hat{p} - \bar{\Delta}\left(\bar{q},\bar{\tau}\right)K_\tau\bar{\tau}\Big)\Big) \end{aligned} \tag{5.21}$$

where $K_\tau \in \mathbb{R}^{n\times 3}$, $K_p \in \mathbb{R}^{n\times n}$, $K_p > 0$, are constant matrices, and $\bar{\tau} = \tau - \tau_d$, renders the following:

a. The set $\{(\bar{q},\bar{p},\tau) : \bar{p} = 0, \tau = \tau_d\}$ asymptotically stable for the closed-loop system provided that $\bar{G}\left(\bar{q}\right)^{-1}$ is well defined locally around the set, and the origin of the dynamics (5.20) *is asymptotically stable.*

b. The set $\{(\bar{q},\bar{p},\tau) : \bar{p} = 0, \tau = \tau_d\}$ globally asymptotically stable for the closed-loop system provided that $\bar{G}\left(\bar{q}\right)^{-1}$ is well defined for all $\bar{q}$ in the reach space of (5.9)*, and the origin of the dynamics* (5.20) *is globally asymptotically stable.*

Proof. Part a. follows directly from the previous developments and Theorem III.2 in [14].

The same applies to Part b. provided that all closed-loop solution are well defined. This follows directly, from (5.19), if the reach space of the manipulator is bounded. ■

5.2.2 Hamiltonian-based approach

The first strategy relies on the direct readings of the camera system without any assumption on the invertibility of the interaction matrix. The second proposed strategy does require that assumption though. It is realized via a change of variables that represents a new adapted momenta which is in terms of a more general function that depends directly on the geometry of the vision system, and the kinematics of the robot manipulator. Furthermore, this strategy depends on potential energy shaping $\frac{\partial \bar{H}(\bar{q},\bar{p})}{\partial \bar{q}}$ with $\bar{H}(\bar{q},\bar{p})$ as in (2.34), and damping injection via the image features error $\bar{\tau}$.

Consider a matrix $\bar{\Delta}(\bar{q},\bar{\tau}) \in \mathbb{R}^{3\times n}$,

$$\bar{\Delta}(\bar{q},\bar{\tau}) = \Delta(\tau)\, \mathscr{J}(q) \tag{5.22}$$

with the geometric Jacobian $\mathscr{J}(q) \in \mathbb{R}^{6\times n}$, and an interaction matrix $\Delta(\tau) \in \mathbb{R}^{3\times 6}$, such that its right inverse $\bar{\Delta}(\bar{q},\bar{\tau})^{\dagger}$ is given by

$$\bar{\Delta}(\bar{q},\bar{\tau})^{\dagger} = \bar{\Delta}(\bar{q},\bar{\tau})^{\top} \left(\bar{\Delta}(\bar{q},\bar{\tau})\bar{\Delta}(\bar{q},\bar{\tau})^{\top}\right)^{-1} \tag{5.23}$$

Using the change of variables

$$\tilde{p} = \phi_{\bar{p}}(\bar{q},\bar{p},\bar{\tau}) \tag{5.24}$$

$$= \bar{p} + \theta(\bar{q},\bar{\tau}) \tag{5.25}$$

with $\theta(\bar{q},\bar{\tau}) \in \mathbb{R}^n$, where

$$\theta(\bar{q},\bar{\tau}) = \bar{T}(\bar{q})^{\top} \bar{\Delta}(\bar{q},\bar{\tau})^{\dagger} \bar{\tau} \tag{5.26}$$

We get the following.

Theorem 5.2.3 *Consider the port-Hamiltonian system* (5.9)*, nonsingular matrices* $\bar{G}(\bar{q}) \in \mathbb{R}^{n\times n}$*,* $\bar{\Delta}(\bar{q},\bar{\tau}) \in \mathbb{R}^{3\times n}$ *as in* (5.22)*, and a matrix* $C > 0$*,* $C \in \mathbb{R}^{n\times n}$*. Then, the control input*

$$\begin{aligned} v = \bar{G}(\bar{q})^{-1} \Bigg[& \bar{T}(\bar{q})^{-1} \frac{\partial \bar{H}(\bar{q},\bar{p})}{\partial \bar{q}} + (\bar{J}_2(\bar{q},\bar{p}) - \bar{D}(\bar{q},\bar{p}))\, \bar{T}(\bar{q})^{\top} \bar{\Delta}(\bar{q},\bar{\tau})^{\dagger} \bar{\tau} \\ & - \beta_1(\bar{q},\bar{\tau})\, \tilde{p} - \beta_2(\bar{q},\bar{\tau})\, \bar{\tau} - \bar{T}(\bar{q})^{-1} \bar{\Delta}(\bar{q},\bar{\tau})^{\top} \bar{\tau} \Bigg] \end{aligned} \tag{5.27}$$

with $\bar{\tau} = \tau - \tau_d$ *and* τ_d *a constant desired image features and with*

$$\beta_1(\bar{q},\bar{\tau}) = -\frac{\partial\theta(\bar{q},\bar{\tau})^\top}{\partial\bar{q}}\bar{T}(\bar{q})^{-\top} + \frac{\partial\theta(\bar{q},\bar{\tau})^\top}{\partial\bar{\tau}}\bar{\Delta}(\bar{q},\bar{\tau})\bar{T}(\bar{q})^{-\top} + C \tag{5.28}$$

$$\beta_2(\bar{q},\bar{\tau}) = -\frac{\partial\theta(\bar{q},\bar{\tau})^\top}{\partial\bar{q}}\bar{\Delta}(\bar{q},\bar{\tau})^\dagger - \frac{\partial\theta(\bar{q},\bar{\tau})^\top}{\partial\bar{\tau}} \tag{5.29}$$

asymptotically stabilizes the system (5.9) *at* $\tau = \tau_d$.

Proof. From (2.31) we obtain

$$\dot{\bar{q}} = \dot{q} = M(q)^{-1} p = \bar{T}(\bar{q})^{-\top}\bar{p} \tag{5.30}$$

and based on the adapted momenta $\tilde{p}$ as in (5.25) we write

$$\dot{\bar{q}} = -\bar{T}(\bar{q})^{-\top}\theta(\bar{q},\bar{\tau}) + \bar{T}(\bar{q})^{-\top}\tilde{p} \tag{5.31}$$

and if we substitute $\theta(\bar{q},\bar{\tau})$ as in (5.26) in (5.31) we obtain

$$\dot{\bar{q}} = -\bar{T}(\bar{q})^{-\top}\bar{T}(\bar{q})^{\top}\bar{\Delta}(\bar{q},\bar{\tau})^\dagger\bar{\tau} + \bar{T}(\bar{q})^{-\top}\tilde{p} = -\bar{\Delta}(\bar{q},\bar{\tau})^\dagger\bar{\tau} + \bar{T}(\bar{q})^{-\top}\tilde{p} \tag{5.32}$$

From (5.25) we know that

$$\dot{\tilde{p}} = \dot{\bar{p}} + \frac{\partial\theta(\bar{q},\bar{\tau})^\top}{\partial\bar{q}}\dot{\bar{q}} + \frac{\partial\theta(\bar{q},\bar{\tau})^\top}{\partial\bar{\tau}}\dot{\bar{\tau}} \tag{5.33}$$

Furthermore, from (5.9) we have

$$\dot{\bar{p}} = -\bar{T}(\bar{q})^{-1}\frac{\partial\bar{H}(\bar{q},\bar{p})}{\partial\bar{q}} + (\bar{J}_2(\bar{q},\bar{p}) - \bar{D}(\bar{q},\bar{p}))\frac{\partial\bar{H}(\bar{q},\bar{p})}{\partial\bar{p}} + \bar{G}(\bar{q})v \tag{5.34}$$

and with $\dot{\bar{\tau}} = \dot{\tau}$, and $\dot{\bar{q}} = \dot{q}$, then from (5.6), (5.22), (5.26), (5.30), and (5.31), we obtain

$$\begin{aligned}
\dot{\bar{\tau}} &= \Delta(\tau)\mathscr{J}(q)\dot{q} \\
&= \Delta(\tau)\mathscr{J}(q)\bar{T}(\bar{q})^{-\top}\left(-\bar{T}(\bar{q})^{\top}\bar{\Delta}(\bar{q},\bar{\tau})^\dagger\bar{\tau} + \tilde{p}\right) \\
&= -\underbrace{\Delta(\tau)\mathscr{J}(q)}_{\bar{\Delta}(\bar{q},\bar{\tau})}\bar{\Delta}(\bar{q},\bar{\tau})^\dagger\bar{\tau} + \underbrace{\Delta(\tau)\mathscr{J}(q)}_{\bar{\Delta}(\bar{q},\bar{\tau})}\bar{T}(\bar{q})^{-\top}\tilde{p} \\
&= -\bar{\tau} + \bar{\Delta}(\bar{q},\bar{\tau})\bar{T}(\bar{q})^{-\top}\tilde{p}
\end{aligned} \tag{5.35}$$

where $\bar{\Delta}(\bar{q},\bar{\tau})\bar{\Delta}(\bar{q},\bar{\tau})^\dagger = I_{3\times3}$. If we substitute $\dot{\bar{q}}$, $\dot{\tilde{p}}$, and $\dot{\bar{\tau}}$, as in (5.32), (5.34), and (5.35), in the right side of (5.33) we obtain the open-loop dynamics of our adapted momenta $\dot{\tilde{p}}$,

i.e.,

$$\dot{\tilde{p}} = -\bar{T}(\bar{q})^{-1}\frac{\partial \bar{H}(\bar{q},\bar{p})}{\partial \bar{q}} + (\bar{J}_2(\bar{q},\bar{p}) - \bar{D}(\bar{q},\bar{p}))\frac{\partial \bar{H}(\bar{q},\bar{p})}{\partial \bar{p}} + \bar{G}(\bar{q})v + \frac{\partial \theta(\bar{q},\bar{\tau})^\top}{\partial \bar{q}}\left(\bar{\Delta}(\bar{q},\bar{\tau})^\dagger \bar{\tau} + \bar{T}(\bar{q})^{-\top}\tilde{p}\right) + \frac{\partial \theta(\bar{q},\bar{\tau})^\top}{\partial \bar{\tau}}\left(-\bar{\tau} + \bar{\Delta}(\bar{q},\bar{\tau})\bar{T}(\bar{q})^{-\top}\tilde{p}\right) \tag{5.36}$$

and given the control law v as in (5.27) with $\beta_1(\bar{q},\bar{\tau})$, and $\beta_2(\bar{q},\bar{\tau})$ as in (5.28), (5.29), respectively, we then obtain the closed-loop dynamics of $\dot{\tilde{p}}$ in terms of $(\bar{q},\tilde{p},\bar{\tau})$, i.e.,

$$\begin{aligned}
\dot{\tilde{p}} = {} & -\bar{T}(\bar{q})^{-1}\frac{\partial \bar{H}(\bar{q},\bar{p})}{\partial \bar{q}} + (\bar{J}_2(\bar{q},\bar{p}) - \bar{D}(\bar{q},\bar{p}))\frac{\partial \bar{H}(\bar{q},\bar{p})}{\partial \bar{p}} \\
& + \frac{\partial \theta(\bar{q},\bar{\tau})^\top}{\partial \bar{q}}\left(-\bar{\Delta}(\bar{q},\bar{\tau})^\dagger \bar{\tau} + \bar{T}(\bar{q})^{-\top}\tilde{p}\right) + \frac{\partial \theta(\bar{q},\bar{\tau})^\top}{\partial \bar{\tau}}\left(-\bar{\tau} + \bar{\Delta}(\bar{q},\bar{\tau})\bar{T}(\bar{q})^{-\top}\tilde{p}\right) \\
& + \bar{G}(\bar{q})\bar{G}(\bar{q})^{-1}\left[\bar{T}(\bar{q})^{-1}\frac{\partial \bar{H}(\bar{q},\bar{p})}{\partial \bar{q}} + (\bar{J}_2(\bar{q},\bar{p}) - \bar{D}(\bar{q},\bar{p}))\bar{T}(\bar{q})^\top \bar{\Delta}(\bar{q},\bar{\tau})^\dagger \bar{\tau}\right. \\
& - \left(-\frac{\partial \theta(\bar{q},\bar{\tau})^\top}{\partial \bar{q}}\bar{T}(\bar{q})^{-\top} + \frac{\partial \theta(\bar{q},\bar{\tau})^\top}{\partial \bar{\tau}}\bar{\Delta}(\bar{q},\bar{\tau})\bar{T}(\bar{q})^{-\top} + C\right)\tilde{p} \\
& \left. - \left(-\frac{\partial \theta(\bar{q},\bar{\tau})^\top}{\partial \bar{q}}\bar{\Delta}(\bar{q},\bar{\tau})^\dagger - \frac{\partial \theta(\bar{q},\bar{\tau})^\top}{\partial \bar{\tau}}\right)\bar{\tau} - \bar{T}(\bar{q})^{-1}\bar{\Delta}(\bar{q},\bar{\tau})^\top \bar{\tau}\right] \\
= {} & (\bar{J}_2(\bar{q},\bar{p}) - \bar{D}(\bar{q},\bar{p}) - C)\tilde{p} - \bar{T}(\bar{q})^{-1}\bar{\Delta}(\bar{q},\bar{\tau})^\top \bar{\tau}
\end{aligned} \tag{5.37}$$

with $J_2(\bar{q},\bar{p})$ as in (2.37). We choose a smooth function $\tilde{U}(\bar{q},\bar{p},\bar{\tau})$ such that

$$\tilde{U}(\bar{q},\bar{p},\bar{\tau}) = \bar{p}^\top \theta(\bar{q},\bar{\tau}) - \bar{V}(\bar{q}) + \frac{1}{2}\theta(\bar{q},\bar{\tau})^\top \theta(\bar{q},\bar{\tau}) + \frac{1}{2}\bar{\tau}^\top \bar{\tau} \tag{5.38}$$

with $\bar{V}(\bar{q})$ from (2.35). We then realize a candidate Lyapunov function $\tilde{H}(\tilde{p},\bar{\tau}) > 0$ based on Hamiltonian $\bar{H}(\bar{q},\bar{p})$ as in (2.34), $\tilde{U}(\bar{q},\bar{p},\bar{\tau})$ as in (5.38), and $\tilde{p}$ as in (5.25), i.e,

$$\begin{aligned}
\tilde{H}(\tilde{p},\bar{\tau}) &= \bar{H}(\bar{q},\bar{p}) + \tilde{U}(\bar{q},\bar{p},\bar{\tau}) \\
&= \frac{1}{2}\bar{p}^\top \bar{p} + \bar{V}(\bar{q}) + \bar{p}^\top \theta(\bar{q},\bar{\tau}) - \bar{V}(\bar{q}) + \frac{1}{2}\theta(\bar{q},\bar{\tau})^\top \theta(\bar{q},\bar{\tau}) + \frac{1}{2}\bar{\tau}^\top \bar{\tau} \\
&= \frac{1}{2}(\bar{p} + \theta(\bar{q},\bar{\tau}))^\top (\bar{p} + \theta(\bar{q},\bar{\tau})) + \frac{1}{2}\bar{\tau}^\top \bar{\tau} \\
&= \frac{1}{2}\tilde{p}^\top \tilde{p} + \frac{1}{2}\bar{\tau}^\top \bar{\tau}
\end{aligned} \tag{5.39}$$

Given now the nonsingular functions $\bar{q} = \phi_{\bar{q}}^{-1}(\bar{\tau})$ as in Remark 5.2.1, $\bar{p} = \phi_{\bar{p}}^{-1}(\tilde{p})$ as in

(5.24), we rewrite $\bar{J}_2(\bar{q},\bar{p})$, $\bar{D}(\bar{q},\bar{p})$, $\bar{\Delta}(\bar{q},\bar{\tau})$, and $\bar{T}(\bar{q})$, as

$$\bar{J}_2(\bar{q},\bar{p}) = \bar{J}_2\left(\phi_{\bar{q}}^{-1}(\bar{\tau}),\phi_{\bar{p}}^{-1}(\tilde{p})\right) = \tilde{J}_2(\tilde{p},\bar{\tau}) \tag{5.40}$$

$$\bar{D}(\bar{q},\bar{p}) = \bar{D}\left(\phi_{\bar{q}}^{-1}(\bar{\tau}),\phi_{\bar{p}}^{-1}(\tilde{p})\right) = \tilde{D}(\tilde{p},\bar{\tau}) \tag{5.41}$$

$$\bar{\Delta}(\bar{q},\bar{\tau}) = \bar{\Delta}\left(\phi_{\bar{q}}^{-1}(\bar{\tau}),\bar{\tau}\right) = \hat{\Delta}(\bar{\tau}) \tag{5.42}$$

$$\bar{T}(\bar{q}) = \bar{T}\left(\phi_{\bar{q}}^{-1}(\bar{\tau})\right) = \tilde{T}(\bar{\tau}) \tag{5.43}$$

Hence, the dynamics $\dot{\tilde{p}}$ as in (5.37), and $\dot{\bar{\tau}}$ as in (5.35), results in

$$\dot{\tilde{p}} = \left(\tilde{J}_2(\tilde{p},\bar{\tau}) - \tilde{D}(\tilde{p},\bar{\tau}) - C\right)\frac{\partial \tilde{H}(\tilde{p},\bar{\tau})}{\partial \tilde{p}} - \tilde{T}(\bar{\tau})^{-1}\hat{\Delta}(\bar{\tau})^{\top}\frac{\partial \tilde{H}(\tilde{p},\bar{\tau})}{\partial \bar{\tau}} \tag{5.44}$$

$$\dot{\bar{\tau}} = \hat{\Delta}(\bar{\tau})\tilde{T}(\bar{\tau})^{-\top}\frac{\partial \tilde{H}(\tilde{p},\bar{\tau})}{\partial \tilde{p}} - \frac{\partial \tilde{H}(\tilde{p},\bar{\tau})}{\partial \bar{\tau}} \tag{5.45}$$

where resulting in the closed-loop system

$$\begin{bmatrix} \dot{\tilde{p}} \\ \dot{\bar{\tau}} \end{bmatrix} = \begin{bmatrix} \tilde{J}_2(\tilde{p},\bar{\tau}) - \tilde{D}(\tilde{p},\bar{\tau}) - C & -\tilde{T}(\bar{\tau})^{-1}\hat{\Delta}(\bar{\tau})^{\top} \\ \hat{\Delta}(\bar{\tau})\tilde{T}(\bar{\tau})^{-\top} & -I_{3\times 3} \end{bmatrix} \begin{bmatrix} \dfrac{\partial \tilde{H}(\tilde{p},\bar{\tau})}{\partial \tilde{p}} \\ \dfrac{\partial \tilde{H}(\tilde{p},\bar{\tau})}{\partial \bar{\tau}} \end{bmatrix} \tag{5.46}$$

with Hamiltonian (5.39), and $\tilde{H}(\tilde{p},\bar{\tau}) \geqslant 0$. We now compute the power balance $\dot{\tilde{H}}(\tilde{p},\bar{\tau})$ as

$$\begin{aligned} \dot{\tilde{H}}(\tilde{p},\bar{\tau}) &= \frac{\partial \tilde{H}(\tilde{p},\bar{\tau})}{\partial \tilde{p}}^{\top}\dot{\tilde{p}} + \frac{\partial \tilde{H}(\tilde{p},\bar{\tau})}{\partial \bar{\tau}}^{\top}\dot{\bar{\tau}} \\ &= -\tilde{p}^{\top}\left(\tilde{D}(\tilde{p},\bar{\tau}) + C\right)\tilde{p} - \bar{\tau}^{\top}\bar{\tau} \leqslant 0 \end{aligned} \tag{5.47}$$

Since $\tilde{D}(\tilde{p},\bar{\tau}) \geqslant 0$, and $C > 0$, thus (5.47) holds. The closed-loop system (5.46) is asymptotically stable at $(\tilde{p},\bar{\tau}) = (0,0)$, and hence $\tau = \tau_d$. ■

Remark 5.2.4 The constant matrix C of the control law (5.27) represents damping injection in the closed-loop system (5.46) when we define an output $\tilde{y}$ such that

$$\tilde{y} = \bar{G}(\bar{q})^{\top}\frac{\partial \tilde{H}(\tilde{p},\bar{\tau})}{\partial \tilde{p}} = \bar{G}(\bar{q})^{\top}\tilde{p} \tag{5.48}$$

with $\tilde{H}(\tilde{p},\bar{\tau})$ as in (5.39), and $\bar{G}(\bar{q}) = I_{n\times n}$.

5.3 Discussion

Via the control law of Theorem 5.2.2 in (5.21), and Theorem 5.2.3 in (5.27), we are able to stabilize the system in (5.9) to the desired image features, $\tau = \tau_d$, which means that the end-effector is in a grasping distance configuration. The realization of an adapted momenta is the key in the development of our control law strategies. The adapted momenta $\hat{p}$ and $\tilde{p}$ as in (5.12) and (5.25), respectively, depend on the error in the image features variables $\bar{\tau}$, and the mass-inertia matrix decomposition $\bar{T}(\bar{q})$. Moreover, $\tilde{p}$ also depends on invertibility properties of the interaction matrix $\bar{\Delta}(\bar{q}, \bar{\tau})$. The control law in (5.21) uses a reduction-design approach [14, 49] to prove asymptotic (exponential) stability of a closed-loop system with the help of the candidate Lyapunov function (5.18). The advantage of (5.21) is that there is no dependence of the inverse of the interaction matrix, while the control law in (5.27) implies the computation of a right inverse matrix (5.23). Moreover, via the second control law, we have realized a closed-loop PH system. Since the system is PH, interconnection and structure preservation is possible with other PH systems. The implementation of both control laws is given in the following section, where we demonstrate their applicability via simulations.

5.4 Example

In this Section we apply the designed controllers in Section 5.2 to a three-dof robot manipulator model with an eye-in-hand camera configuration. First, we derive the PH model (2.35) using the *Denavit-Hartenberg* parameters of the robot, [53]. Then, we obtain the interaction matrix $\bar{\Delta}(\bar{q}, \bar{\tau})$ of the camera dynamics. Finally, we present simulation results for both control approaches.

We use a three-dof shoulder and elbow Philips Experimental Robot Arm (PERA), [45]. A picture of the PERA is shown in Figure 2.1. The shoulder and elbow of the PERA consist of two links actuated by four motors. The Denavit-Hartenberg parameters are given in Table 5.1.

Table 5.1: Denavit-Hartenberg parameters for the shoulder and elbow links of the PERA.

Link i	a_i	α_i	d_i	q_i
1	0	$\frac{\pi}{2}$	0	q_1
2	0.32	0	0	q_2
3	0.28	$\frac{\pi}{2}$	0	q_3

The model of the arm consists of masses m_i, link lengths a_i, distances to the center of masses equal to a_{C_i}, and moments of inertia $\mathscr{I}_i$, with $i = 1,2,3$ the number of dof. The states of the system are $x = (q,p)^\top$, where $(q,p) \in \mathbb{R}^3$ are the generalized coordinates and the generalized momenta, respectively, and q_i being the angle of the Link i. Based now on Table 1, we are able to compute the mass-inertia matrix $M(q) \in \mathbb{R}^{3\times 3}$ as

$$M(q) = \begin{bmatrix} \bar{m}_1 & 0 & 0 \\ 0 & \bar{m}_2 & \bar{m}_3 \\ 0 & \bar{m}_3 & \bar{m}_4 \end{bmatrix} \tag{5.49}$$

where

$$\begin{aligned}
\bar{m}_1 &= \mathscr{I}_1 + \mathscr{I}_2 + \mathscr{I}_3 + \frac{1}{2}a_{C_3}^2(m_2+m_3) + \frac{1}{2}a_2^2 m_3(1+\cos(2q_2)) \\
&\quad + a_{C_3}^2\left(\frac{1}{2}m_2\cos(2q_2) + \frac{1}{2}m_3\cos(2q_2+2q_3) + a_2^2 m_3(\cos(q_3)+\cos(2q_2+q_3))\right) \\
\bar{m}_2 &= \mathscr{I}_2 + \mathscr{I}_3 + a_{C_3}^2(m_2+m_3) + a_2^2 m_3\left(1+2a_{C_3}^2\cos(q_3)\right) \\
\bar{m}_3 &= \mathscr{I}_3 + a_{C_3}^2 m_3\left(1+a_2^2\cos(q_3)\right) \\
\bar{m}_4 &= \mathscr{I}_3 + a_{C_3}^2 m_3
\end{aligned}$$

which can be decomposed in a lower triangular matrix given by

$$T(q) = \begin{bmatrix} \sqrt{\bar{m}_1} & 0 & 0 \\ 0 & \sqrt{\bar{m}_2} & 0 \\ 0 & \dfrac{\bar{m}_3}{\sqrt{\bar{m}_2}} & \sqrt{\dfrac{\bar{m}_2\bar{m}_4 - \bar{m}_3^2}{\bar{m}_2}} \end{bmatrix} \tag{5.50}$$

and since $\bar{m}_k > 0$, with $k = 0,1,2,3$, holds, $M(q) = T(q)\,T(q)^\top$ as in (2.33). Furthermore,

the potential energy vector is given by

$$\frac{\partial V(q)}{\partial q} = \begin{bmatrix} \bar{g}_1 \\ \bar{g}_2 \\ \bar{g}_3 \end{bmatrix} \tag{5.51}$$

with $\bar{g}_1$, $\bar{g}_2$, and $\bar{g}_3$ given by

$$\begin{aligned} \bar{g}_1 &= g\sin(q_1)\left(a_{C_3} m_2 \cos(q_2) + m_3\left(a_2\cos(q_2) + a_{C_3}\cos(q_2+q_3)\right)\right) \\ \bar{g}_2 &= g\cos(q_1)\left(a_{C_3} m_2 \sin(q_2) + m_3\left(a_2\sin(q_2) + a_{C_3}\sin(q_2+q_3)\right)\right) \\ \bar{g}_3 &= m_3 g a_{C_3}\cos(q_1)\sin(q_2+q_3) \end{aligned}$$

respectively, where $g = 9.81 m/s^2$ is the gravitational acceleration. We have included in our model a dissipation matrix $D(q,p)$ as in (2.2), such that

$$D(\dot{q}) = \begin{bmatrix} d_1(\dot{q}_1) & 0 & 0 \\ 0 & d_2(\dot{q}_2) & 0 \\ 0 & 0 & d_3(\dot{q}_3) \end{bmatrix} \tag{5.52}$$

with

$$d_i = \left(F_{c_i} + (F_{s_i} - F_{c_i}) e^{|\dot{q}_i||\dot{q}_{s_i}^{-1}|}\right)\left(\alpha_{f_i} + \dot{q}_i^2\right)^{-0.5} + F_{v_i}\dot{q}_i \tag{5.53}$$

and where F_{c_i}, F_{s_i}, and F_{v_i} are the Coulomb, static, and viscous friction coefficients, respectively; the Coulomb friction force is approximated as in [20] with positive (small) constants α_i; the constant due to the Stribeck velocity [1] is $\dot{q}_{s_i}$, and $i = 1,2,3$. The system is then described in the port-Hamiltonian form by

$$\begin{bmatrix} \dot{q} \\ \dot{p} \end{bmatrix} = \begin{bmatrix} 0_{3\times3} & I_{3\times3} \\ -I_{3\times3} & D(\dot{q}) \end{bmatrix} \begin{bmatrix} \dfrac{\partial V(q)}{\partial q} \\ M(q)^{-1} p \end{bmatrix} + \begin{bmatrix} 0 \\ G(q) \end{bmatrix} u \tag{5.54}$$

with an input matrix $G = I_{3\times3}$ (fully actuated), an output $y = G^\top M(q)^{-1} p$, with $M(q)$ as in (5.49), the potential energy vector $\dfrac{\partial V(q)}{\partial q}$ as in (5.51), a dissipation matrix $D(\dot{q})$ as in (5.52), and a Hamiltonian of the form

$$H(q,p) = \frac{1}{2} p^\top M(q)^{-1} p + V(q) \tag{5.55}$$

5.4.1 Dynamics of the vision system

Here. we present a derivation of the camera dynamics based on the interaction matrix $\Delta(\tau)$ as in (5.3), and the matrix $\tilde{\Delta}(\bar{q},\bar{\tau})$ as in (5.22). We furthermore give the invertibility condition in order to chose between the control law in Theorem 5.2.2 or the one in Theorem 5.2.3. We make use of the geometric Jacobian of the robot arm which is realized via the Denavit-Hartenberg parameters of Table 1. Subsequently, the geometric Jacobian $\mathscr{J}(q) \in \mathbb{R}^{3\times 6}$ is given by the linear and angular Jacobians as in (5.5).

The matrices $\mathscr{J}_v(q) \in \mathbb{R}^{3\times 3}$, and $\mathscr{J}_\omega(q) \in \mathbb{R}^{3\times 3}$ are then given by

$$\mathscr{J}_\omega(q) = \begin{bmatrix} 0 & \sin(q_1) & \sin(q_1) \\ 0 & -\cos(q_1) & \cos(q_1) \\ 1 & 0 & 0 \end{bmatrix} \tag{5.56}$$

$$\mathscr{J}_v(q) = \begin{bmatrix} \eta_{v_{11}} & \eta_{v_{21}} & \eta_{v_{31}} \\ \eta_{v_{12}} & \eta_{v_{22}} & \eta_{v_{32}} \\ \eta_{v_{13}} & \eta_{v_{23}} & \eta_{v_{33}} \end{bmatrix} \tag{5.57}$$

$$\begin{aligned}
\eta_{v_{11}} &= -\sin(q_1)\left(a_{l_2}\cos(q_2) + a_{C_3}\cos(q_2+q_3)\right) \\
\eta_{v_{12}} &= \cos(q_1)\left(a_{l_2}\cos(q_2) + a_{C_3}\cos(q_2+q_3)\right) \\
\eta_{v_{13}} &= 0 \\
\eta_{v_{21}} &= -\cos(q_1)\left(a_{l_2}\sin(q_2) + a_{C_3}\sin(q_2+q_3)\right) \\
\eta_{v_{22}} &= -\sin(q_1)\left(a_{l_2}\sin(q_2) + a_{C_3}\sin(q_2+q_3)\right) \\
\eta_{v_{23}} &= a_{l_2}\cos(q_2) + a_{C_3}\cos(q_2+q_3) \\
\eta_{v_{31}} &= -a_{C_3}\cos(q_1)\cos(q_2+q_3) \\
\eta_{v_{32}} &= a_{C_3}\sin(q_1)\sin(\,q_2+q_3) \\
\eta_{v_{33}} &= a_{C_3}\cos(q_2+q_3)
\end{aligned}$$

Subsequently, we obtain the origin point for the end-effector, i.e., $o(x,y,z)$, in terms of the generalized coordinates of the system (5.54), i.e.,

$$o(x,y,z) = o(q) = \begin{bmatrix} \cos(q_1)\left(a_{l_2}\cos(q_2) + a_{l_3}\cos(q_2+q_3)\right) \\ \sin(q_1)\left(a_{l_2}\cos(q_2) + a_{l_3}\cos(q_2+q_3)\right) \\ a_{l_2}\sin(q_2) + a_{l_3}\sin(q_2+q_3) \end{bmatrix} \tag{5.58}$$

Based on the interaction matrix $\Delta(\tau)$ as in (5.3), the geometric Jacobian $\mathscr{J}(q)$, with $\mathscr{J}_\omega(q)$ and $\mathscr{J}_v(q)$, as in (5.56), and (5.57), respectively, the matrix $\bar{\Delta}(\bar{q},\bar{\tau})$ as in (5.6) is

given as

$$\bar{\Delta}(\bar{q},\bar{\tau}) = \begin{bmatrix} -\frac{l}{L} & 0 & \frac{l\mu}{fL} & \frac{\mu\nu}{f} & -f-\frac{\mu^2}{f} & \nu \\ 0 & -\frac{l}{L} & \frac{l\nu}{fL} & f+\frac{\nu^2}{f} & -\frac{\nu\mu}{f} & -\mu \\ 0 & 0 & -\frac{l^2}{fL} & \frac{l\nu}{f} & -\frac{l\mu}{f} & 0 \end{bmatrix} \begin{bmatrix} \eta_{v_{11}} & \eta_{v_{21}} & \eta_{v_{31}} \\ \eta_{v_{12}} & \eta_{v_{22}} & \eta_{v_{32}} \\ \eta_{v_{13}} & \eta_{v_{23}} & \eta_{v_{33}} \\ 0 & \sin q_1 & \sin q_1 \\ 0 & -\cos q_1 & \cos q_1 \\ 1 & 0 & 0 \end{bmatrix}$$
$$= \begin{bmatrix} \zeta_{11} & \zeta_{12} & \zeta_{13} \\ \zeta_{21} & \zeta_{22} & \zeta_{23} \\ \zeta_{31} & \zeta_{32} & \zeta_{33} \end{bmatrix} \tag{5.59}$$

and the invertibility condition of $\bar{\Delta}(\bar{q},\bar{\tau})$ in (5.59) is given by $\det\bar{\Delta}(\bar{q},\bar{\tau}) \neq 0$ which means that

$$\begin{aligned} \det\bar{\Delta}(\bar{q},\bar{\tau}) &= \zeta_{11}\det\begin{vmatrix} \zeta_{22} & \zeta_{23} \\ \zeta_{32} & \zeta_{33} \end{vmatrix} - \zeta_{12}\det\begin{vmatrix} \zeta_{21} & \zeta_{23} \\ \zeta_{31} & \zeta_{33} \end{vmatrix} + \zeta_{13}\det\begin{vmatrix} \zeta_{21} & \zeta_{22} \\ \zeta_{31} & \zeta_{32} \end{vmatrix} \\ &= \zeta_{11}(\zeta_{22}\zeta_{33}-\zeta_{32}\zeta_{23}) - \zeta_{12}(\zeta_{21}\zeta_{33}-\zeta_{31}\zeta_{23}) + \zeta_{13}(\zeta_{21}\zeta_{32}-\zeta_{31}\zeta_{22}) \neq 0 \end{aligned} \tag{5.60}$$

We have determined numerically that the condition (5.60) holds, which means that we can compare the performance of our two proposed IBVS controllers for our model; we will do so in the sequel.

5.4.2 Simulation results

Here, we perform a simulation of the system in (5.54) that includes the dynamics of the camera. The two developed IBVS control laws, i.e., (5.21) and (5.27), are tested in the model of our robot manipulator. We have determined experimentally the parameters of the shoulder and the elbow of the PERA given by: $F_{c_i} = \{0.5, 0.5, 0.25\}$, $F_{s_i} = \{0.9, 0.9, 0.5\}$, $F_{v_i} = \{0.5, 0.5, 0.2\}$, and $\dot{q}_{s_i} = \{0.2, 0.2, 0.15\}$: masses $m_i = \{2.9, 2.9, 1\}\,kg$, link lengths $a_i = \{0.32, 0.32, 0.28\}\,m$, length to the center of masses $a_{C_i} = \{0.16, 0.16, 0.14\}\,m$, (we assume here that the masses of the links are equally distributed along the link), moments of inertia $\mathscr{I}_i = \{1, 1, 0.5\}$, and constant matrices $K_\tau = diag\,(1, 1, 0.5)$, and $K_p = C = diag\,(0.5, 0.5, 0.5)$. The matrices K_p and C are chosen equal in order to have a fair comparison between the damping injection effect of the controllers (Remark 5.2.4). The camera is assumed to have an image sensor with focal length of $10mm$. The object is assumed to have $38 \times 7.2mm$, and a height $h = 10mm$ (Figure 5.1). The goal is to bring the center of the object to the center of the camera $(\mu_d, \nu_d) = (0, 0)$ (as seen in Figure 5.2),

with a desired object length in the image plane set to $l_d = 2mm$.

Figures 5.3a, 5.3b and 5.3c show that the error trajectories for the camera states $\tau = (\mu, \nu, l)$ converge to zero, which means that the camera positions $o(x, y, z)$ converge to the object position $P(X, Y, Z)$. Moreover, we observe how the control law (5.21) (solid line) exhibits better performance compared to the control law (5.27) (dashed line), which involves the computation of an extra inverse matrix (5.22) that depends on the camera dynamics.

5.5 Concluding remarks

We have presented a PH approach to visual servo control of a standard mechanical system. We have realized an extended model of the system that includes a camera dynamics based on perspective projection modeling, and which introduces nonlinearities in the system. We have developed and implemented in our simulations an interaction matrix that includes the depth information in its structure. The control law strategies presented here stabilize the system in desired image features based on a change of variables, where adaptations to our generalized momenta with the dynamics of the camera system play a key role. Lastly, we have shown the performance of the controllers via simulation results.

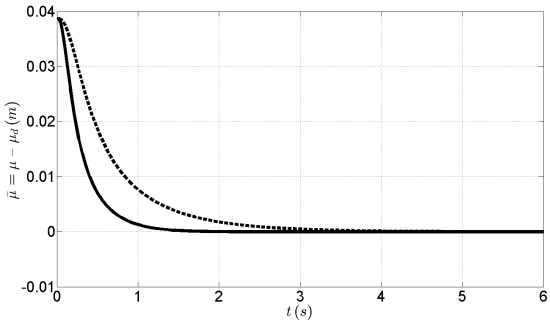

(a) Image feature error $\bar{\mu} = \mu - \mu_d\,(m)$. Initial conditions $\mu\,(0) = 38mm$. Desired image feature $\mu_d = 0mm$.

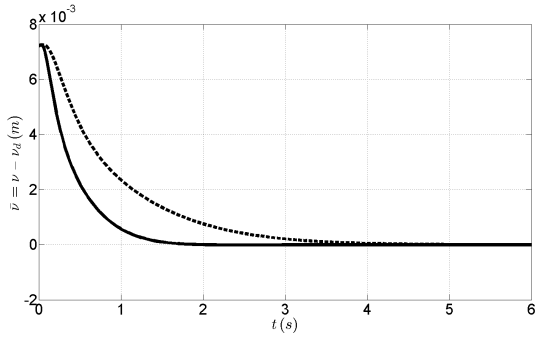

(b) Image feature error $\bar{\nu} = \nu - \nu_d\,(m)$. Initial conditions $\nu\,(0) = 7.2mm$. Desired image feature $\nu_d = 0mm$.

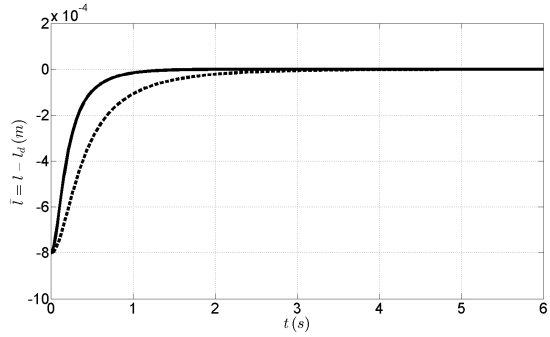

(c) Image feature error $\bar{l} = l - l_d\,(m)$. Initial conditions $l\,(0) = 10mm$. Desired image feature $l_d = 2mm$.

Figure 5.3: Simulation results and performance of the IBSV control strategies. Solid line: control law (5.21), and dashed line control law (5.27).

Chapter 6

Trajectory tracking control of a robot manipulator

In this chapter, we focus on a passivity-based control method, called *stabilization via a canonical transformation*. With this so-called canonical transformation a PH system can be transformed into another representation, while the structure of the original is preserved. When a system cannot be stabilized by conventional state-feedback, the canonical transformations become of particular interest, because they are capable of dealing with a more general class of systems, e.g., time-varying systems [17]. Consequently, the inclusion of a time variable in a PH system as in (2.1), allows us to stabilize mechanical systems to desired time-varying trajectories.

The trajectory tracking control problem for mechanical systems has been addressed by control design methodologies in the EL framework, see [40,52], and the references therein. Basic results on Hamiltonian systems were introduced in [16, 52]. The first approach to stabilization of time-varying PH systems, with the method of generalized canonical transformations was presented by [17, 19]. Examples can be also found in [18]. The later work of [6–8] shows tracking control with only position measurements.

The main contribution of this chapter is to introduce a trajectory tracking control strategy for PH systems. This strategy is based on a canonical transformation that deals with a PH system with a nonconstant mass-inertia matrix. Such transformation realizes an equivalent PH system with a constant mass-inertia matrix. Moreover, we make use of the measurement of forces sensors. The force sensors include the internal and external forces of the system. Lastly, experimental results preformed on a two-DOF robotic manipulator are presented, in order to validate the effectiveness of the control strategy presented here. The results here are inspired by the previous results of [6, 7].

The chapter is organized as follows. Section 6.1 introduces a canonical transformation in the PH system in order to obtain an equivalent PH system with a constant mass-inertia matrix. The transformation introduced in Section 6.1 allows us to embed a desired trajectory in the structure of the PH system. Furthermore, a trajectory tracking control strategy for mechanical systems in the PH framework is given. In Section 6.2, we provide simulation results of the two-DOF link manipulator in (2.7) of Example 2.1.2. Finally, experimental results are presented in Section 6.3, and concluding remarks in Section 6.4.

6.1 Control law

In this Section, we introduce a trajectory tracking control law for the mechanical systems described in (2.2). A PH approach is used during our control design methodology. We follow a canonical transformation of the PH system proposed in [17, 19]. Consequently, we provide a change of variables that transforms the PH system in (2.2) with a nonconstant mass-inertia matrix into an equivalent PH system with a constant mass-inertia matrix, as in [56]. Such transformation provides the means to embed our desired trajectory in the equivalent PH system. A control law is realized based on the *error system* stabilization methodology of [17]. It is of particular interest here the inclusion of force sensors in the proposed control law.

Denote the total forces on the system (2.2), and measured by n available force sensors, by $f(q,p)$, such that

$$f(q,p) = -\frac{\partial H(q,p)}{\partial q} - D(q,p)\frac{\partial H(q,p)}{\partial p} + B(q)f_e \tag{6.1}$$

with $H(q,p)$ as in (2.4), $f_e \in \mathbb{R}^n$ being the vector of external forces with input matrix $B(q) \in \mathbb{R}^{n\times n}$, and $D(q,p) \geqslant 0$ being the dissipation matrix.

We assume that the desired trajectory $q_d \in \mathscr{C}^2$ is known, and bounded. Consider the system (2.1) with nonconstant $M(q)$, and a coordinate transformation as

$$\bar{x} = \Phi_t(x) = \Phi_t(q,p) \triangleq \begin{pmatrix} \bar{q} \\ \bar{p} \end{pmatrix} = \begin{pmatrix} q - q_d \\ T(q)^{-1} p - T(q)^\top \dot{q}_d \end{pmatrix} = \begin{pmatrix} q - q_d \\ T(q)^\top (\dot{q} - \dot{q}_d) \end{pmatrix} \tag{6.2}$$

where $T(q)$ is a lower triangular matrix such that

$$T(q) = T\left(\Phi_t^{-1}(q,p)\right) = \bar{T}(\bar{q}) \tag{6.3}$$

and

$$M(q) = T(q)T(q)^\top = \bar{T}(\bar{q})\bar{T}(\bar{q})^\top \tag{6.4}$$

as in (2.33). From (6.2), and the potential energy $V(q)$ of (2.4), we know that

$$\bar{V}(\bar{q}) = V\left(\Phi_t^{-1}(\bar{q})\right) \tag{6.5}$$

Based on the *completing the square* technique, we introduce a scalar function $U(q,p)$ given by

$$U(q,p) = -\frac{1}{2}\left(p^\top \dot{q}_d + \dot{q}_d^\top p\right) + \frac{1}{2}\dot{q}_d^\top T(q)T(q)^\top \dot{q}_d \tag{6.6}$$

a change of variables $\Phi_t(q,p)$ as in (6.2), and $\bar{V}(q)$ in (6.5), we transform our Hamiltonian

$H(q,p)$ to $\bar{H}(\bar{q},\bar{p})$. It follows that

$$\begin{aligned}\bar{H}(\bar{q},\bar{p}) &= H(q,p)+U(q,p)\\ &= \frac{1}{2}p^{\top}M^{-1}(q)\,p+V(q)-\frac{1}{2}\left(p^{\top}\dot{q}_d+\dot{q}_d^{\top}p\right)+\frac{1}{2}\dot{q}_d^{\top}T(q)\,T(q)^{\top}\dot{q}_d\\ &= \frac{1}{2}\left(T(q)^{\top}(\dot{q}-\dot{q}_d)\right)^{\top}T(q)^{\top}(\dot{q}-\dot{q}_d)+\frac{1}{2}p^{\top}M^{-1}(q)\,p-\frac{1}{2}\dot{q}^{\top}M(q)\,\dot{q}+V(q)\\ &= \frac{1}{2}\bar{p}^{\top}\bar{p}+\bar{V}(\bar{q}) \end{aligned} \tag{6.7}$$

Note that the new Hamiltonian $H(q,p)$ in (6.7) has a constant mass-inertia matrix, i.e. $M(q)=I_{n\times n}$. We proceed to derive a vector $\beta(q,p)\in\mathbb{R}^n$ as in (2.25), and a scalar $\alpha(q,p)$ as in (2.26). We first compute $\dfrac{\partial\Phi_t(q,p)}{\partial(q,p,t)}$ with $\Phi_t(q,p)$ as in (6.2), i.e.,

$$\begin{aligned}\frac{\partial\Phi_t(q,p)}{\partial(q,p,t)} &= \frac{\partial}{\partial(q,p,t)}\begin{pmatrix}\bar{q}\\ \bar{p}\end{pmatrix}=\frac{\partial}{\partial(q,p,t)}\begin{pmatrix}q-q_d\\ T(q)^{-1}p-T(q)^{\top}\dot{q}_d\end{pmatrix}\\ &= \begin{bmatrix}\dfrac{\partial\bar{q}}{\partial q} & \dfrac{\partial\bar{q}}{\partial p} & \dfrac{\partial\bar{q}}{\partial t}\\ \dfrac{\partial\bar{p}}{\partial q} & \dfrac{\partial\bar{p}}{\partial p} & \dfrac{\partial\bar{p}}{\partial t}\end{bmatrix}\\ &= \begin{bmatrix}I_{n\times n} & 0_{n\times n} & \dot{q}-\dot{q}_d\\ \dfrac{\partial\left(T(q)^{\top}(\dot{q}-\dot{q}_d)\right)}{\partial q} & T(q)^{-1} & -\dfrac{\partial\left(T(q)^{\top}\dot{q}_d\right)}{\partial t}\end{bmatrix}\end{aligned} \tag{6.8}$$

together with the partial derivative of $U(q,p)$ as in (6.6), i.e $\dfrac{\partial U(q,p)}{\partial x}$, such that

$$\frac{\partial U(q,p)}{\partial(q,p)}=\begin{bmatrix}\dfrac{\partial U(q,p)}{\partial q}\\ \dfrac{\partial U(q,p)}{\partial p}\end{bmatrix}^{\top}=\begin{bmatrix}\dfrac{\partial\left(\dot{q}_d^{\top}M(q)\,\dot{q}_d\right)}{\partial q}^{\top}\\ -\dot{q}_d(t)\end{bmatrix} \tag{6.9}$$

Furthermore, consider the partial derivative in (6.9), and the input vector $g(x)=g(q,p)=col\,(0_{n\times n},G(q))$, with $G(q)\in\mathbb{R}^{n\times n}$ being the input matrix of system in (2.2). We substitute the aforementioned results in equation (2.26) in order to obtain the scalar $\alpha(q,p)$. Hence,

$$\alpha(q,p)=\begin{bmatrix}0_{n\times n}\\ G(q)\end{bmatrix}^{\top}\begin{bmatrix}\dfrac{\partial\left(\dot{q}_d^{\top}M(q)\,\dot{q}_d\right)}{\partial q}^{\top}\\ -\dot{q}_d(t)\end{bmatrix}=-G(q)^{\top}\dot{q}_d \tag{6.10}$$

We now give our attention to the PDE in (2.25). We substitute there the previous results in (6.8), and (6.9), together with the matrices, $J(q,p)$, $R(q,p)$, $D(q,p)$, and $G(q)$ of system (2.2), with the Hamiltonian $H(q,p)$ as in (2.4), and matrices $K(q,p)=0$, and $S(q,p)=0$. Thus, we obtain the following result

$$\begin{aligned}
\begin{bmatrix} \mathscr{P}_1(q,p) \\ \mathscr{P}_2(q,p) \end{bmatrix} &\triangleq \frac{\partial \Phi(q,p)}{\partial(q,p,t)} \left(\begin{bmatrix} 0_{n\times n} & I_{n\times n} \\ -I_{n\times n} & -D(q,p) \end{bmatrix} \begin{bmatrix} \frac{\partial U}{\partial q} \\ \frac{\partial U}{\partial p} \end{bmatrix}^{\top} + \begin{bmatrix} 0_{n\times n} \\ G(q)\beta(q,p) \end{bmatrix} \right) \\
&\quad \cdot (-1) \\
&\Leftrightarrow \begin{bmatrix} \frac{\partial \bar{q}}{\partial q} & \frac{\partial \bar{q}}{\partial p} & \frac{\partial \bar{q}}{\partial t} \\ \frac{\partial \bar{p}}{\partial q} & \frac{\partial \bar{p}}{\partial p} & \frac{\partial \bar{p}}{\partial t} \end{bmatrix} \begin{bmatrix} \frac{\partial U}{\partial p}^{\top} \\ -\frac{\partial U}{\partial q}^{\top} - D(q,p)\frac{\partial U}{\partial p}^{\top} + G(q)\beta(q,p) \\ -1 \end{bmatrix} \\
&\Leftrightarrow \begin{bmatrix} \frac{\partial \bar{q}}{\partial q}\frac{\partial U}{\partial p}^{\top} + \frac{\partial \bar{q}}{\partial p}\left(-\frac{\partial U}{\partial q}^{\top} - D(q,p)\frac{\partial U}{\partial p}^{\top} + G(q)\beta(q,p) \right) - \frac{\partial \bar{q}}{\partial t} \\ \frac{\partial \bar{p}}{\partial q}\frac{\partial U}{\partial p}^{\top} + \frac{\partial \bar{p}}{\partial p}\left(-\frac{\partial U}{\partial q}^{\top} - D(q,p)\frac{\partial U}{\partial p}^{\top} + G(q)\beta(q,p) \right) - \frac{\partial \bar{p}}{\partial t} \end{bmatrix}
\end{aligned} \tag{6.11}$$

We have left out the arguments of $U(q,p)$ for notational simplicity. We simplify $\mathscr{P}_1(q,p)$ and $\mathscr{P}_2(q,p)$, such that

$$\mathscr{P}_1(q,p) = \frac{\partial U}{\partial p}^{\top} - \frac{\partial \bar{q}}{\partial t} = -\dot{q}_d + \dot{q}_d = 0 \tag{6.12}$$

$$\begin{aligned}
\mathscr{P}_2(q,p) = &\frac{\partial\left(T(q)^{-1}p - T(q)^{\top}\dot{q}_d\right)}{\partial q}\frac{\partial U}{\partial p}^{\top} - \frac{\partial\left(T(q)^{\top}\dot{q}_d\right)}{\partial t} \\
&+ T(q)^{-1}\left(-\frac{\partial U}{\partial q}^{\top} - D(q,p)\frac{\partial U}{\partial p}^{\top} + G(q)\beta(q,p) \right)
\end{aligned} \tag{6.13}$$

It follows from (6.13) that $\beta(q,p)$ can be written as

$$\begin{aligned}
\beta(q,p) &= G(q)^{-1}\left(\frac{\partial \bar{p}}{\partial p}^{-1}\left(-\frac{\partial \bar{p}}{\partial q}\frac{\partial U}{\partial p}^{\top}+\frac{\partial \bar{p}}{\partial t}\right)+\frac{\partial U}{\partial q}^{\top}+D(q,p)\frac{\partial U}{\partial p}^{\top}\right)\\
&= G(q)^{-1}\left[T(q)\frac{\partial\left(T(q)^{\top}\dot{q}_d\right)}{\partial t}+\frac{\partial U}{\partial q}^{\top}\right.\\
&\quad\left.+\left(-T(q)\frac{\partial\left(T(q)^{-1}p-T(q)^{\top}\dot{q}_d\right)}{\partial q}+D(q,p)\right)\frac{\partial U}{\partial p}^{\top}\right]\\
&= G(q)^{-1}\left[T(q)\frac{\partial\left(T(q)^{\top}\dot{q}_d\right)}{\partial t}+\frac{\partial\left(\dot{q}_d(t)^{\top}M(q)\dot{q}_d\right)}{\partial q}^{\top}\right.\\
&\quad\left.-\left(T(q)\frac{\partial\left(T(q)^{-1}p-T(q)^{\top}\dot{q}_d\right)}{\partial q}+D(q,p)\right)\dot{q}_d\right] \qquad (6.14)
\end{aligned}$$

The next result follows from Theorem 2.2.1, and the previous developments.

Theorem 6.1.1 *Consider the PH system in* (2.2) *with an output y as in* (2.3)*, a mass-inertia matrix $M(q)$, a lower triangular matrix $T(q)$ as in* (6.3)*, a dissipation matrix $D(q,p)$, a vector $\beta(q,p)\in\mathbb{R}^n$ as in* (6.14)*, and a scalar $\alpha(q,p)$ as in* (6.10)*. Furthermore, consider the force sensor readings $f(q,p)$ as in* (6.1)*, an invertible input matrix $G(q)$, and positive matrices $C>0$, and $K_t>0$. Then, the control law*

$$u = G(q)^{-1}\left(-f(q,p)+K_t(q-q_d)\right)-\beta(q,p)-C\left(y+\alpha(q,p)\right) \qquad (6.15)$$

asymptotically stabilizes the PH system (2.2) *to $(q,p)=(q_d,0)$.*

Proof. The mechanical system (2.2) is asymptotically stable in $(q,p)=(q_d,0)$ when the control law (6.15) with the vector $\beta(q,p)$ as in (6.14), and the scalar $\alpha(q,p)$ as in (6.10), is applied. This follows directly from Theorem 2.2.1 with the passivity condition (2.30) of Theorem 2.2.2. ■

It is worth noticing that in the control law (6.15) we make use of our available force sensors readings, i.e $f(q,p)$ as in (6.1), in order to compensate for steady-state and delay errors. In the sequel, we validate our results by applying the control law to a robot manipulator. Simulations and experimental results are provided in the following sections.

6.2 Simulation results: two-DOF Example

Consider the two-DOF robot manipulator model (2.7) in Example 2.1.2, with the parameters of the simulation results in Section 3.4. Furthermore, consider the desired trajectories $q_d = col\,(q_{d_1}, q_{d_2}) \in \mathbb{R}^2$, such that

$$q_{d_i} = A_{t_i} \sin(\omega_i t + \varphi_i) + B_{t_i} \tag{6.16}$$

with an amplitude, frequency, phase, and bias (offset) given by the scalars A_{t_i}, ω_i, φ_i, and B_{t_i}, respectively, and $i = 1, 2$. The parameters for our desired trajectories q_d of the link of the PERA are given by $A_t = \left\{\frac{2\pi}{9}, 0\right\}$ *rad*, $\omega = \left\{\frac{\pi}{10}, 0\right\}$ *Hz*, $\varphi = \left\{-\frac{\pi}{2}, 0\right\}$ *rad*, and $B_t = \left\{\frac{2\pi}{9}, 0\right\}$ *rad*. We apply the control law (6.15) to the system (2.7) with output y in (2.8), and with the matrices $K_t = diag\,(45, 45)$, and $C = diag\,(10, 10)$. The simulation results are shown in Figure 6.1, with an error shown in Figure 6.2. We observe in Figure 6.2 that the proposed control law in (6.15) achieves a trajectory tracking with an error of ± 0.013 *rad* $\approx \pm 0.750^\circ$

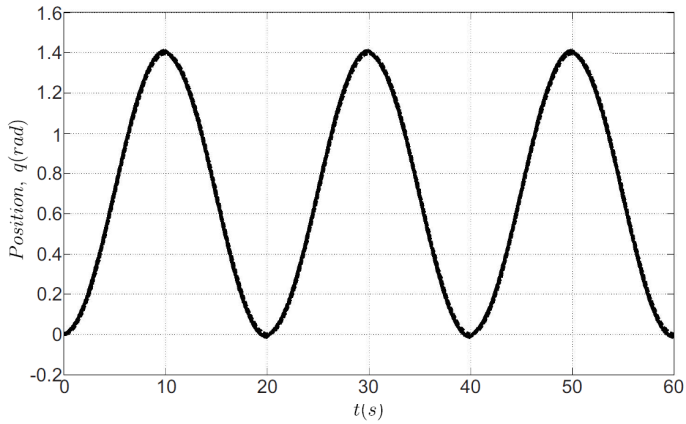

Figure 6.1: Trajectory tracking control of link q_1 of the PERA in (2.7). Desired trajectory given by (6.16)(dashed line). Simulation results obtained with our control law (6.15) (solid line). Frequency of $\omega_1 = \frac{1}{30}$.

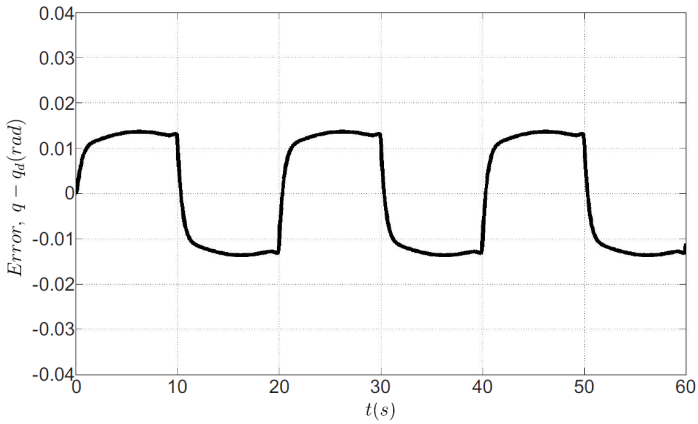

Figure 6.2: Trajectory tracking control error of link q_1 of the PERA in (2.7). Simulation results obtained with our control law (6.15). Frequency of $\omega_1 = \dfrac{1}{30}$.

6.3 Experimental results

The experimental setup is shown in Figure 2.1. The parameters of our desired trajectory in (6.16) for the first link of the PERA, i.e. q_{d_1} are given by $A_t = \left\{\dfrac{2\pi}{9}, 0\right\}$ *rad*, $\omega_1 = \left\{\dfrac{1}{10}, \dfrac{1}{20}, \dfrac{1}{30}\right\}$ *Hz*, $\omega_2 = 0$ *Hz*, $\varphi = \{0,0\}$ *rad*, and $B_t = \left\{\dfrac{2\pi}{9}, 0\right\}$ *rad*. Additionally, we implement the control law in (6.15) with $K_t = diag\,(45,45)$, and $C = diag\,(10,10)$ as in Section 6.2. Note that we have tested the proposed controller in this chapter for three different frequencies in order to demonstrate that our control law is consistent. Experimental results are shown in Figures 6.3, and 6.4. We observe in Figure 6.4 how a higher frequency means a smaller error. Thus, a speed of convergence plays an important role in the proposed controller (6.15). The error of the experiment performed at a frequency of $\omega_3 = \dfrac{1}{30}$ *Hz* (Figure 6.4c) is ± 0.017 *rad* $\approx \pm 0.974^\circ$. The results here validate our simulations results performed at the same frequency (Figure 6.2).

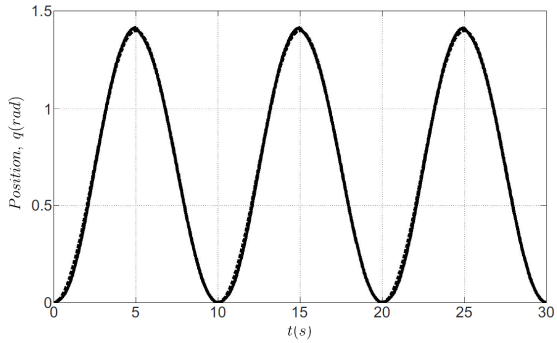

(a) Frequency $\omega_1 = \dfrac{1}{10}\ Hz$.

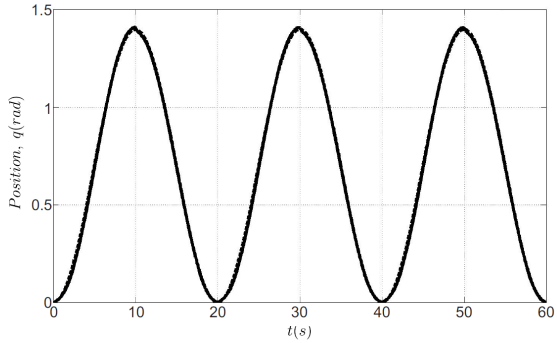

(b) Frequency $\omega_2 = \dfrac{1}{20}\ Hz$.

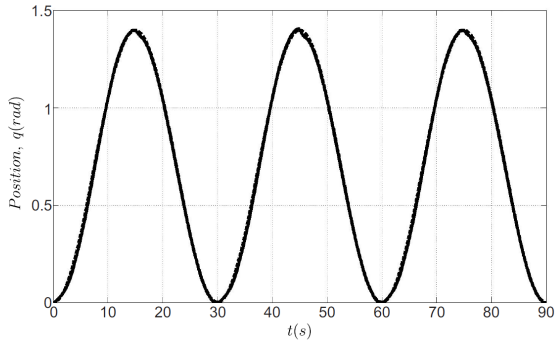

(c) Frequency $\omega_3 = \dfrac{1}{30}\ Hz$.

Figure 6.3: Trajectory tracking control of link q_1 of the PERA in (2.7). Desired trajectory given by (6.16) (dashed line). Experimental results obtained with our control law (6.15) (solid line).

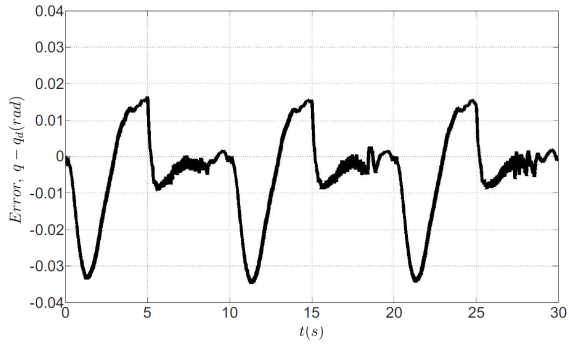

(a) Frequency $\omega_1 = \dfrac{1}{10}\ Hz$.

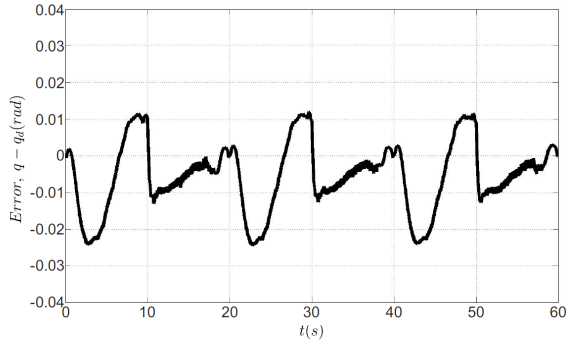

(b) Frequency $\omega_2 = \dfrac{1}{20}\ Hz$.

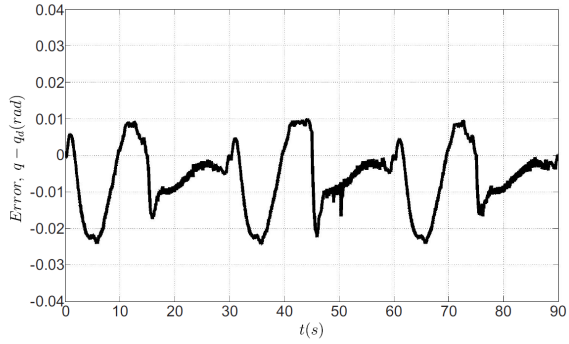

(c) Frequency $\omega_3 = \dfrac{1}{30}\ Hz$.

Figure 6.4: Trajectory tracking control error of link q_1 of the PERA in (2.7). Experimental results obtained with our control law (6.15).

6.4 Concluding remarks

This chapter addresses a trajectory tracking control problem with force feedback for mechanical systems in the PH framework. The control problem becomes one of stabilization due to the canonical transformations implemented. The canonical transformations for PH systems are previously introduced by [17, 19]. The main contributions of this chapter are the development of a control strategy, and its implementation to a real system for validation, i.e. the robot manipulator shown in Figure 2.1. The incorporation of (real) measurements from force sensors bring consistency to the proposed control strategy. The control law asymptotically stabilizes the robot manipulator to an a priori chosen time-varying trajectory. Moreover, we have validated the effectiveness of the control law via simulation and experimental results. The performance of our controller reduces the trajectory tracking error to $q - q_d < 1^\circ$, and remains consistent after different tests.

Chapter 7
Conclusions and recommendations

This final chapter summarizes the most important contributions of the present thesis. General remarks about PH systems, and more specifically the control design methodologies for position, force, grasping impedance, and trajectory tracking are included. Furthermore, we recapitulate the importance of the incorporation of force measurements in the input of the system during a noncontact to contact transition. Lastly, future work is recommended to connect with our PH setting for mechanical systems.

7.1 Concluding remarks

This thesis is realized under the PH modeling framework, because this energy setting allows us to include a larger class of (nonlinear) physical system. The main objective of this thesis is to design control methods that deal with mechanical systems in the PH framework. We have addressed control problems for mechanical systems, e.g., robot manipulators, with an energy setting perspective. Furthermore, we have shown that the incorporation of measurements of force sensors increases the dexterity of the mechanical systems, specially during a noncontact to contact transition. Novel strategies for force control and impedance grasping are developed, which increase the manipulation skills of robotic systems, and the physical interconnection with the environment is straightforwardly, achieved thanks to the tools for analysis of the PH framework. Furthermore, the problem of position control is addressed in presence of external forces, force feedback, and the incorporation of the dynamics of a camera system. Lastly, time-varying position control has been addressed, i.e., the trajectory tracking control problem. A canonical transformation in the PH framework, and a force feedback are our main strategies to achieve a robust solution for a trajectory tracking control problem.

In Chapter 2, we recapitulate the important theorems, properties and examples for systems analysis used in this thesis. We have provided a general background of the PH framework. Furthermore, we have described a PH system with a nonconstant mass-inertia matrix in a equivalent PH system that has a constant mass-inertia matrix. We make use of this canonical transformation in order to simplify the control strategies developed in the thesis. Moreover, a Hamilton-Jacobi inequality is revisited, which we use to analyze a

closed-loop system for disturbance attenuation properties in the following chapter. Lastly, we provide the constructive procedure of [29] to modify the Hamiltonian function of a forced PH system in order to generate a Lyapunov function for nonzero equilibria.

Chapter 3 is devoted to the development of strategies for position control via force feedback for mechanical systems under the PH framework. An alternative solution to the classical methods for position control problem via force feedback is this chapter main goal. The resulting framework with force feedback provides better tuning capabilities for the control strategies, which have been validated via simulation results. Structure preservation in the PH setting is not straightforward when we incorporate the force measurements in the input of the system. However, we have shown that via a change of variables we are able to realize force feedback while preserving the PH structure. We have introduced a control strategy based on modeled internal forces of a mechanical system with a nonconstant mass-inertia matrix. When the external forces acting on the aforementioned system are constant nonzero, we have shown that a type of integral control compensates for position errors. Subsequently, we assume that force sensors are present to give measurements of the (real) total forces in the system, i.e., the internal and external forces. Lastly, we show that we can use the force measurements to realize rejection of the total forces in the system. This final result is used in the following Chapters of the thesis.

Chapter 4 addressed the development of new strategies of force control and impedance grasping control in the PH framework. The strategies become of importance in a non-contact to contact transition of end-effector (gripper) of the mechanical system, and the environment (object). The main motivation is the proposition of an alternative solution to the the classical force control and impedance grasping control strategies of [21] and [23], respectively. A type of integral action over the force sensor output, and a change of variables, are the main strategies to realize a force control in presence of external forces. Force control is then realizable when we have (total) measurements of the internal and external forces of our system. This connects with our results of total force rejection presented in Chapter 3. Furthermore, we have given an impedance graping strategy realized via a virtual spring force. The incorporation of a virtual spring force with a variable rest-length that can be varied fundamentally improves the mechanical impedance between the system and the environment. The additional (co)dissipation term in the power balance of the system results in lower convergence and lower impact forces in comparison with the classical strategy of [23]. Lastly, simulation and experimental results have validated our control laws.

In Chapter 5, we have presented a PH approach to visual servo control of a standard mechanical system. An extended model of the system that includes the dynamics of a camera based on perspective projection modeling is realized. The PH setting of our mechanical system deals with the nonlinearities introduced by the vision system. A

depth variable that includes a reference of the object with respect to the end-effector played a fundamental role during our developments, and it is a change of variables with the incorporation of an adapted momenta our main strategy during the control design methodology. The adapted momenta includes the information of the dynamics of the camera system. We have achieved asymptotic stability to a desired image features, which means that we are able to control the end-effector to a grasping distance. Lastly, we have examined the performance of the controllers via simulation results.

Finally, Chapter 6 is devoted to the trajectory tracking control problem with force feedback for mechanical systems in the PH framework. The canonical transformations previously introduced by [17, 19] have played an key role during the stabilization of the mechanical system. The main contributions of this Chapter are the development of a control strategy, and its implementation to a real system for validation purposes, i.e., the robot manipulator shown in Figure 2.1. The incorporation of (real) measurements of force sensors bring robustness to our framework. The control law asymptotically stabilizes the robot manipulator to an a priori chosen time-varying trajectory.

7.2 Recommendations for future research

In this thesis, we have presented simulations and experimental results based on our control strategies. Experimental results are implemented in our robot manipulator, shown in Figure 2.1. We have introduced the use of two links of the shoulder, which model is presented in Example 2.1.2, and one dimensional system, i.e. the gripper, presented in the Example 2.1.3. Then, future work can include more links of the robot manipulator where the proposed control methods can be tested. For instance, we can add the links of the *elbow* and the *wrist* of the robot manipulator in order to perform complex tasks. Furthermore, a real camera system can be integrated, and experimental results for the proposed image-based servo control strategies can validate the simulation results shown in 5.4. We can investigate vision control work and the connection with the proposed impedance grasping strategy in order to obtain a more general experimental setup.

Appendix A

Model of a seven-DOF robot manipulator

This appendix introduces the model of the Philips Experimental Robot Arm shown in Figure 2.1, and with the Denavit-Hartenberg representation, see [53], in Figure 2.2. Partial modeling results are the two-DOF of the shoulder from Example 2.1.2, the end-effector (gripper) from Example 2.1.3, and the three-DOF system (shoulder and elbow) from Section 5.4, with the Table 5.1.

The Denavit-Hartenberg parameters of the PERA are shown in the Table A.1. Subsequently, the PH modeling is given by (2.2), with a Hamiltonian $H(q,p)$ as in (2.4). The generalized coordinates are given by q_i, with m_i being the masses, $\mathscr{I}_i$ being the inertias, and $i = \{1,\ldots,7\}$. Furthermore, the lengths of the shoulder, elbow and wrist of the PERA are d_{q_3}, d_{q_5}, and a_{q_7}, respectively. Finally, we consider that the masses of the links are uniformly distributed.

Table A.1: Denavit-Hartenberg parameters for the PERA

Link i	a_i	α_i	d_i	q_i
1	0	$\frac{\pi}{2}$	0	q_1
2	0	$-\frac{\pi}{2}$	0	q_2
3	0	$\frac{\pi}{2}$	d_{q_3}	q_3
4	0	$-\frac{\pi}{2}$	0	q_4
5	0	$-\frac{\pi}{2}$	d_{q_5}	q_5
6	0	$\frac{\pi}{2}$	0	q_6
7	a_{q_7}	$-\frac{\pi}{2}$	0	q_7

We are able to compute the mass-inertia matrix, i.e., $M(q) \in \mathbb{R}^{7\times 7}$ with elements $\bar{m}_{ij}$ for $i,j = \{1,\ldots,7\}$, given by

$$
\begin{aligned}
\bar{m}_{11} =& \mathscr{I}_1 + \mathscr{I}_2 + \mathscr{I}_3 + \mathscr{I}_4 + \mathscr{I}_5 + \mathscr{I}_6 + \mathscr{I}_7 + d_{q_3}^2 m_4 + d_{q_3}^2 m_5 + d_{q_3}^2 m_6 + d_{q_3}^2 m_7 + d_{q_5}^2 m_6 \\
&+ d_{q_5}^2 m_7 - d_{q_3}^2 m_4 cos(q_2)^2 - d_{q_3}^2 m_5 cos(q_2)^2 - d_{q_3}^2 m_6 cos(q_2)^2 - d_{q_3}^2 m_7 cos(q_2)^2 \\
&- d_{q_5}^2 m_6 cos(q_3)^2 - d_{q_5}^2 m_7 cos(q_3)^2 + 2 d_{q_3} d_{q_5} m_6 cos(q_4) + 2 d_{q_3} d_{q_5} m_7 cos(q_4) \\
&+ d_{q_5}^2 m_6 cos(q_2)^2 cos(q_3)^2 - d_{q_5}^2 m_6 cos(q_2)^2 cos(q_4)^2 + d_{q_5}^2 m_7 cos(q_2)^2 cos(q_3)^2 \\
&+ d_{q_5}^2 m_6 cos(q_3)^2 cos(q_4)^2 - d_{q_5}^2 m_7 cos(q_2)^2 cos(q_4)^2 + d_{q_5}^2 m_7 cos(q_3)^2 cos(q_4)^2 \\
&- d_{q_5}^2 m_6 cos(q_2)^2 cos(q_3)^2 cos(q_4)^2 - d_{q_5}^2 m_7 cos(q_2)^2 cos(q_3)^2 cos(q_4)^2 \\
&- 2 d_{q_3} d_{q_5} m_6 cos(q_2)^2 cos(q_4) - 2 d_{q_3} d_{q_5} m_7 cos(q_2)^2 cos(q_4) \\
&+ 2 d_{q_3} d_{q_5} m_6 cos(q_2) cos(q_3) sin(q_2) sin(q_4) \\
&+ 2 d_{q_3} d_{q_5} m_7 cos(q_2) cos(q_3) sin(q_2) sin(q_4) \\
&+ 2 d_{q_5}^2 m_6 cos(q_2) cos(q_3) cos(q_4) sin(q_2) sin(q_4) \\
&+ 2 d_{q_5}^2 m_7 cos(q_2) cos(q_3) cos(q_4) sin(q_2) sin(q_4) \\
\bar{m}_{12} =& - d_{q_5} sin(q_3)(m_6 + m_7)(d_{q_3} cos(q_2) sin(q_4) - d_{q_5} cos(q_3) sin(q_2) \\
&+ d_{q_5} cos(q_2) cos(q_4) sin(q_4) + d_{q_5} cos(q_3) cos(q_4)^2 sin(q_2)) \\
\bar{m}_{13} =& \mathscr{I}_3 cos(q_2) + \mathscr{I}_4 cos(q_2) + \mathscr{I}_5 cos(q_2) + \mathscr{I}_6 cos(q_2) + \mathscr{I}_7 cos(q_2) \\
&+ d_{q_5}^2 m_6 cos(q_2) + d_{q_5}^2 m_7 cos(q_2) - d_{q_5}^2 m_6 cos(q_2) cos(q_4)^2 \\
&- d_{q_5}^2 m_7 cos(q_2) cos(q_4)^2 + d_{q_5}^2 m_6 cos(q_3) cos(q_4) sin(q_2) sin(q_4) \\
&+ d_{q_5}^2 m_7 cos(q_3) cos(q_4) sin(q_2) sin(q_4) + d_{q_3} d_{q_5} m_6 cos(q_3) sin(q_2) sin(q_4) \\
&+ d_{q_3} d_{q_5} m_7 cos(q_3) sin(q_2) sin(q_4) \\
\bar{m}_{14} =& sin(q_2) sin(q_3)(\mathscr{I}_4 + \mathscr{I}_5 + \mathscr{I}_6 + \mathscr{I}_7 + d_{q_5}^2 m_6 + d_{q_5}^2 m_7 + d_{q_3} d_{q_5} m_6 cos(q_4) \\
&+ d_{q_3} d_{q_5} m_7 cos(q_4)) \\
\bar{m}_{15} =& (cos(q_2) cos(q_4) - cos(q_3) sin(q_2) sin(q_4))(\mathscr{I}_5 + \mathscr{I}_6 + \mathscr{I}_7) \\
\bar{m}_{16} =& - (\mathscr{I}_6 + \mathscr{I}_7)(cos(q_5) sin(q_2) sin(q_3) + cos(q_2) sin(q_4) sin(q_5) \\
&+ cos(q_3) cos(q_4) sin(q_2) sin(q_5)) \\
\bar{m}_{17} =& \mathscr{I}_7 cos(q_2) cos(q_4) cos(q_6) - \mathscr{I}_7 cos(q_3) cos(q_6) sin(q_2) sin(q_4) \\
&+ \mathscr{I}_7 cos(q_2) cos(q_5) sin(q_4) sin(q_6) - \mathscr{I}_7 sin(q_2) sin(q_3) sin(q_5) sin(q_6) \\
&+ \mathscr{I}_7 cos(q_3) cos(q_4) cos(q_5) sin(q_2) sin(q_6)
\end{aligned}
$$

$$
\begin{aligned}
\bar{m}_{21} =& -d_{q_5} sin(q_3)(m_6+m_7)(d_{q_3} cos(q_2) sin(q_4) - d_{q_5} cos(q_3) sin(q_2) \\
&+ d_{q_5} cos(q_2) cos(q_4) sin(q_4) + d_{q_5} cos(q_3) cos(q_4)^2 sin(q_2)) \\
\bar{m}_{22} =& \mathscr{I}_2 + \mathscr{I}_3 + \mathscr{I}_4 + \mathscr{I}_5 + \mathscr{I}_6 + \mathscr{I}_7 + d_{q_3}^2 m_4 + d_{q_3}^2 m_5 \\
&+ d_{q_3}^2 m_6 + d_{q_3}^2 m_7 + d_{q_5}^2 m_6 cos(q_3)^2 + d_{q_5}^2 m_6 cos(q_4)^2 \\
&+ d_{q_5}^2 m_7 cos(q_3)^2 + d_{q_5}^2 m_7 cos(q_4)^2 + 2 d_{q_3} d_{q_5} m_6 cos(q_4) \\
&+ 2 d_{q_3} d_{q_5} m_7 cos(q_4) - d_{q_5}^2 m_6 cos(q_3)^2 cos(q_4)^2 - d_{q_5}^2 m_7 cos(q_3)^2 cos(q_4)^2 \\
\bar{m}_{23} =& -d_{q_5} sin(q_3) sin(q_4)(m_6+m_7)(d_{q_3} + d_{q_5} cos(q_4)) \\
\bar{m}_{24} =& cos(q_3)(\mathscr{I}_4 + \mathscr{I}_5 + \mathscr{I}_6 + \mathscr{I}_7 + d_{q_5}^2 m_6 + d_{q_5}^2 m_7 + d_{q_3} d_{q_5} m_6 cos(q_4) \\
&+ d_{q_3} d_{q_5} m_7 cos(q_4)) \\
\bar{m}_{25} =& sin(q_3) sin(q_4)(\mathscr{I}_5 + \mathscr{I}_6 + \mathscr{I}_7) \\
\bar{m}_{26} =& -(cos(q_3) cos(q_5) - cos(q_4) sin(q_3) sin(q_5))(\mathscr{I}_6 + \mathscr{I}_7) \\
\bar{m}_{27} =& \mathscr{I}_7 cos(q_6) sin(q_3) sin(q_4) - \mathscr{I}_7 cos(q_3) sin(q_5) sin(q_6) \\
&- \mathscr{I}_7 cos(q_4) cos(q_5) sin(q_3) sin(q_6)
\end{aligned}
$$

$$
\begin{aligned}
\bar{m}_{31} =& \mathscr{I}_3 cos(q_2) + \mathscr{I}_4 cos(q_2) + \mathscr{I}_5 cos(q_2) + \mathscr{I}_6 cos(q_2) + \mathscr{I}_7 cos(q_2) + d_{q_5}^2 m_6 cos(q_2) \\
&+ d_{q_5}^2 m_7 cos(q_2) - d_{q_5}^2 m_6 cos(q_2) cos(q_4)^2 - d_{q_5}^2 m_7 cos(q_2) cos(q_4)^2 \\
&+ d_{q_5}^2 m_6 cos(q_3) cos(q_4) sin(q_2) sin(q_4) + d_{q_5}^2 m_7 cos(q_3) cos(q_4) sin(q_2) sin(q_4) \\
&+ d_{q_3} d_{q_5} m_6 cos(q_3) sin(q_2) sin(q_4) + d_{q_3} d_{q_5} m_7 cos(q_3) sin(q_2) sin(q_4) \\
\bar{m}_{32} =& -d_{q_5} sin(q_3) sin(q_4)(m_6+m_7)(d_{q_3} + d_{q_5} cos(q_4)) \\
\bar{m}_{33} =& \mathscr{I}_3 + \mathscr{I}_4 + \mathscr{I}_5 + \mathscr{I}_6 + \mathscr{I}_7 + d_{q_5}^2 m_6 sin(q_4)^2 + d_{q_5}^2 m_7 sin(q_4)^2 \\
\bar{m}_{34} =& 0 \\
\bar{m}_{35} =& cos(q_4)(\mathscr{I}_5 + \mathscr{I}_6 + \mathscr{I}_7) \\
\bar{m}_{36} =& -sin(q_4) sin(q_5)(\mathscr{I}_6 + \mathscr{I}_7) \\
\bar{m}_{37} =& \mathscr{I}_7 cos(q_4) cos(q_6) + \mathscr{I}_7 cos(q_5) sin(q_4) sin(q_6)
\end{aligned}
$$

$$
\begin{aligned}
\bar{m}_{41} =& sin(q_2)sin(q_3)(\mathscr{I}_4+\mathscr{I}_5+\mathscr{I}_6+\mathscr{I}_7+d_{q_5}^2m_6+d_{q_5}^2m_7+d_{q_3}d_{q_5}m_6cos(q_4)\\
&+d_{q_3}d_{q_5}m_7cos(q_4))\\
\bar{m}_{42} =& cos(q_3)(\mathscr{I}_4+\mathscr{I}_5+\mathscr{I}_6+\mathscr{I}_7+d_{q_5}^2m_6+d_{q_5}^2m_7+d_{q_3}d_{q_5}m_6cos(q_4)\\
&+d_{q_3}d_{q_5}m_7cos(q_4))\\
\bar{m}_{43} =& 0\\
\bar{m}_{44} =& \mathscr{I}_4+\mathscr{I}_5+\mathscr{I}_6+\mathscr{I}_7+d_{q_5}^2m_6+d_{q_5}^2m_7\\
\bar{m}_{45} =& 0\\
\bar{m}_{46} =& -cos(q_5)(\mathscr{I}_6+\mathscr{I}_7)\\
\bar{m}_{47} =& -\mathscr{I}_7sin(q_5)sin(q_6)
\end{aligned}
$$

$$
\begin{aligned}
\bar{m}_{51} =& (cos(q_2)cos(q_4)-cos(q_3)sin(q_2)sin(q_4))(\mathscr{I}_5+\mathscr{I}_6+\mathscr{I}_7)\\
\bar{m}_{52} =& sin(q_3)sin(q_4)(\mathscr{I}_5+\mathscr{I}_6+\mathscr{I}_7)\\
\bar{m}_{53} =& cos(q_4)(\mathscr{I}_5+\mathscr{I}_6+\mathscr{I}_7)\\
\bar{m}_{54} =& 0\\
\bar{m}_{55} =& \mathscr{I}_5+\mathscr{I}_6+\mathscr{I}_7\\
\bar{m}_{56} =& 0\\
\bar{m}_{57} =& \mathscr{I}_7cos(q_6)
\end{aligned}
$$

$$
\begin{aligned}
\bar{m}_{61} =& -(\mathscr{I}_6+\mathscr{I}_7)(cos(q_5)sin(q_2)sin(q_3)\\
&+cos(q_2)sin(q_4)sin(q_5)+cos(q_3)cos(q_4)sin(q_2)sin(q_5))\\
\bar{m}_{62} =& -(cos(q_3)cos(q_5)-cos(q_4)sin(q_3)sin(q_5))(\mathscr{I}_6+\mathscr{I}_7)\\
\bar{m}_{63} =& -sin(q_4)sin(q_5)(\mathscr{I}_6+\mathscr{I}_7)\\
\bar{m}_{64} =& -cos(q_5)(\mathscr{I}_6+\mathscr{I}_7)\\
\bar{m}_{65} =& 0\\
\bar{m}_{66} =& \mathscr{I}_6+\mathscr{I}_7\\
\bar{m}_{67} =& 0
\end{aligned}
$$

$$
\begin{aligned}
\bar{m}_{71} =& \mathscr{I}_7 cos(q_2)cos(q_4)cos(q_6) - \mathscr{I}_7 cos(q_3)cos(q_6)sin(q_2)sin(q_4) \\
&+ \mathscr{I}_7 cos(q_2)cos(q_5)sin(q_4)sin(q_6) - \mathscr{I}_7 sin(q_2)sin(q_3)sin(q_5)sin(q_6) \\
&+ \mathscr{I}_7 cos(q_3)cos(q_4)cos(q_5)sin(q_2)sin(q_6) \\
\bar{m}_{72} =& \mathscr{I}_7 cos(q_6)sin(q_3)sin(q_4) - \mathscr{I}_7 cos(q_3)sin(q_5)sin(q_6) \\
&- \mathscr{I}_7 cos(q_4)cos(q_5)sin(q_3)sin(q_6) \\
\bar{m}_{73} =& \mathscr{I}_7 cos(q_4)cos(q_6) + \mathscr{I}_7 cos(q_5)sin(q_4)sin(q_6) \\
\bar{m}_{74} =& - \mathscr{I}_7 sin(q_5)sin(q_6) \\
\bar{m}_{75} =& \mathscr{I}_7 cos(q_6) \\
\bar{m}_{76} =& 0 \\
\bar{m}_{77} =& \mathscr{I}_7
\end{aligned}
$$

Lastly, the vector of potential energy, i.e., $\dfrac{\partial V(q)}{\partial q} \in \mathbb{R}^7$ with elements $\bar{g}_i$ for $i = \{1,\ldots,7\}$, with $g = 9.81\ \dfrac{m}{s^2}$ being the acceleration of the gravity, is given by

$$
\begin{aligned}
\bar{g}_1 =& g m_6 (d_{q_5}(sin(q_4)(cos(q_1)sin(q_3) + cos(q_2)cos(q_3)sin(q_1)) + cos(q_4)sin(q_1)sin(q_2)) \\
&+ d_{q_3} sin(q_1)sin(q_2)) + g m_7 (d_{q_5}(sin(q_4)(cos(q_1)sin(q_3) + cos(q_2)cos(q_3)sin(q_1)) \\
&+ cos(q_4)sin(q_1)sin(q_2)) + d_{q_3} sin(q_1)sin(q_2)) + g d_{q_3} m_4 sin(q_1)sin(q_2) \\
&+ g d_{q_3} m_5 sin(q_1)sin(q_2) \\
\bar{g}_2 =& - g m_6 (d_{q_5}(cos(q_1)cos(q_2)cos(q_4) - cos(q_1)cos(q_3)sin(q_2)sin(q_4)) \\
&+ d_{q_3} cos(q_1)cos(q_2)) - g m_7 (d_{q_5}(cos(q_1)cos(q_2)cos(q_4) \\
&- cos(q_1)cos(q_3)sin(q_2)sin(q_4)) + d_{q_3} cos(q_1)cos(q_2)) - g d_{q_3} m_4 cos(q_1)cos(q_2) \\
&- g d_{q_3} m_5 cos(q_1)cos(q_2) \\
\bar{g}_3 =& g d_{q_5} m_6 sin(q_4)(cos(q_3)sin(q_1) + cos(q_1)cos(q_2)sin(q_3)) \\
&+ g d_{q_5} m_7 sin(q_4)(cos(q_3)sin(q_1) + cos(q_1)cos(q_2)sin(q_3)) \\
\bar{g}_4 =& g d_{q_5} m_6 (cos(q_4)(sin(q_1)sin(q_3) - cos(q_1)cos(q_2)cos(q_3)) \\
&+ cos(q_1)sin(q_2)sin(q_4)) + g d_{q_5} m_7 (cos(q_4)(sin(q_1)sin(q_3) \\
&- cos(q_1)cos(q_2)cos(q_3)) + cos(q_1)sin(q_2)sin(q_4)) \\
\bar{g}_5 =& 0 \\
\bar{g}_6 =& 0 \\
\bar{g}_7 =& 0
\end{aligned}
$$

Bibliography

[1] S. Andersson, A. Soderberg, and S. Bjorklund. Friction models for sliding dry, boundary and mixed lubricated contacts. *Tribology International*, 40(4):580–587, 2007.

[2] I. Asimov. *I, Robot*. Doubleday & Company, New York, USA, 1950.

[3] M. Bol. *Force and position control of the Philips Experimental Robot Arm in a energy-based setting*. University of Groningen, Groningen, The Netherlands, 2012.

[4] C. Canudas de Wit, B. Siciliano, and G. Bastin. *Theory of Robot Control*. Springer, London, UK, 1996.

[5] N. Diolaiti, C. Melchiorri, and S. Stramigioli. Contact impedance estimation for robotic systems. *IEEE Transactions on Robotics*, 21(5):925–935, 2005.

[6] D.A. Dirksz and J.M.A. Scherpen. Passivity-based tracking control of port-Hamiltonian mechanical systems with only position measurements. In *Proceedings European Control Conference*, pages 4689–4694, Budapest, Hungary, 2009.

[7] D.A. Dirksz and J.M.A. Scherpen. Apdative tracking control of fully actuated port-Hamiltonian mechanical systems. In *Proceedings IEEE Muli-Conference on Systems and Control*, pages 4689–4694, Yokohama, Japan, 2010.

[8] D.A. Dirksz and J.M.A. Scherpen. Power-based adaptive and integral control of standard mechanical systems. In *Proceedings of the 49th IEEE Conference on Decision and Control*, pages 4612–4617, Atlanta, Georgia, USA, 2010.

[9] D.A. Dirksz and J.M.A. Scherpen. A port-Hamiltonian approach to visual servo control of a pick and place system. In *Proceedings of 51st Conference on Decision and Control*, pages 5661–5666, Maui, Hawaii, USA, 2012.

[10] D.A. Dirksz and J.M.A. Scherpen. Power-based control: Canonical coordinate transformations, integral and adaptive control. *Automatica*, 48(6):1046–1056, 2012.

[11] D.A. Dirksz, J.M.A. Scherpen, and M. Steinbuch. A port-Hamiltonian approach to visual servo control of a pick and place system. *Asian Journal of Control*, 16(3):703–713, 2014.

[12] A. Donaire and S. Junco. On the addition of integral control action to port-controlled Hamiltonian systems. *Automatica*, 45(8):1910–1916, 2009.

[13] V. Duindam, A. Macchelli, S. Stramigioli, and H. Bruyninckx. *Modeling and Control of Complex Physical Systems: The Port-Hamiltonian Approach*. Springer, Berlin, Germany, 2009.

[14] M. I. El-Hawwary and M. Maggiore. Reduction principles and the stabilization of closed sets for passive systems. *IEEE Transactions on Automatic Control*, 55(4):982–987, 2010.

[15] B. Espiau, F. Chaumette, and P. Rives. A new approach to visual servoing in robotics. *IEEE Transactions on Robotics and Automation*, 8(3):313–326, 1992.

[16] H. Flashner and J. M. Skowronski. Model tracking control of Hamiltonian systems. *ASME, Journal of Dynamics Systems, Measurement and Control*, 111:656–659, 1989.

[17] K. Fujimoto, K. Sakura, and T. Sugie. Trajectory tracking of port-controlled Hamiltonian systems via generalized canonical transformation. *Automatica*, 39(12):2059–2069, 2003.

[18] K. Fujimoto and T. Sugie. Time-varying stabilization of nonholonomic Hamiltonian systems via canonical transformations. In *Proceedings of American Control Conference*, pages 3269–3273, Chicago, USA, 2000.

[19] K. Fujimoto and T. Sugie. Canonical transformation and stabilization of generalized Hamiltonian systems. *Systems and Control Letters*, 42(3):217–227, 2001.

[20] F. Gomez-Estern and A.J. van der Schaft. Physical damping in ida-pbc controlled underactuated mechanical systems. *European Journal on Control*, 10:451–468, 2004.

[21] D. Gorinevsky, A. Formalsky, and A. Scheiner. *Force Control of Robotics Systems*. CRC, Moscow, Russia, 1997.

[22] P. Harmo, T. Taipalus, J. Knuuttila, J. Vallet, and A. Halme. Needs and solutions-home automation and service robots for the elderly and disabled. In *IEEE/RSJ International Conference on Intelligent Robots and Systems*, pages 3201–3206. IEEE, 2005.

[23] N. Hogan. Impedance control, an approach to manipulation, parts i, ii, and iii. *ASME Journal Dynamic Systems, Measurement, and Control*, 107(1):1–24, 1985.

[24] S.A. Hutchinson, G.D. Hager, and P.I. Corke. A tutorial on visual servo control. *IEEE Transactions on Robotics and Automation*, 12(5):651–670, 1996.

[25] H. Khalil. *Nonlinear Systems*. Prentice-Hall, USA, 1996.

[26] F. Koops. *Trajectory Tracking Control of the Philips Experimental Robot Arm in the Port-Hamiltonian Framework*. University of Groningen, Groningen, The Netherlands, 2014.

[27] R. Mahony and S. Stramigioli. A port-Hamiltonian approach to image-based visual servo control for dynamic systems. *The International Journal of Robotic Research*, 31(11):1303–1319, 2012.

[28] R. Mahony, S. Stramigioli, and J. Trumpf. Vision based control of aerial robotic vehicles using the port-Hamiltonian framework. In *Proceedings of 50th IEEE Conference on Decision and Control and European Control Conference*, pages 3526–3532, Orlando, Florida, USA, 2011.

[29] B. Maschke, R. Ortega, and A.J. van der Schaft. Energy-based lyapunov functions for forced Hamiltonian systems with dissipation. *IEEE Transactions on Automatic Control*, 45(8):1498–1502, 2000.

[30] B.M. Maschke and A.J. van der Schaft. Port-controlled Hamiltonian systems: modeling origins and system-theoretic properties. In *Proceedings of the IFAC Symposium on Nonlinear Control Systems*, pages 282–288, Bordeaux, France, 1992.

[31] M. Munoz-Arias, J.M.A. Scherpen, and D.A. Dirksz. A class of standard mechanical systems with force feedback in the port-Hamiltonian framework. In *Proceedings of the 4th IFAC Workshop on Lagrangian and Hamiltonian Methods for Nonlinear Control*, pages 90–95, Bertinoro, Italy, 2012.

[32] M. Munoz-Arias, J.M.A. Scherpen, and D.A. Dirksz. Force feedback of a class of standard mechanical system in the port-Hamiltonian framework. In *Proceedings of the 20th International Symposium on Mathematical Theory of Networks and Systems*, Melbourne, Australia, 2012.

[33] M. Munoz-Arias, J.M.A. Scherpen, and D.A. Dirksz. Force control of a class of standard mechanical system in the port-Hamiltonian framework. In *Proceedings of the 9th IFAC Symposium on Nonlinear Control Systems*, pages 377–382, Toulouse, France, 2013.

[34] M. Munoz-Arias, J.M.A. Scherpen, and D.A. Dirksz. Position control via force feedback for a class of standard mechanical systems in the port-Hamiltonian framework. In *Proceedings of the 52nd IEEE Conference on Decision and Control*, pages 1622–1627, Florence, Italy, 2013.

[35] M. Munoz-Arias, J.M.A. Scherpen, and D.A. Dirksz. Position control via force feedback for a class of standard mechanical systems in the port-Hamiltonian framework. *submitted*, 2014.

[36] M. Munoz-Arias, J.M.A. Scherpen, and A. Macchelli. An impedance grasping strategy. In *Proceedings of the 53rd IEEE Conference on Decision and Control*, Los Angeles, CA, USA.

[37] M. Munoz-Arias, J.M.A. Scherpen, and A. Macchelli. An impedance grasping strategy. *submitted*, 2015.

[38] R.M. Murray, L. Zexiang, and S.S. Sastry. *Mathematical Introduction to Robot Manipulation*. CRC, USA, 1994.

[39] A.M. Okamura, M.J. Mataric, and H. I. Christensen. Medical and health-care robotics. *Robotics and Automation Magazine*, 17(3):26–27, 2010.

[40] R. Ortega, A. Loria, P.J. Nicklasson, and H. Sira-Ramirez. *Passivity-Based Control of Euler-Lagrange Systems*. Springer, London, UK, 1998.

[41] R. Ortega and J. G. Romero. Robust integral control of port-Hamiltonian systems: the case of non-passive outputs with unmatched disturbances. *Systems and Control Letters*, 61:11–17, 2011.

[42] R. Ortega, M. Spong, F. Gomez, and G. Blankenstein. Stabilization of underactuated mechanical systems via interconnection and damping assignment. *IEEE Transactions on Automatic Control*, 45(8):1498–1502, 2000.

[43] R. Ortega, A. van der Schaft, B. Maschke, and G. Escobar. Interconnection and damping assignment passivity-based control of port-controlled Hamiltonian systems. *Automatica*, 38:585–596, 2002.

[44] R. Ortega, A.J. van der Schaft, I. Mareels, and B. Maschke. Putting energy back in control. *Control Systems, IEEE*, 21(2):18–33, 2001.

[45] R. Rijs, R. Beekmans, S. Izmit, and D. Bemelmans. *Philips Experimental Robot Arm: User Instructor Manual*. Koninklijke Philips Electronics N.V., Eindhoven, The Netherlands, 2010.

[46] H. Sadeghian, M. Keshmiri, L. Villani, and B. Siciliano. Null-space impedance control with disturbance observer. In *Proceedings of the IEEE/RSJ International Conference on Intelligent Robots and Systems*, pages 2795–2800, Vilamoura, Algarve, Portugal, 2012.

[47] Y. Sakagami, R. Watanabe, C. Aoyama, S. Matsunaga, N. Higaki, and K. Fujimura. The intelligent asimo: System overview and integration. In *IEEE/RSJ International Conference on Intelligent Robots and Systems*, volume 3, pages 2478–2483. IEEE, 2002.

[48] S. Sakai and S. Stramigioli. Casimir based impedance control. In *Proceedings of the IEEE International Conference on Robotics and Automation*, pages 1384–1391, St. Paul, Minnesota, USA, 2012.

[49] P. Seibert and J. S. Florio. On the reduction to a subspace of stability properties of systems in metric spaces. *Annali di Matematica pura ed applicata*, CLXIX:291–320, 1995.

[50] R. Serway and J. Jewett. *Physics for scientists and engineers*. Cengage Learning, 2013.

[51] B. Siciliano and O. Kathib. *Springer Handbook of Robotics*. Springer, Berlin, Germany, 2008.

[52] J.-J. E. Slotine and W. Li. Composite adaptive control of robot manipulators. *Automatica*, 25(4):613–618, 1989.

[53] M. Spong, S. Hutchinson, and M. Vidjasagar. *Robot modeling and control*. Wiley, USA, 2006.

[54] S. Stramigioli. *Modeling and IPC control of interactive mechanical systems: a coordinate-free approach*. Springer-Verlag, London, UK, 2001.

[55] A.J. van der Schaft. *L_2-Gain and Passivity Techniques in Nonlinear Control*. Springer, London, UK, 2000.

[56] G. Viola, R. Ortega, R. Banavar, J. A. Acosta, and A. Astolfi. Total energy shaping control of mechanical systems simplifying the matching equations via coordinate changes. *IEEE Transactions on Automatic Control*, 52(6):1093–1099, 2007.

Summary

Modern society demands robotic systems that are able to perform complex tasks under different circumstances. The rising production requirements of industry, the ever increasing standards, and applications in emerging domains such as domotics and mobile robotics,require fast and accurate intelligent systems.

This thesis answers the aforementioned requirements by the development of new control methods for nonlinear mechanical systems in an energy-based setting known as port-Hamiltonian (PH) systems. The control methods investigated are position, force, impedance grasping, and the trajectory tracking problem. Our novel control strategies are well suited for general mechanical systems, we focus our simulations and experimental results on a robotic manipulator. The robot manipulator illustrates the application of the aforementioned control strategies.

Control laws in the PH framework are derived with a clear physical interpretation via direct shaping of the closed-loop energy, interconnection, and dissipation structure of the system. The PH formalism leads to the selection of an energy storage function (Hamiltonian) that ensures a desired behavior of the mechanical system. PH systems include a large family of physical nonlinear systems. Since the PH framework is an efficient way to describe the environment, the physical systems, and the interactions between them, the dynamics of nonlinear controllers have a more suitable interpretation.

The first contribution of this thesis is about position control strategies via force feedback, presented for standard mechanical systems in the PH framework. The introduced control strategies require change of variables, since structure preservation of the PH system is not straightforward. The proposed control strategy offers an alternative solution to position control with more tuning freedom, and exploits knowledge of the system dynamics.

As a second contribution, we develop a new force control strategy, and we provide a force control law that asymptotically stabilizes a mechanical system to a constant desired

force. Furthermore, we introduce an impedance strategy for mechanical systems in the PH framework, where another change of variables is required in order to guarantee structure preservation. We then achieve impedance grasping control via a virtual spring with a variable rest-length. The force that is exerted by the virtual spring leads to a dissipation term in the impedance grasping controller, which is needed to obtain a smoother noncontact to contact transition.

Subsequently, we develop vision control strategies for standard mechanical systems in the PH framework. The strategies make use of an interaction matrix that includes the depth information together with the image features variables of the image plane. This procedure allows us to include the nonlinear dynamics of a vision system in order to attain a desired position.

Finally, in this thesis we make use of a passivity-based control method, called stabilization via canonical transformations. When a system cannot be stabilized by conventional state-feedback, the canonical transformations become of particular interest, because they are capable of dealing with a more general class of systems, e.g., time-varying systems.

Samenvatting

De moderne maatschappij vraagt naar robotsystemen die complexe taken kunnen uitvoeren onder verschillende omstandigheden. De steeds hogere eisen vanuit de industrie, hogere standaards en toepassingen in opkomende gebieden zoals domotica en mobiele robots, vereisen intelligente systemen die snel en nauwkeurig zijn.

Dit proefschrift beschrijft de ontwikkeling van nieuwe regelmethoden voor niet-lineaire mechanische systemen volgens de energiegebaseerde benadering van port Hamiltonse (PH) systemen. De ontwikkelde regelmethoden bieden een oplossing om te voldoen aan de eis van snelle en nauwkeurige intelligente systemen. In dit proefschrift wordt de regeling van positie, traject, kracht en impedantie-grijpen onderzocht. De ontwikkelde regelmethoden zijn geschikt voor algemene mechanische systemen, met simulaties en experimenten van een robot-manipulator. De robot-manipulator dient als voorbeeld ter illustratie van de eerder genoemde regelmethoden.

Regelmethoden in het PH raamwerk worden op basis van een duidelijke fysische interpretatie afgeleid, door de gesloten-lus energie, interconnectie en dissipatiestructuur van het systeem te veranderen. De PH benadering leid tot een energiefunctie (Hamiltoniaan) dat ervoor zorgt dat het systeem het gewenste gedrag vertoont. PH systemen omvatten een grote groep niet-lineaire systemen in verschillende fysische domeinen. Door de fysische interpretatie van het PH raamwerk wordt de interpretatie van de ontwikkelde regelsystemen ook duidelijker.

De eerste bijdrage van dit proefschrift is het realiseren van positieregeling van standaard mechanische systemen in het PH raamwerk door terugkoppeling van de kracht. Het behouden van de PH structuur bij krachtterugkoppeling is niet eenvoudig en vereist een coördinaattransformatie. De voorgestelde regeling is een alternatief voor positieregeling die meer vrijheid biedt bij het instellen van de regelparameters, met behulp van de systeemdynamica.

De tweede bijdrage van dit proefschrift is een regelmethode waarbij de kracht van een

mechanisch systeem wordt geregeld naar een constante gewenste waarde. Een regelmethode gebaseerd op de impedantie wordt voorgesteld, waarbij ook weer een coördinaattransformatie nodig is om de PH structuur te behouden. Impedantie-grijpen regeling wordt gerealiseerd door middel van een virtuele veer met een variabele rustlengte. De kracht geleverd door de virtuele veer zorgt voor een dissipatieve term in de impedantie-grijpen regeling, welke nodig is voor een meer geleidelijke overgang van niet-contact naar contact.

Vervolgens worden beeldgebaseerde regelstrategieën gepresenteerd. De regelmethode hierbij gebruikt een interactiematrix met informatie over de diepte en kenmerken van het beeldvlak. Hierdoor wordt het mogelijk om de niet-lineaire dynamica van het visionsysteem te gebruiken om een gewenste positie te realiseren.

Tenslotte wordt in dit proefschrift gebruik gemaakt van een passiviteitsgebaseerde regelmethode bekend als stabilisatie via kanonieke transformaties. De kanonieke transformaties maken het mogelijk om met een meer algemene klasse van systemen te werken, namelijk tijdsvariërende systemen. Dit is vooral interessant voor systemen die niet via de conventionele toestandsterugkoppeling gestabiliseerd kunnen worden.

Resumen

La sociedad moderna demanda sistemas robóticos con capacidad de desarrollar tareas complejas bajo diferentes circunstancias. La elevadas expectativas de producción en la industria, el siempre incremento de estándares, y aplicaciones en campos emergentes tales cómo la *domótica* y robots móviles, requieren rápidos y precisos sistemas inteligentes.

Esta tesis responde a los citados requisitos mediante el desarrollo de nuevos métodos de control para sistemas mecánicos no lineales en una configuración basada en energía. Esta configuración es conocida cómo *sistemas Hamiltonianos con puertos* (sHp). Los métodos investigados son el control de: posición, fuerza, impedancia mecánica de sujeción y seguimiento de trayectorias. Esta tesis solo incluye simulaciones y resultados experimentales obtenidos en un manipulador robótico, a pesar de que estas estrategias de control se adaptan adecuadamente a sistemas mecánicos generales. El trabajo con el sistema robótico valida la efectividad de los nuevos controladores.

Las leyes de control en el marco de los sHp son derivadas con un clara interpretación física mediante un moldeo de la energía en lazo cerrado, y mediante la interconexión y disipación en la estructura del sistema. El formalismo de los sHp lleva a seleccionar una función de almacenamiento de energía (Hamiltoniano) que asegura un comportamiento deseado en el sistema mecánico. Los sHp incluyen una extensa familia de sistemas físicos no lineales. Dado que el marco de los sHp es una forma eficiente de describir el entorno, los sistemas físicos y las interacciones entre estos; se tiene una interpretación física más adecuada de la dinámica de los controladores no lineales.

La primera contribución de esta tesis consiste en el desarrollo de estrategias de control de posición en sistemas dinámicos por medio de realimentación de fuerza. Estas estrategias con sHp no se pueden aplicar de forma directa en el sistema mecánico dado que se pierde las propiedades de pasividad de los sHp. Se requiere entonces de un cambio de variables que involucra la lectura de vectores de fuerza del sistema. La estrategia de control propuesta ofrece una solución alternativa a control de posición más clásico, ofreciendo

más libertad de ajuste.

Cómo segunda contribución se desarrolla una estrategia para el control de fuerza. Se presenta una ley de control que estabiliza asintóticamente la fuerza ejercida por un sistema mecánico a un valor constante. Además, se introduce una estrategia para controlar la impedancia mecánica en el marco de los sHp, donde se requiere de un nuevo cambio de variables para garantizar la pasividad del sistema. Cómo consecuencia, un control de sujeción con impedancia mecánica es posible mediante un resorte virtual. La fuerza que se ejerce con el resorte virtual genera un elemento disipador en el controlador, el cuál es necesario para obtener una transición de no contacto a contacto más suave por el sistema mecánico a una superficie.

Posteriormente, esta tesis dirige su atención a sistemas mecánicos con sensorización visual en el marco de los sHp. Las estrategias para el control de posición de estos sistemas hacen uso de una matriz de interacción que incluye información de las características de la imagen y del plano visual, dando una interpretación física del sistema controlado.

Finalmente, en esta tesis se hace uso de un método de control basado en pasividad llamado estabilidad por medio de *transformaciones canónicas*. Cuando un sistema no se puede estabilizar por medio de una realimentación de estados, las transformaciones canónicas se vuelven interesantes porque son capaces de hacerle frente a este problema. Tal es el caso del problema de control de trayectorias para robot manipuladores.